Data Compilation and Evaluation of SPACE SHIELDING PROBLEMS

Volume III

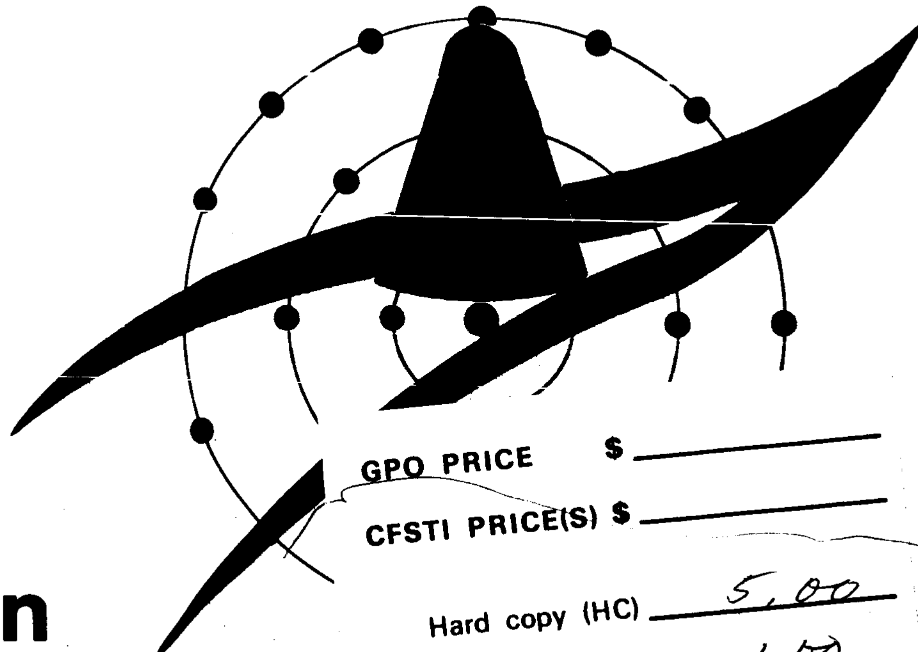

GPO PRICE $ ______

CFSTI PRICE(S) $ ______

Hard copy (HC) 5.00

Microfiche (MF) 1.00

ff 653 July 65

Radiation Hazards in Spac[redacted]

CONTRACT NAS8-11164

N67 11966 (ACCESSION NUMBER) ______ (THRU)

182 (PAGES) 1 (CODE)

CR-76511 (NASA CR OR TMX OR AD NUMBER) 29 (CATEGORY)

FACILITY FORM 602

ER-7777

LOCKHEED NUCLEAR PRODUCTS

Lockheed-Georgia Company -- A Division of Lockheed Aircraft Corporation

ER 7777
April 1966

DATA COMPILATION AND EVALUATION OF SPACE SHIELDING PROBLEMS

RADIATION HAZARDS IN SPACE
VOLUME III

Prepared For:

GEORGE C. MARSHALL SPACE FLIGHT CENTER

Prepared By:

C. W. Hill
W. B. Ritchie
K. M. Simpson, Jr.

[redacted]

LOCKHEED NUCLEAR PRODUCTS
Lockheed-Georgia Company - A Division of Lockheed Aircraft Corporation

Contract NAS 8-11164
Code U

FOREWORD

Volume III, ER 7777, Data Compilation and Evaluation of Space Shielding Problems - Radiation Hazards in Space, is a technical summary report of a study performed under Contract NAS 8-11164 to the George C. Marshall Space Flight Center, NASA, Huntsville, Alabama. The Technical Contract Monitor is M. O. Burrell of the Research Projects Division.

TABLE OF CONTENTS

PRECEDING PAGE BLANK NOT FILMED.

TABLE OF CONTENTS
(Continued)

LIST OF TABLES AND FIGURES

LIST OF TABLES AND FIGURES
(Continued)

LIST OF TABLES AND FIGURES
(Continued)

LIST OF TABLES AND FIGURES
(Continued)

LIST OF TABLES AND FIGURES
(Continued)

ABSTRACT

This report presents the results of parametric studies investigating the hazards of space radiations in relation to various local and interplanetary missions. The radiation types include proton and alpha particles emitted in solar flux events and proton and electron particles trapped in the magnetosphere of the Earth. The missions are three Mars expeditions, three 14-day Lunar expeditions, and 29 orbital studies. Detectors are located in the eye and abdomen of a man model placed in a cylindrical vehicle composed of either aluminum or polyethylene. The vehicle wall thickness ranges from 1 to 30 gm/cm^2. Descriptions of the principal computer programs employed in these studies are contained in this report.

1.0 INTRODUCTION

This volume represents a continuation of investigations into the hazards of space radiation and associated shielding problems. Presented here are the results of parametric studies of interplanetary and local space missions. Also included is a description of an additional computer program not contained in Volume II[25], and modifications to the Dose program initially described in Volume II. The additional program provides proton and alpha spectra, integral in energy, due to solar flux events. The modifications to the Dose program permit the calculation of alpha and electron doses (or dose rates) as well as proton doses (or dose rates).

These parametric studies are described in Section 2.0, and the results are presented in Appendix E. Dose estimates are obtained for three Mars missions and three Lunar missions with four alpha and proton spectra for each mission. The vehicle wall thicknesses for these missions are 1, 2, 5, 10, 20, and 30 gm/cm^2 of aluminum and the same set of thicknesses for polyethylene. The dose estimates are made in the right eye and abdomen of a man model placed in the vehicle. The results of these 1152 dose calculations are presented graphically. In addition to the Mars and Lunar missions, dose calculations are performed for the aluminum vehicle in orbit about the Earth. Proton and electron dose rates are obtained for three angles of inclination (0°, 30°, and 90°) and for ten altitudes ranging from 150 to 15,000 nautical miles. The same shield thicknesses and detector locations as in the Mars and Lunar missions are employed. The results of the orbital missions are also presented graphically. The spectra involved in the various missions are presented in tabular form in Appendix D. Associated with each spectrum resulting from solar activity is a probability that that particular hazard will be exceeded during that mission. The spectra associated with Earth orbits are projected for the 1968 time period.

Section 3.0 describes a mathematical model used to predict proton and alpha total mission flux, integral in energy, due to solar flux events. The integral fluxes are

PRECEDING PAGE BLANK NOT FILMED.

tabulated at 10, 30, 50, 100, 200, 400, 1000, and 1500 MeV. At each energy, there are 55 flux values and the associated probability, at each flux value, of exceeding that value. Flux event clustering and summer-winter asymmetry are available as options. This model is incorporated into a Fortran IV language computer program acceptable to either the IBM 7094 or System 360/50.

The Dose program modifications are presented in Section 4.0. The alpha dose calculation employs the same techniques as the proton dose calculation; therefore, the calculational methods of Section 5.1, Volume II, are repeated for the reader's convenience in Section 4.1 of this volume. The calculation of electron dose (or dose rate) is described in Section 4.2. The results of the electron transport methods are compared with the Monte Carlo results of Berger and Seltzer.[11,12]

The computer programs described in this report and in previous space radiation shielding reports may be obtained from Radiation Shielding Information Center, Oak Ridge National Laboratory, P. O. Box X, Oak Ridge, Tennessee, 37831.

2.0 MISSION STUDIES

This section investigates radiation dose estimates for several local and interplanetary missions. The vehicle configuration is described; calculational limitations are listed; mission source spectra are discussed; and conclusions are listed. In Appendix E, the results of these investigations are graphically displayed along with a table of dose tolerances for comparison. Appendix D contains tabulations of the various mission spectra.

Several points should be remembered in connection with the present calculations. The Mars and Lunar mission dose calculations do not include contributions from the trapped radiation belts. The orbital mission calculations do not include a solar flux event component. No provision is made for estimating electron bremsstrahlung or the penetration of solar flare radiation into the geomagnetic field. These capabilities will be added to the system in the near future. Cosmic ray dose is not included; this component depends on solar activity, position in the solar system, and shielding. Finally, the question of biological effectiveness is avoided by the use of physical dose units.

Considerations of various transmitted proton spectra[5], energy loss[24], and RBE[19] indicate that biological dose should be approximately equal to physical dose for shields ranging from 1 to 50 grams per square centimeter in thickness. Below this range, some solar flares with large low energy fluxes may produce skin biological dose much larger than physical dose. Above this range, secondary neutrons may raise the biological dose above physical dose. Similar considerations for alphas indicate that biological dose may be two to five times greater than physical dose for the same shield thicknesses. Electron energy loss data[13] and RBE[19] data indicate that biological dose is equal to physical dose for electron energies below 300 MeV.

2.1 GEOMETRIC CONFIGURATION

A simple vehicle configuration is chosen in order to expedite the analysis and ease the computation. The vehicle is a circular cylinder, surmounted by spherical end caps. The internal diameter is eight feet and the length is twenty feet. One standing man model is located along the vehicle mid-line with his feet at the center of the vehicle. Detector points are located in his right eye and the center of his abdomen. Vehicle walls are one inch thick. The wall density is specified so that mass thickness is one gram per square centimeter. The mass thickness is increased for purposes of a parametric survey by means of the "FF" factors in the Dose program. The material, aluminum or polyethylene, is specified in Dose program data. A sketch of the configuration is shown in Figure 2-1. This simple configuration is used in estimating doses for Mars missions, Lunar missions, and Earth orbital missions.

2.2 MARS MISSION RADIATION HAZARDS

An estimate of solar flare radiation hazards is made for three Mars missions by means of the Flare program and Dose program described in Sections 3.0 and 4.0.

The mission launch dates are October 9, 1977, December 28, 1981, and April 16, 1986. Each mission is approximately 450 days in length, with a Mars stay time of 20 days. The return trajectory passes inside the orbit of Venus. A total of 1000 histories are processed by the Flare program for each mission. A history is a stochastic representation of the course of solar flux events throughout the mission.

The cumulative proton and alpha integral flux distributions constructed by the Flare program are used to derive a set of integral flux spectra for a mission. A percent is associated with each cumulative integral flux spectrum; this percent represents the probability that the cumulative integral flux at each energy is exceeded. For a given probability, the integral flux spectrum is processed by the LSSC[23] program to generate

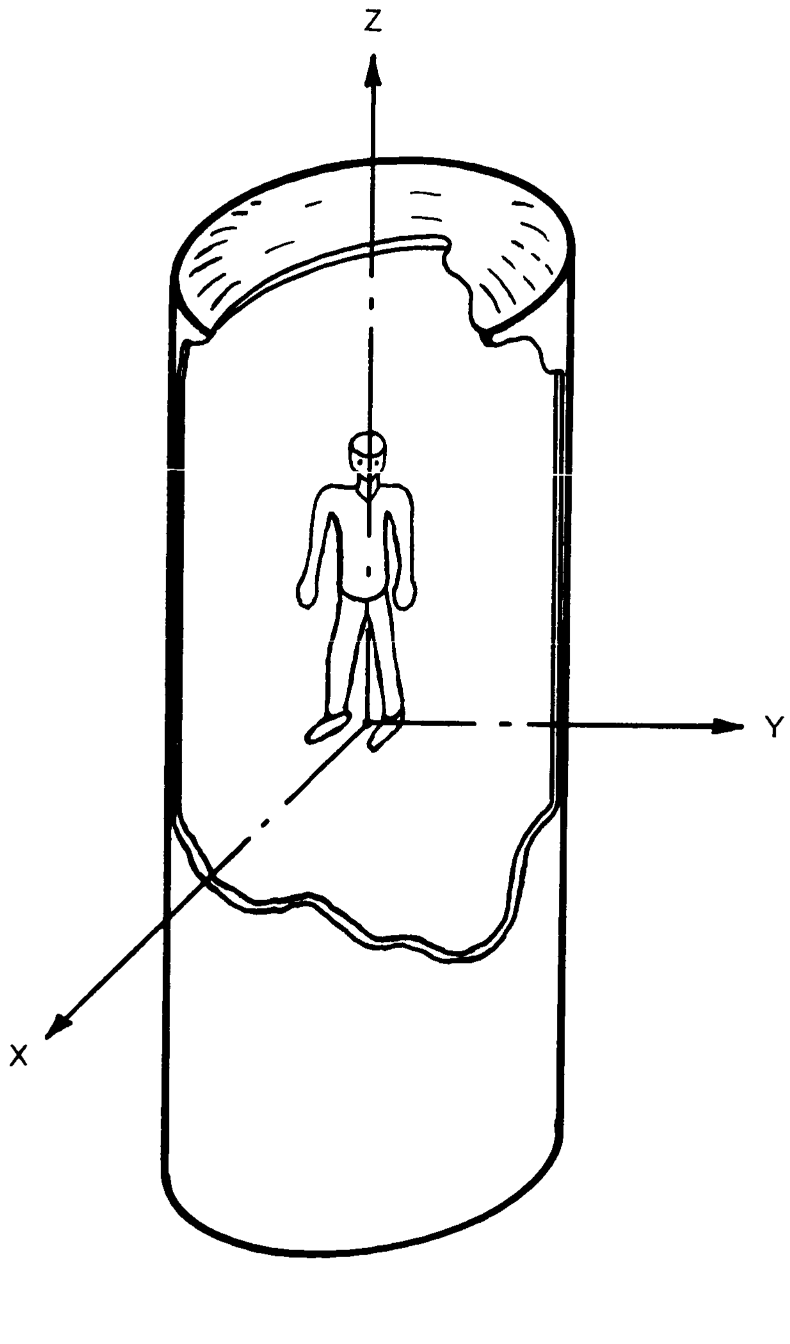

FIGURE 2-1 GEOMETRIC CONFIGURATION

a spectrum differential in energy. The spectra for three Mars missions, at the 0.1, 1.0, 10, and 50 percent probability levels, are tabulated in Appendix D.

Doses received at the eye and at the center of the abdomen of the man model within the configuration of Section 2.1 are shown graphically in Figures E1 - E12 of Appendix E. Caution should be used in the interpretation of the results presented in Appendix E. These data assume that future solar cycles will exhibit the same activity as the one just past, which, according to sunspot indices, was the most active in the last two centuries.[4] The model described in Section 3.0 permits flux events much larger than those observed in the last cycle. The manner of computing doses at the 0.1 and 1.0 percent probability levels may be conservative. Finally, the statistics at the low probability levels are fairly poor.

With the above cautions in mind, a few tentative conclusions may be stated with regard to these Mars missions.

(1) On a mass thickness basis, polyethylene is a better shield than aluminum, improving with increasing shield thickness.

(2) The alpha hazard is smaller than the proton hazard in all cases of interest.

(3) For the mission encountering the greatest hazard (1981), 15 gm/cm^2 of aluminum or 11 gm/cm^2 of polyethylene reduce eye dose to 100 rads with 90 percent probability.

(4) During solar minimum, a 10 gm/cm^2 aluminum or 7 gm/cm^2 polyethylene shield provides adequate protection against maximum permissible single acute emergency exposure[14] with greater than 99 percent probability.

(5) As probability of occurrence becomes smaller, the proton spectrum becomes

harder.

(6) For the mission encountering the greatest hazard, a 30 gm/cm^2 shield would not provide adequate protection with 99 percent probability.

Conclusions 5 and 6 may justly be regarded as questionable pending further investigation of the Flare model.

2.3 LUNAR MISSIONS

The term "Lunar missions" is intended to include voyages at one astronomical unit from the Sun and near the orbital plane of the Earth but effectively outside the magnetosphere. Synchronous orbital missions approximate these conditions. The vehicle configuration is the same as that of the Mars missions. The duration of the Lunar missions is 14 days. The number of histories processed for each mission is 10,000.

The same considerations and cautions applied to the Mars mission data generally hold for the Lunar mission results. However, the statistical uncertainty in the 0.1 percent probability curves is reduced. One feature of the Flare program mathematical model, not discussed explicitly in connection with the Mars mission results, acquires great importance in these shorter missions. The Flare program assumes a summer-winter asymmetry in the occurence of solar flux events. The asymmetry parameter is set to 0.4. A description of the summer-winter asymmetry option is given in Section 3.0. The Lunar mission dates (June 1-14, 1969, January 1-14, 1970, and June 1-14, 1971) are chosen to illustrate the effect of this asymmetry.

The proton and alpha fluxes computed for lunar missions are tabulated in Appendix D. The doses computed from these fluxes are plotted in Figures E13 - E24 of Appendix E.

Several interesting features may be inferred from the graphs.

(1) In no case is there a 50 percent or greater probability of receiving one rad behind a one gm/cm^2 shield.

(2) For the mission encountering the greatest radiation hazard (June 1969), a 10 gm/cm^2 aluminum shield reduces eye dose to 100 rads with 99 percent probability.

(3) For the same mission (June 1969), 16 gm/cm^2 polyethylene or 22 gm/cm^2 aluminum are required to keep eye dose below 25 rads with 99 percent probability.

(4) For the same mission (June 1969), 5 gm/cm^2 aluminum will restrict abdomen dose to 25 rads with 99 percent probability.

As in the Mars mission results, polyethylene is a better shield than aluminum; the alpha hazard is negligible for shields thicker than 5 gm/cm^2; and the proton spectrum becomes harder with decreasing probability of occurrence.

2.4 EARTH ORBITAL MISSIONS

Eye and abdomen dose rates within the configuration of Section 2.1 are estimated for circular orbits in the trapped radiation belts. These orbits have angular inclinations of 0, 30, and 90 degrees and altitudes ranging from 150 to 15,000 nautical miles. The primary radiations considered include protons and electrons.

Radiation intensities are taken from orbital integrations of the AP 3 (proton) flux map and the projected 1968 electron environment furnished by James I. Vette.[36, 37] These flux spectra, integral in energy, are converted to spectra, differential in energy, by means of the LSSC[23] program. These radiation spectra are tabulated in Appendix D.

Proton eye and abdomen dose rates versus thickness are shown in Figures E25 - E28 of Appendix E for various altitudes and angles of inclination. Electron eye dose rates versus altitude are shown in Figures E29 and E30 of Appendix E for two shield thicknesses and three angles of inclination.

3.0 FLARE PROGRAM

The Flare program is a Fortran IV, Monte Carlo code presently operating on the IBM 7094 and System 360/50. Its purpose is to provide an estimate, at various probability levels, of the proton and alpha fluxes in space which arise from solar flares. To this end, the Flare program processes a specified number of mission histories. The number of days per mission may range from 1 to 1000. The program considers each day in turn and determines whether a flux event occurs by sampling from a probability distribution function (pdf). The proton flux above 30 MeV is sampled from another pdf. A spectral parameter is sampled from a third pdf and this parameter also specifies the proton to alpha ratio. The proton and alpha flux, integral in energy, is computed at eight energies; 10, 30, 50, 100, 200, 400, 1000 and 1500 MeV. Then 40, 70, 90, or 100 percent of these fluxes are accumulated depending on whether 0, 1, 2 or more than 2 days remain in the mission. An inverse square correction is applied for interplanetary missions.

After each flux event, the presence of a "clustered" event is tested by means of sampling. If a clustered event occurs, it is forced to follow the primary event by 2 days. Again, the proton and alpha fluxes are determined and spread over a 4 day interval.

After each mission history is completed, the fluxes in each energy group are tabulated according to magnitude. After all histories are completed, the tabulation is converted to percent of histories which exceed certain flux levels for each energy group.

The mathematical model is based upon interpretations of data principally from the nineteenth solar cycle, 1954 - 1964. The validity of the results is, of course, dependent upon the validity of the data and upon the assumption that future activity cycles will follow the pattern of the nineteenth.

3.1 FLARE PROGRAM DESCRIPTION

There appear to be well established patterns of solar activity.[1,3,22,33,35] Allen[4] states that sunspot activity is known with high reliability back to about 1830, with fair reliability to 1749, and with low reliability to 1700. The cycle is approximately 11 years in duration, varying from 8 to 14 years. Prior to 1700, direct evidence of the solar activity cycle is not available; however, indirect observations implying cyclical patterns are available. An 11 year pattern has been found in tree rings which may be related to the solar cycle, though the causative mechanism has not been clearly defined. Brooks[15] has found that a negative correlation exists between tropical temperature and sunspots, a positive correlation exists between pressure contrasts and sunspots, and a positive precipitation correlation exists where the pressure correlation is negative and vice versa. Baktai et al[10] have detected a seven year cycle in petrified tree rings from 25 to 30 million years ago.

Various efforts have been made to study the relationship between sunspots and solar flux event (SFE) secondary characteristics such as polar cap absorption (PCA) and geomagnetic storms.[2,6,8,20] The correlation coefficient is generally determined to be about 0.7[32], a significant but not conclusive level. It is doubtful that hazardous SFE's achieve better correlation. Indeed, Warwick[39] and Bailey[8] have pointed out that the major SFE's of the nineteenth cycle occurred on the ascending and descending portion of the sunspot cycle, with no large events at the maximum.

Recently Gnevyshev[20] has shown a correlation between coronal glow and geomagnetic activity which reaches a value of 0.98. This very high correlation is understandable if the plasma storms which cause geomagnetic storms excite the upper reaches of the solar atmosphere as they leave the sun. It is reasonable to inquire whether high energy particle eruptions also follow the coronal cycle. No serious attempt has been made to verify such a relationship in the present study. However, since the coronal cycle is double peaked in the 11 year sunspot cycle with two to three years between the two peaks of a cycle,[7,20] the hypothetical relationship should be apparent from data on SFE's. The best documented characteristic of SFE's is found in the records of PCA's.

The tabulations of PCA's published by Malitson and Webber,[28] and by Bailey are combined and plotted as a bar graph in Figure 3-1. Here, the PCA's are collected in yearly increments. The plot suggests a possible double peak. The smooth curve fitted to the bar graph represents the sum of two beta distributions with an arbitrary minimum set equal to three percent of the largest maximum.

A possible seasonal effect has been suggested by Anderson.[6] Such an effect has been sought in the present data. Despite relatively poor statistics, a winter-summer asymmetry does appear as shown by the bar graph of Figure 3-2.

The difference between the average number of winter SFE's and summer SFE's over ten years of the nineteenth cycle has been tested by the "t" test of significance between two sample means for paired variates.[26] The probability that this difference is random is less than 0.12. Over the five most active years, the probability that this difference is random is 0.032. These results indicate that the winter-summer asymmetry should not be ignored. In order to realize this asymmetry, a sinusoidal variation is imposed on the pdf as shown in Figure 3-2.

The smooth curve of Figure 3-1 is constructed from the sum of two beta distributions as shown in Figure 3-3.

$$F(t) = f_1(t) + f_2(t) \qquad 0 \leq t \leq 1 \qquad (3\text{-}1)$$

where

$f(t) = kt^{\alpha}(1-t)^{\beta}$, and

t = number of days from start of cycle/4017.

The three constants for each function are computed from input data; t_1, t_2, t_3, y_1,

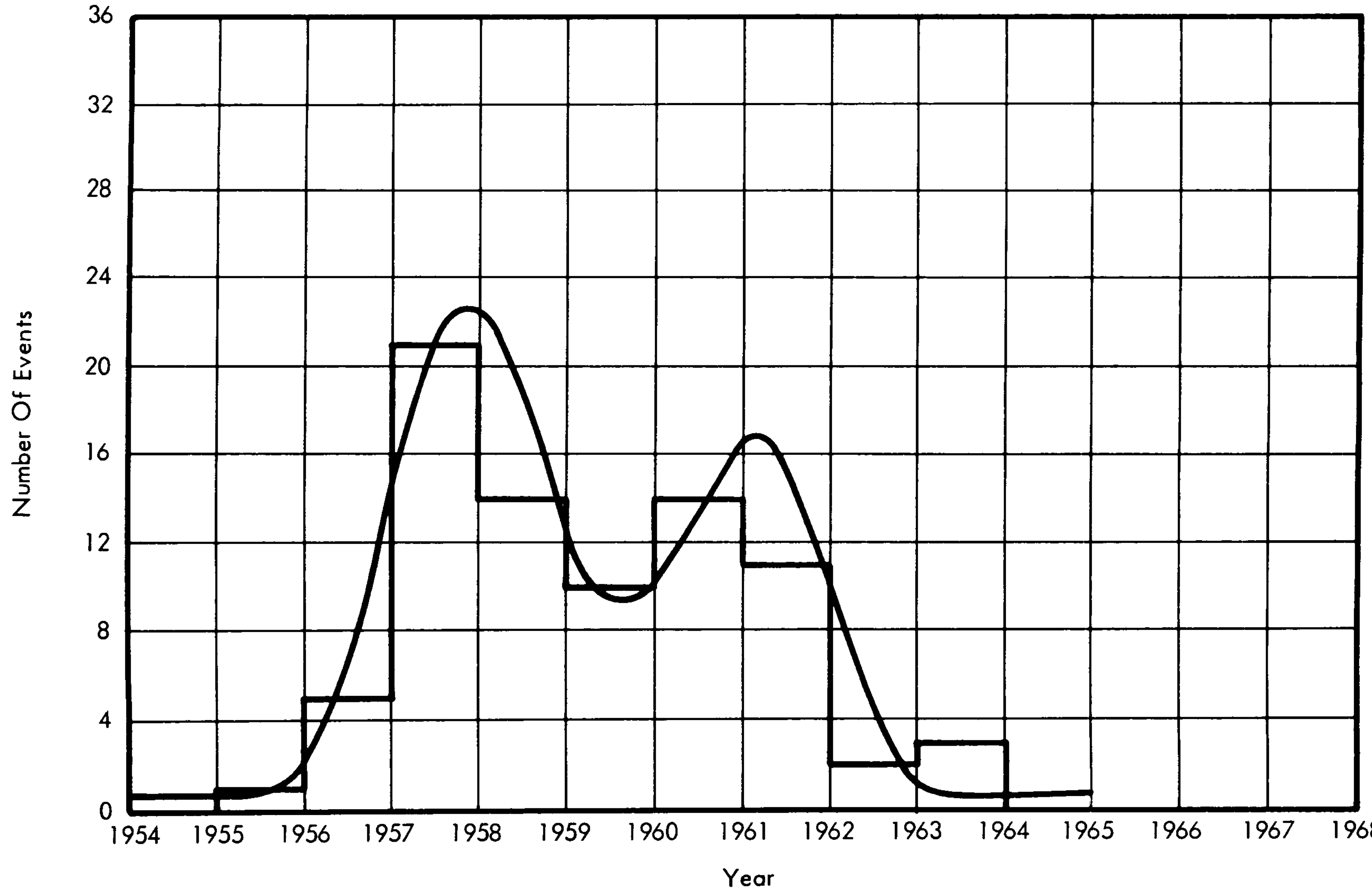

FIGURE 3-1 SOLAR FLUX EVENTS IN THE 19TH CYCLE

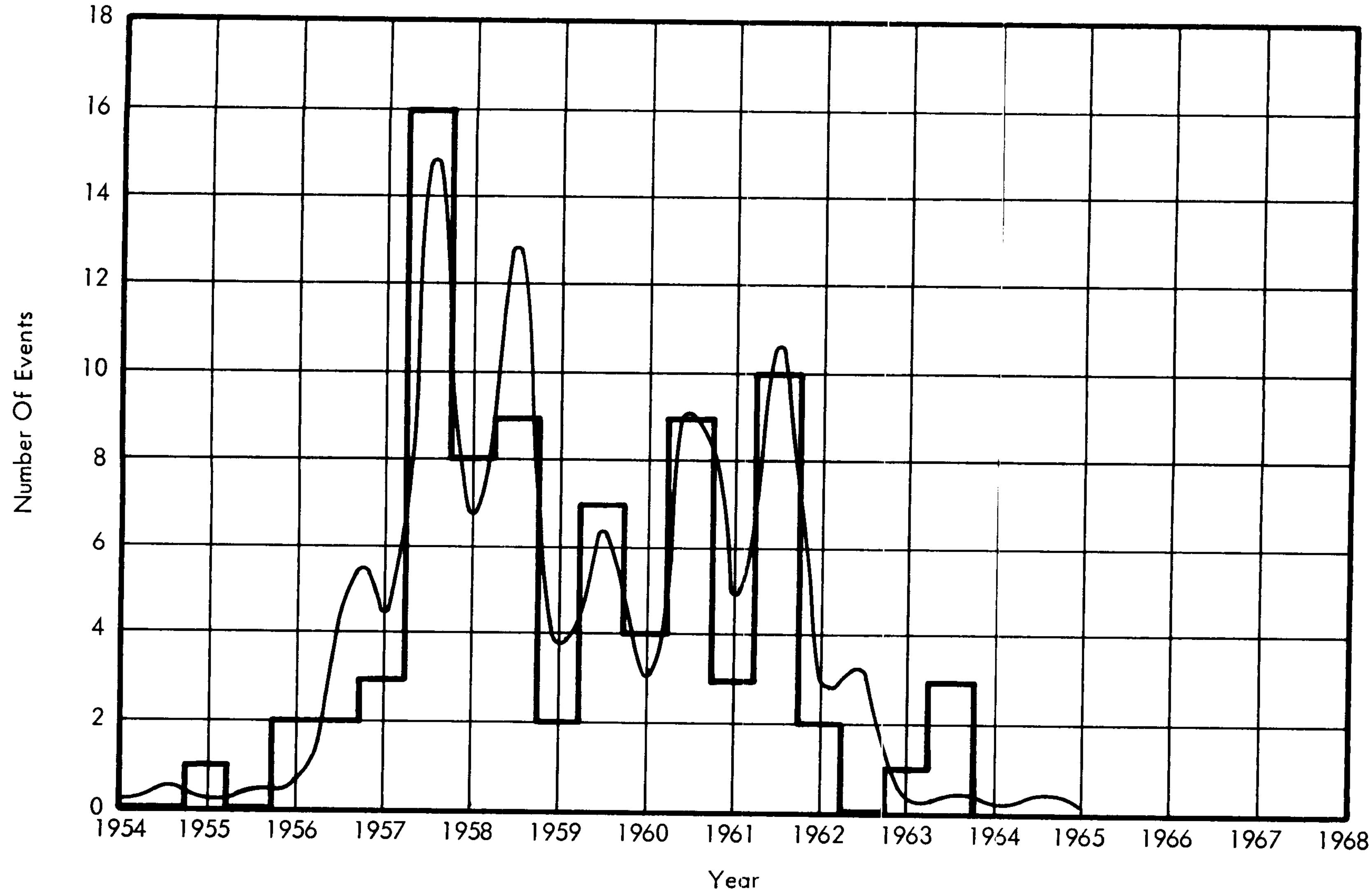

FIGURE 3-2 SOLAR FLUX EVENTS IN THE 19TH CYCLE SHOWING SUMMER-WINTER ASYMMETRY - C = 0.4

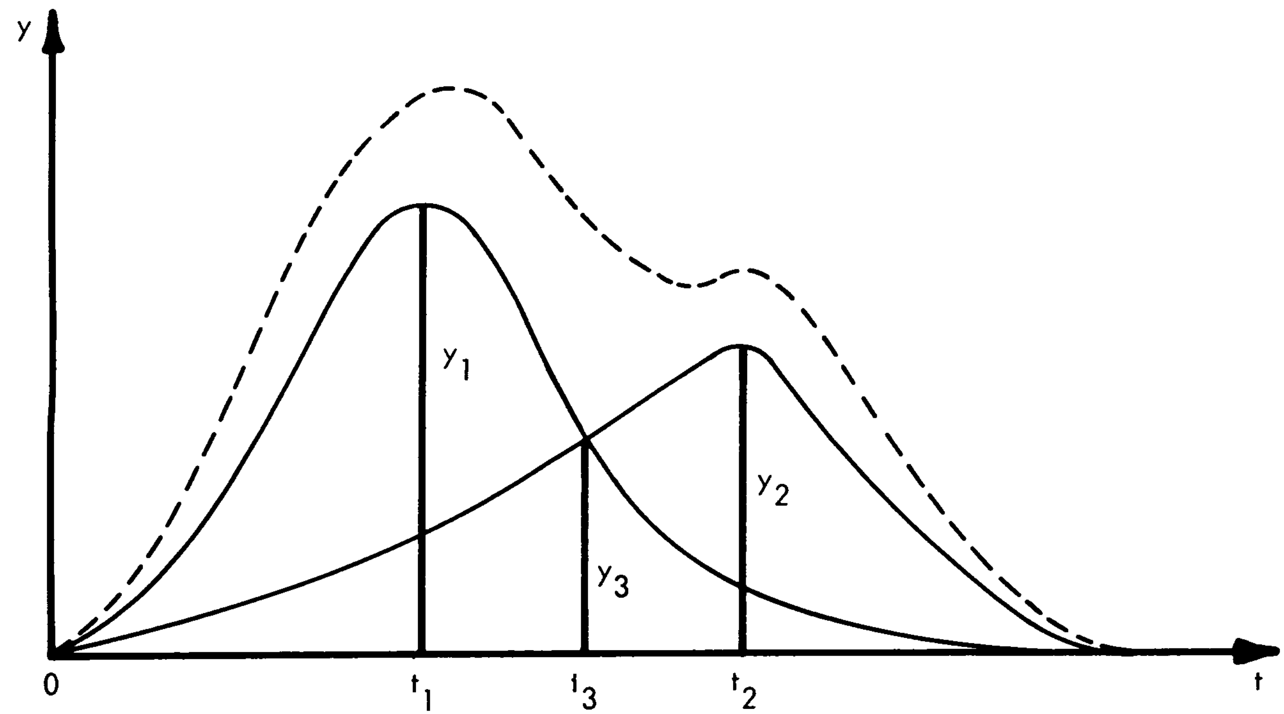

FIGURE 3-3 SUM OF TWO BETA DISTRIBUTIONS

y_2, and y_3. The first beta distribution is determined by the values t_1, t_3, y_1, and y_3.

$$f_1(t) = y(t) = k\, t^{\alpha} (1 - t)^{\beta}$$

The derivative of $y(t)$ at t_1 is zero; this condition permits the evaluation of α in terms of β and t_1.

$$\alpha = \frac{\beta\, t_1}{1 - t_1} \tag{3-2}$$

At t_1 and t_3, respectively,

$$y_1 = k\, t_1^{\alpha} (1 - t_1)^{\beta}$$
$$y_3 = k\, t_3^{\alpha} (1 - t_3)^{\beta}$$

Dividing, taking logarithms, and solving,

$$\beta = \frac{\ln (y_3/y_1)}{\frac{t_1}{1 - t_1} \ln (t_3/t_1) + \ln \frac{1 - t_3}{1 - t_1}} \tag{3-3}$$

Finally,

$$k = \frac{y_1}{t_1^{\alpha} (1 - t_1)^{\beta}} \tag{3-4}$$

The second beta distribution is determined in a similar manner using t_2, t_3, y_2, and y_3. Because the probability distribution function is too small near the endpoints of Figure 3-1, these values are raised to three percent of the highest peak.

A sinusoidal variation, to depict the summer-winter asymmetry, is imposed on the above probability distribution function in the following manner.

$$F(t) = (f_1(t) + f_2(t))\,(1 + C \sin(wt + \gamma)) \qquad (3\text{-}5)$$

where

$w = 22\pi$, and

$\gamma = -\pi/2$.

The constant "C" is termed the summer-winter asymmetry parameter. A value of 0.4 produces the curve shown in Figure 3-2. The pdf, $F(t)$, is normalized to the number of primary solar flux events during the solar cycle.

The occurrence of a solar flux event on any given day of a mission history is determined stochastically from $F(t)$. If an event occurs, the Flare program selects the magnitude of the flux greater than 30 MeV from a pdf. The "size" pdf is constructed from the tabulated fluxes in Appendix A. The events for which no fluxes are indicated in Appendix A are assumed to have integral fluxes between 10^6 and 10^7 particles per square centimeter above 30 MeV because the sensitivity threshold of the instruments measuring PCA's lies in this range for fairly short events. Gregory[21] states that radio backscatter techniques are much more sensitive than riometers. A list of 1960 SFE's detected by the radio backscatter technique but not detected as PCA's is given in Appendix B. In the present study, such events are assumed to have integral fluxes between 10^5 and 10^6 particles/cm^2 above 30 MeV. If the ratio of 1960 events with fluxes greater than 10^5 to those with fluxes greater than 10^6 is applied to all PCA events in the nineteenth cycle, then the total number of events with fluxes greater than 10^5 is approximately 250. These data are plotted on Figure 3-4. The points lie approximately on a straight line on a log-log scale. The cumulative distribution, $G(\Phi)$, versus flux, Φ, of Figure 3-4 may be expressed as:

$$G(\Phi) = H\,\Phi^Q + \text{constant} \qquad (3\text{-}6)$$

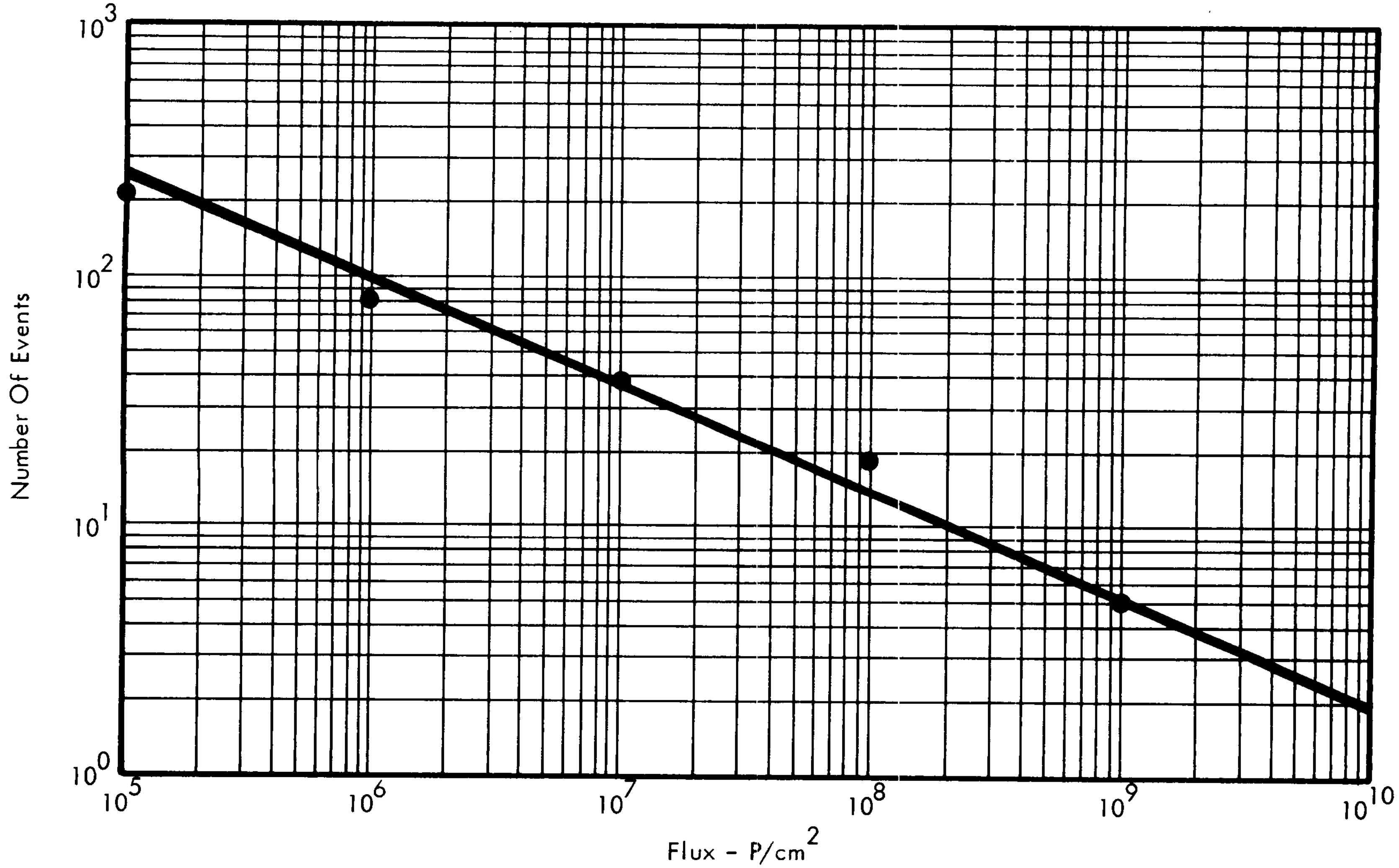

FIGURE 3-4 CUMULATIVE EVENT DISTRIBUTION VERSUS TIME-INTEGRATED OMNIDIRECTIONAL FLUX

The differential distribution is:

$$g(\Phi) = H\,Q\,\Phi^{Q-1} \tag{3-7}$$

The constants H and Q are evaluated from the following equations.

$$G(10^5) = 250 = \int_{10^5}^{\infty} H\,Q\,\Phi^{Q-1}\,d\Phi = -H\,10^{5Q}$$

$$G(10^9) = 5 = \int_{10^9}^{\infty} H\,Q\,\Phi^{Q-1}\,d\Phi = -H\,10^{9Q}$$

With the values of H and Q determined, it is now possible to sample from the normalized cumulative size distribution function above 10^5 P/cm^2 per flare.

$$R = \int_{10^5}^{\Phi} H\,Q\,X^{Q-1}\,dX = H\Phi^{Q} - H\,10^{5Q}; \tag{3-8}$$

where R is a random number from the uniform distribution between zero and one. This distribution would occasionally select very large SFE's. In the present study, the maximum size is restricted to a value of 10^{11}, many times the largest observed. By modifying Equation 3-8,

$$R = \frac{\int_{10^5}^{\Phi} H\,Q\,X^{Q-1}\,dX}{\int_{10^5}^{10^{11}} H\,Q\,X^{Q-1}\,dX} = \frac{H\,\Phi^{Q} - H\,10^{5Q}}{H\,10^{11Q} - H\,10^{5Q}}, \tag{3-9}$$

or

$$\Phi = \left[R\,(10^{11Q} - 10^{5Q}) + 10^{5Q}\right]^{1/Q} \tag{3-10}$$

The value of Φ given in Equation 3-10 refers to time-integrated proton flux above 30 MeV for one flare.

The problem of determining the proton spectrum for a given flare is made difficult by a scarcity of data. The spectrum of the time-integrated flux may be exponential in rigidity or occasionally power law in energy. It is not yet feasible to demonstrate spectral dependence on flux magnitude. In this study all spectra are assumed to be exponential in rigidity from 10 to 1500 MeV and independent of the size of the event. The former assumption is probably not valid below 30 MeV. The available data for 31 time-integrated spectra[40] are plotted in Figure 3-5. Here, the number of flares with characteristic rigidity greater than p_o is plotted versus p_o, where p_o is defined as:

$$\Phi(p) = \Phi_o e^{-p/p_o} \qquad (3\text{-}11)$$

The points exhibit a reasonably small scatter about a straight line so it is possible to represent the cumulative number of flares, N, versus p_o as:

$$\ln \left[N(p_o) \right] = a\,p_o + b \qquad (3\text{-}12)$$

The observed values of p_o range from 50 to 270 MV. Arbitrary bounds of 40 and 300 MV are imposed in this study. The constants a and b are evaluated using points obtained from the straight line on Figure 3-5.

$$\ln \left[N(40) \right] = \ln(40) = a \cdot 40 + b$$

$$\ln \left[N(300) \right] = \ln(.37) = a \cdot 300 + b.$$

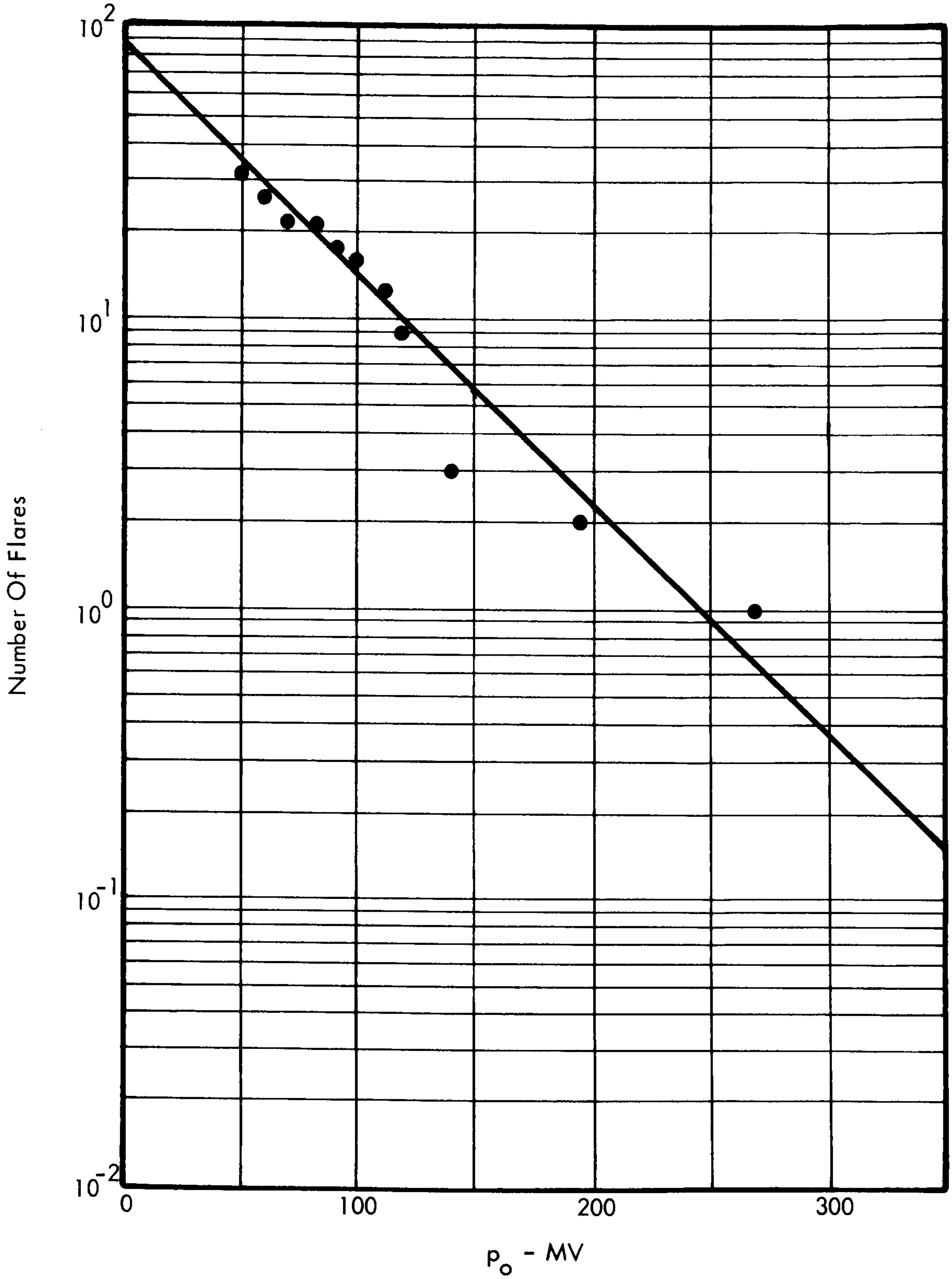

FIGURE 3-5 CUMULATIVE NUMBER OF FLARES CHARACTERIZED BY p_o OR GREATER VERSUS p_o

Let

$$K = \frac{\ln (40/.37)}{260};$$

Then $$a = -K, \tag{3-13}$$

and $$b = \ln 40 + 40\, K; \tag{3-14}$$

thus, $$N(p_o) = 40\, e^{K(40 - p_o)}. \tag{3-15}$$

Differentiating, integrating, truncating, normalizing, and setting the pdf equal to a random number as before,

$$R = \frac{-\int_{40}^{p_o} 40\, K\, e^{K(40 - X)}\, dX}{-\int_{40}^{300} 40\, K\, e^{K(40 - X)}\, dX} \tag{3-16}$$

which reduces to

$$p_o = 40 - \frac{260}{\ln (40/.37)} \ln \left[1 - R \left(1 - \frac{.37}{40}\right) \right] \tag{3-17}$$

as a means of selecting p_o.

Determination of the alpha particle component of solar flux events is based on a smaller body of available data[40] than parameters derived heretofore. Where data is available, the alpha spectrum, integral in rigidity, is usually parallel to the corresponding proton spectrum for the same event. Thus, the same value of p_o may be used for protons and alphas. Webber[40] presents the data plotted in Figure 3-6. This plot shows that the proton to alpha ratio approximates a power law function of p_o (averaged over an event) for the nine cases studied. For p_o less than 80 MV, the proton to alpha ratio is unity. Note that for a given rigidity p, the proton flux, integral in rigidity, above p is a factor of P/α larger than the alpha flux, integral in rigidity, above the same rigidity. Given the value p_o from Equation 3-17, the P/α ratio from Figure 3-6 is:

$$P/\alpha = 1 \qquad 40 \le p_o \le 80$$

$$P/\alpha = \exp\left[\frac{\ln (p_o/80) \ln 60}{\ln (275/80)}\right] \qquad 80 < p_o \le 300 \qquad (3\text{-}18)$$

With the aid of the model described above, the proton and alpha spectra, integral in energy, may be derived.

The Flare code determines the value of such spectra at eight energies; 10, 30, 50, 100, 200, 400, 1000, and 1500 MeV. Rigidities corresponding to these energies are computed for the protons as follows:

$$p_i = (E_i^2 + 2 \cdot 938.21\ E_i)^{1/2}\ . \qquad (3\text{-}19)$$

For the alphas, the equation is:

$$p_i = \frac{1}{2}\ (E_i^2 + 2 \cdot 3727.23\ E_i)^{1/2}\ . \qquad (3\text{-}20)$$

If the value of proton rigidity corresponding to 30 MeV is denoted as p_{30}, then the proton flux, integral in energy, at E_i is:

$$\Phi_P (E_i) = \Phi_P (p_i) = \Phi_P (p_{30})\ e^{(p_{30} - p_i)/p_o}\ . \qquad (3\text{-}21)$$

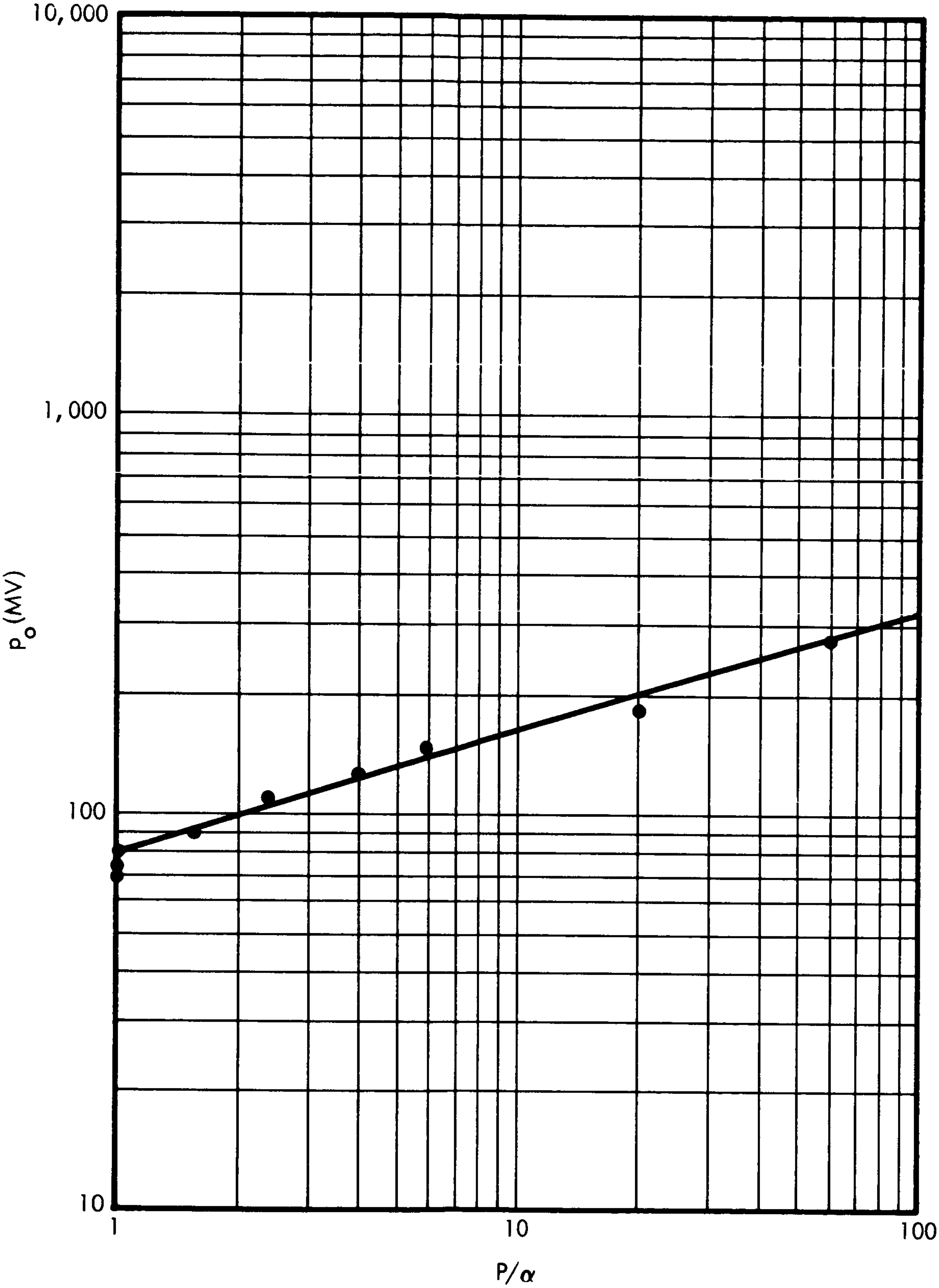

FIGURE 3-6 PROTON/ALPHA RATIO AS FUNCTION OF P_o

The alpha flux, integral in energy, is

$$\Phi_\alpha (E_i) = \Phi_\alpha (p_i) = \frac{\Phi_p (p_{30})\, e^{(p_{30} - p_i)/p_o}}{P/\alpha} \tag{3-22}$$

The Flare program assumes that the probability of encountering an SFE is independent of distance from the Sun. The flux intensities, derived above, may be attenuated by an inverse square law if desired. For this purpose, an elliptical transfer trajectory may be specified for the trip from the Earth to a planet together with a second elliptical trajectory for the return trip. The Sun is at one focus of both trajectories. The influence of other bodies in the solar system is ignored. The method used to compute the distance from the Sun to the vehicle as a function of time is derived from a program[17] originated at the George C. Marshall Space Flight Center, NASA.

The distance from the Sun to a point on the trajectory in polar coordinates is:

$$r = \frac{a\,(1 - \epsilon)}{1 + \epsilon \cos \theta} \tag{3-23}$$

where

a = semi-major axis of ellipse,

ϵ = eccentricity of ellipse, and

θ = initial angle in polar coordinates.

A variable, y, may be defined:

$$y = \frac{a - r}{a \epsilon} = \frac{\epsilon - \cos \theta}{1 + \epsilon \cos \theta} \tag{3-24}$$

Time, expressed as a function of position, is:[34]

$$t = \frac{a^{3/2}}{\mu^{1/2}} \left[\sin^{-1}\left(\frac{\sqrt{1 - \epsilon^2}\,\sin\theta}{1 + \epsilon\cos\theta}\right) - \frac{\sqrt{1 - \epsilon^2}\,\sin\theta}{1 + \epsilon\cos\theta} \right] \qquad (3\text{-}25)$$

which transforms to

$$t = a^{3/2}\,\mu^{-1/2}\,(\cos^{-1} y - \epsilon\,\sqrt{1 - y^2}) \qquad (3\text{-}26)$$

with

$$\mu^{-1/2} = 58.18\ \text{days/(A.U.)}^{3/2}.$$

Given a value of t, a value of y is obtained by Newton-Raphson iteration. The distance and angle for each day of the trajectory may be obtained from y.

$$r(t) = a\,(1 - \epsilon\,y(t)) \qquad (3\text{-}27)$$

$$\theta(t) = \cos^{-1}\left(\frac{\epsilon - y(t)}{\epsilon\,y(t) - 1}\right) \qquad (3\text{-}28)$$

A subroutine of the Flare program computes the values of r for each day of the mission. The input data required for this calculation includes initial and final values of the time, t, in Julian days and the polar angles, θ, in degrees, plus the eccentricity for each leg of the mission. A Julian calendar is presented in Appendix C.

Having determined the occurrence of an event, its magnitude, and integral spectrum, the total flux for this event is distributed over a four day interval, 40 percent on the day of onset, 30 percent on the day following, 20 percent on the third day, and 10 percent on the fourth day. However, if the mission terminates on any of the first three days, the flux assigned to following days is neglected.

The occurrence of an SFE may herald a series of similar events. The data in Appendices A and B indicate that 75 percent of the primary events are followed within four days by a "secondary" event. Calculations based on the SFE occurrence pdf show that only one third of these clustered events may be attributed to chance. Hence, the Flare program forces a secondary event to follow, in two days, a primary event approximately 50 percent of the time by a stochastic process.

The fluxes in each energy group are accumulated for each mission history. After each history is processed, the magnitude of the integral flux above each energy is tabulated in intervals ranging from 10^2 to $8 \cdot 10^{12}$. At 10 and 30 MeV, each event will produce at least $0.4 \cdot 10^5$ protons per square centimeter because 10^5 is the smallest flux sampled at 30 MeV, and only 40 percent of the flux is accumulated on the last day of the mission. After all histories are processed, this tabulation is converted to percent of missions which exceed various flux levels for each energy group. Sample output is shown in Appendix G.

The computer time required by the Flare program may be estimated as follows. A quantity termed mission days is obtained by multiplying the desired number of mission histories times the number of days in the mission. The time in seconds required by the IBM System 360/50 is the number of mission days divided by 800. The IBM 7094 will require less time.

3.2 GLOSSARY OF INPUT DATA TERMS

RND	the initial random number, a 10 digit odd number
HEAD	the heading information which may be used to identify each case, columns 1 through 72 are available
T1	the number of days from the start of the solar cycle at which the first activity peak occurs (see Figure 3-3), $0 \leq T1 \leq 4017$
T2	the number of days from the start of the solar cycle at which the second activity peak occurs (see Figure 3-3)

T3	the number of days from the start of the solar cycle at which the two beta distributions cross (see Figure 3-3)
Y1	the relative height of the first peak (see Figure 3-3)
Y2	the relative height of the second peak (see Figure 3-3)
Y3	the relative height of each beta distribution at T3 (see Figure 3-3)
C	winter-summer asymmetry parameter, the recommended value is 0.4
SEC	the probability of a single clustered event following a primary event in two days, the recommended value is 0.5
SIZE	the number of solar flux events in a solar activity cycle relative to the number in the nineteenth cycle, a value of unity is used in the present study
NHIS	the number of mission histories to be processed by the Monte Carlo Flare program. If NHIS is negative, the SFE probability will be printed at intervals of (-NHIS) days from JLE to JRE and the flux calculation will be omitted
JLE	the Julian calendar day of the start of the mission
JRE	the Julian calendar day of the end of the mission
JAP	the Julian calendar day at which the vehicle arrives at another planet. A value of zero causes the solar distance to be set to unity for each day of the mission
JLP	the Julian calendar day at which the vehicle leaves another planet. If JAP is zero, JLP may be omitted
TH1	the angle in degrees between the Earth-Sun line and the major axis of the outbound elliptical trajectory at departure time, JLE
TH2	the angle in degrees between the target planet-Sun line and the major axis of the outbound elliptical trajectory at arrival time, JAP
TH3	the angle in degrees between the target planet-Sun line and the major axis of the return elliptical trajectory at departure time, JLP

TH4	the angle in degrees between the Earth-Sun line and the major axis of the return elliptical trajectory at arrival time, JRE
E1	the eccentricity of the outbound elliptical trajectory
E2	the eccentricity of the return elliptical trajectory

3.3 INPUT DATA PREPARATION

The following cards follow the / DATA (360) or the $ DATA (7094) card.

CARD TYPE 1	Columns 1 - 10 contain the initial random number, RND. Format (I10).
CARD TYPE 2	Columns 1 -72 contain heading information, HEAD. Format (18A4).
CARD TYPE 3	This card specifies T1, T2, T3, Y1, Y2, Y3, and C. Format (7E10.1).
CARD TYPE 4	This card specifies SEC and SIZE. Format (2E10.1).
CARD TYPE 5	This card specifies NHIS, JLE, JRE, JAP, and JLP. Format (5I10).
CARD TYPE 6	This card specifies TH1, TH2, TH3, TH4, E1, and E2. This card is omitted if JAP is zero and all Sun-vehicle distances will be set to 1.0 A.U. Format (6E10.1).

NOTE: Additional cases may be run by repeating from Card Type 2.

3.4 FLARE PROGRAM OUTPUT

The Flare program prints the information contained in HEAD and the input data. It then gives the percent of mission histories which encountered no solar flux events. A table whose columns are labeled T, R, and F follows. The quantity T refers to the day in the solar activity cycle in which the mission takes place. The quantity R is the Sun-vehicle distance in astronomical units. If JAP is zero or if NHIS is negative, R will be set to unity. The quantity F is the probability of encountering a primary solar flux event on that day (see Equation 3-5). Following this table, the input random number, the first random number of this case, and the last random number of this case are given. Finally, tables of proton and alpha integral flux probabilities versus flux and energy are presented. Sample problem input and output are shown in Appendix G. The first set of flux probability tables is produced by the IBM 7094. The second set is produced by the IBM System 360/50. The results differ because different random number routines are used.

4.0 DOSE PROGRAM

The Dose program calculates proton, alpha, and electron physical doses (or dose rates) at points associated with a geometric configuration. The doses due to proton and alpha induced secondaries are included in these estimates; however, no bremsstrahlung calculation is attempted. This program obtains the geometric data from a magnetic tape generated by the Geometry program (The Geometry program is described in detail in Section 3 of Volume II). The flux data, range parameters for the materials involved, and other data applicable to the various materials in the configuration are input directly.

The Dose program approximates the proton and alpha input spectra, differential in energy, with from one to one hundred power law representations over the energy range of interest for each radiation type. The electron spectrum is treated in tabular form. Proton and alpha particle attenuation through shield materials is accomplished by the same technique described for protons in Section 5, Volume II. This method is described again in Section 4.1 of this volume for the reader's convenience. The electron transmission calculation is presented in Section 4.2.

The degree of accuracy of these transmission calculations has been established only for protons (Sections 5 and 5.1, Volume II) and electrons; sufficient data pertaining to alpha transport is not presently available. The accuracy of the proton dose calculation is dependent on the incident proton spectrum, the shield materials, and the total thickness. In comparison with the Lockheed Proton Penetration Code (LPPC),[23] the proton dose calculation differs by less than 7 percent from 0 to 100 gm/cm^2 of iron, less than 7 percent from 0 to 100 gm/cm^2 of water and less than 3 percent from 0 to 100 gm/cm^2 of aluminum. Dose calculations involving multi-layer shields of aluminum, iron, polyethylene, and tissue (totalling 20 gm/cm^2) differ from LPPC results by no more than 2.4 percent. The electron transmission calculation is compared with the work of Berger and Seltzer;[11,12] number transmission and transmitted energy spectra for thin shields are exhibited in this comparison.

PRECEDING PAGE BLANK NOT FILMED.

4.1 PROTON AND ALPHA DOSE CALCULATION

An expression of the physical dose or dose rate at a detector is given by:

$$D_j = K \sum_{i=1}^{N} \Omega_{ij} \int_0^\infty B(X_{ij}, E) \cdot P(X_{ij}, E) \cdot S_j(E)\, dE \; ; \qquad (4\text{-}1)$$

where

D_j = dose (rad) or dose rate at the j^{th} detector,

K = energy deposition-to-dose conversion factor,

Ω_{ij} = i^{th} solid angle of the j^{th} detector,

X_{ij} = penetration lengths (gm/cm^2) through all materials in i^{th} solid angle of the j^{th} detector,

$B(X_{ij}, E)$ = correction factor to account for nuclear collision losses of primary particles with energy E and the production and attenuation of secondary radiations,

$P(X_{ij}, E)$ = particle flux, differential in energy, arriving within the i^{th} solid angle of the j^{th} detector, and

$S_j(E)$ = particle stopping power in the j^{th} detector material.

Each of these factors is discussed in turn. The approximations required for computational purposes are illustrated and the transport equations used in the code are detailed.

The basic dose unit is chosen to be the rad. A physical dose, D_j, is calculated rather than a biological dose because information on RBE for the radiations of interest is rather sparse. The use of physical dose units also permits components other than biological specimens to be treated, e.g., photographic emulsion and semiconductors.

The factor, K, converts energy deposition in the detector to dose units. For example, if the units of stopping power are MeV-cm^2/gm and the units of time-integrated particle flux are p/cm^2-MeV-ster, the value of K is 1.602×10^{-8} rad-gm/MeV. If particle flux is given as p/cm^2-sec-MeV-ster, the dose rate may be computed in terms of rad/hr with K equal to 5.76×10^{-5} rad-gm-sec/MeV-hr.

The quantity, Ω_{ij}, represents an incremental solid angle about a vector emanating from the detector. The vector possesses direction cosines α, β, and γ. The maximum size of Ω_{ij} is specified by input data to the Geometry program. Generally, a maximum of 0.2 steradians, generating approximately 100 incremental solid angles, has proved satisfactory.

The quantity X_{ij} in Equation 4-1 represents shield penetration lengths along the vector in Ω_{ij}. The representation is symbolic. Actually, the code treats radiation transport through each layer in sequence in a multi-material shield configuration starting at the outside and going to the detector.

The radiation transport method used in Equation 4-1 makes no explicit reference to the generation and attenuation of secondary radiations, nor to the attenuation of primary particles due to nuclear collisions. To some extent the lack of generating secondary nucleons compensates the lack of attenuation of the primary particles by nuclear collisions which generate the secondaries. In order that the error resulting from this assumption may be corrected, a factor, $B(X_{ij}, E)$, is included in Equation 4-1.

$$B(X_{ij}, E) = \sum_{k=1}^{M} \exp(\epsilon X_{ijk} \cdot A_k/27) \qquad (4\text{-}2)$$

X_{ijk} = k^{th} material thickness in i^{th} solid angle for the j^{th} detector;

A_k = material-dependent parameter (effective atomic weight);

ϵ = .00125, protons; and

ϵ = .050, alphas.

The value of ϵ for protons is derived from comparisons of Dose program results with

LPPC results. The value of ϵ for alphas is estimated indirectly because no transport code similar to LPPC exists for alphas.

Figures F1 through F5 of Appendix F present neutron yield cross sections[30, 31] for proton and alpha particles incident on manganese-55, nickel-58, nickel-62, iron-56, and copper-63. The curves represent the sum of the listed cross sections, each of which are multiplied by the neutron multiplicity for that reaction. These data are, for the most part, derived from activation measurements and are not comprehensive. The neutron yield should rise with increasing energy below 50 to 100 MeV, as shown in Figure F6 for alpha interactions[38] with gold-197 (the Coulomb barrier favors neutron production in heavy neclei). Based upon the incomplete data cited above, the assumption is made that neutron yield from alpha interactions is twice the yield from proton interactions per target nucleus.

The data for charged particle production are also scanty. Bailey[9] gives proton yields from 190 MeV proton and 205 MeV alpha bombardment of aluminum and silver. For aluminum, alphas generate two times more secondary protons above 10 MeV than do protons (secondary protons below 10 MeV generated in the shield do not contribute significantly to the dose). For silver, the ratio is one third.

An indirect measure of the ratio of alpha produced secondaries to proton produced secondaries is available from radiochemical data. Korteling and Hyde[27] have measured the yield of 13 radioisotopes resulting from alpha and proton bombardment of niobium-93 at 320, 500, and 720 MeV, as shown in Table 4-1. Crespo, Alexander, and Hyde[18] have measured sodium-24 and magnesium-28 yields from 700 MeV alpha and proton bombardment of copper, silver, gold, and uranium as shown in Table 4-2. The data of Tables 4-1 and 4-2 show a factor of approximately two in the ratio of alpha and proton produced radioisotopes for medium to heavy nuclides in the energy range 300 to 700 MeV. It is not unreasonable to assume that these ratios are representative of the unreported daughter isotopes. If the daughter isotopes result from

TABLE 4-1

PRODUCTION CROSS SECTIONS FROM ALPHA BOMBARDMENT OF NIOBIUM AND RATIO OF ALPHA TO PROTON INDUCED CROSS SECTIONS[27]

Nuclide	320 MeV		500 MeV		720 MeV	
	σ_α (mb)	σ_α/σ_p	σ_α (mb)	σ_α/σ_p	σ_α (mb)	σ_α/σ_p
Nb-90	129.	2.33	97.2	2.03	83.5	2.24
Nb-89	46.8	2.13	33.5	1.99	27.8	1.99
Zr-89	111.	1.84	81.4	1.80	73.9	1.90
Zr-88	145.	2.01	105.	1.92	93.1	2.19
Zr-87	92.2	2.15	65.8	1.99	55.9	2.12
Cu-67	.0108	2.05	.0715	2.42	.166	1.38
Cu-64	.173	1.65	.145	1.97	4.34	1.54
Cu-61	.0442	1.28	.65	1.55	2.59	1.49
Ni-66	.00106	2.76	.0073	2.53	.0192	2.29
Ni-65	.00607	1.91	.0408	1.83	.121	1.92
Ni-57	.00554	3.03	.036	1.94	.143	1.94
Na-24	.0432	2.89	.113	2.62	.300	2.29
Na-22	.0468	2.92	.0864	3.34	.196	2.27
Average		2.23		2.15		1.97

TABLE 4-2

PRODUCTION CROSS SECTIONS FROM 700 MeV ALPHA BOMBARDMENT AND RATIO OF ALPHA TO PROTON INDUCED CROSS SECTIONS[18]

Target	Na-24		Mg-28	
	σ_α (mb)	σ_α/σ_p	σ_α (mb)	σ_α/σ_p
Cu	.698	1.9	.091	1.85
Ag	.227	2.27	.026	2.17
Au	.308	2.28	.102	1.85
U	.502	2.18	.238	2.07
Average		2.16		1.99

similar de-excitation processes for alpha and proton bombardment, then the ratio of alpha produced secondaries to proton produced secondaries should be approximately two.

In this study, the assumption is made that alpha interactions generate twice as many charged and neutral secondaries per target nucleus as protons. Further, it is observed that the majority of particles in a typical flare spectrum will be stopped in the first gm/cm^2. For a given initial energy, proton range is ten times alpha range. Thus, the secondaries generated by alphas are approximately 2/10 those generated by protons for identical alpha and proton spectra in shields thicker than a few gm/cm^2. This ratio may be realized by setting the quantity ϵ, of Equation 4-2, to 0.05 for alpha fluxes.

In order to compute the particle flux, $P(X_{ij}, E)$, arriving at the j^{th} detector through the i^{th} solid angle, it is necessary to consider the range relations for particles penetrating a multi-layer shield. The range is approximated by Equation 4-3.[16]

$$R(E) = \frac{a}{2b} \cdot \ln(1 + 2bE^r) \qquad (4\text{-}3)$$

where

$R(E)$ = particle range at energy E, and

a, b, r = parameters (particle dependent).

Values of a, b, and r are presented in Volume I of this report for a variety of materials for both proton and alpha particles.

The range of a particle, with energy E_o, incident upon a material of thickness X is related to the range of the transmitted particle, with energy E_1, by:

$$R(E_o) = X + R(E_1) \qquad (4\text{-}4)$$

or

$$\frac{a}{2b} \ln(1 + 2bE_o^{\ r}) = X + \frac{a}{2b} \ln(1 + 2bE_1^{\ r}) \qquad (4\text{-}5)$$

Solving Equation 4-5 for $E_o^{\ r}$:

$$E_o^{\ r} = A + BE_1^{\ r} \qquad (4\text{-}6)$$

where

B = $\exp(2bX/a)$

A = $\frac{B - 1}{2b}$

Equation 4-6 relates the exit energy to the incident energy for particles penetrating one material.

The above treatment may be readily generalized to multilayer shields. Given two layers, X_1 and X_2, of different materials, the exit energies E_1 and E_2 are related to the incident energy E_o by:

$$E_o^r = A_1 + B_1 E_1^r \tag{4-7}$$

$$E_1^r = A_2 + B_2 E_2^r . \tag{4-8}$$

Substituting Equation 4-8 into 4-7,

$$E_o^r = A_1 + B_1 A_2 + B_1 B_2 E_2^r$$

or (4-9)

$$E_o^r = A' + B' E_2^r .$$

For M layers

$$E_o^r = A' + B' E_M^r , \tag{4-10}$$

where

$$B' = B_1 B_2 B_3 \ldots . B_M,$$
$$A' = A_1 + A_2 B_1 + A_3 B_1 B_2 + \ldots . + A_M B_1 B_2 \ldots . B_{M-1},$$
$$B_k = \exp(2b_k X_k / a_k), \text{ and}$$
$$A_k = (B_k - 1)/2b_k .$$

It should be noted that the value of r is assumed to be material independent in the above treatment while a and b are material dependent.

The particle flux penetrating the shield along the i^{th} vector of the j^{th} detector is related to the incident flux by Equation 4-11. This equation presumes conservation of particles. Corrections due to nuclear interactions and secondaries are discussed above.

$$P(X_{ij}, E_M)\, dE_M = P(0, E_o)\, dE_o \qquad (4\text{-}11)$$

The exit energy, E_M, as determined from Equation 4-10, must be non-negative.

The incident flux over an energy interval, E_l to E_{l+1}, is represented by a power law expression:

$$P(0, E_o) = H_l\, E_o^{-q_l}, \qquad E_l \le E_o \le E_{l+1} \qquad (4\text{-}12)$$

One to one hundred intervals may be used over the entire energy range.

The differential of Equation 4-10 is:

$$dE_o = (A' + B'E_M^{\,r})^{\frac{1-r}{r}}\, dE_M\,. \qquad (4\text{-}13)$$

The flux at the detector is obtained by substituting Equations 4-10, 4-12, and 4-13 into 4-11.

$$P(X_{ij}, E_M)\, dE_M = H_l\, B'E_M^{\,r-1}\, (A' + B'E_M^{\,r})^{\frac{1-q_l-r}{r}}\, dE_M \qquad (4\text{-}14)$$

with the restrictions

$$E_l^* \le E_M \le E_{l+1}^*$$

$$(4\text{-}15)$$

$$E_l^* = \text{Max}\left[0, \left(\frac{E_l^{\,r} - A'}{B'}\right)^{\frac{1}{r}}\right]$$

$$E^*_{l+1} = \text{Max}\left[0, \left(\frac{E_{l+1}^{\ r} - A'}{B}\right)^{\frac{1}{r}}\right] . \qquad \text{(4-15 cont'd)}$$

The stopping power of the detector material is given by:

$$S_j(E_M) = \frac{1}{\left(\frac{dR(E)}{dE}\right)_{E_M}} ,$$

where, from Equation 4-3:

$$\frac{dR(E)}{dE} = \frac{a_j r_j E^{r_j - 1}}{(1 + 2b_j E^{r_j})} ,$$

or

$$S_j(E) = \frac{1 + 2b_j E^{r_j}}{a_j r_j E^{r_j - 1}} . \qquad \text{(4-16)}$$

Here, the parameters a, b, and r are subscripted with the detector subscript, j, to indicate that energy is deposited in the detector material. Note that a single value of r must be used for computing slowing of a particle through all shield materials but an optimum value may be used to compute energy deposition by a particle in the detector material to improve accuracy. In general, the values of the parameters a, b, and r will differ with particle type.

Applying Equations 4-2, 4-14, 4-15, and 4-16 to 4-1, the dose at the j^{th} detector may be written as follows:

$$D_j = K \cdot \sum_{i=1}^{N} \Omega_{ij} \prod_{k=1}^{M} \exp(\epsilon X_{ijk} \cdot A_k / 27) \sum_{l=1}^{L-1} H_l \cdot I_l(E^*_l, E^*_{l+1}). \qquad \text{(4-17)}$$

For non-zero shield thickness,

$$I_l(E_l^*, E_{l+1}^*) = B' \int_{E_l^*}^{E_{l+1}^*} \frac{E_M^{r-1} (A' + B'E_M^r)^{\frac{1 - q_l - r}{r}} (1 + 2b_j E_M^{r_j})}{a_j r_j E_M^{r_j - 1}} dE_M \, .$$

(4-18)

The following change of variable transforms Equation 4-18 into a form involving incomplete beta functions.

$$t = \frac{B'E_M^r}{A' + B'E_M^r}, \quad E_M = \left[\frac{A' t}{B'(1 - t)}\right]^{1/r}$$

$$dE_M = \frac{1}{r} \cdot \left(\frac{A'}{B'}\right)^{1/r} \cdot \frac{t^{\frac{1 - r}{r}}}{(1 - t)^{\frac{1 + r}{r}}} dt$$

which leads to

$$I_l(E_l^*, E_{l+1}^*) = K_o \left[\beta_{\alpha_2}(u, v) - \beta_{\alpha_1}(u, v) + K_1 \beta_{\alpha_2}(u', v') - K_1 \beta_{\alpha_1}(u', v')\right]$$

(4-19)

where

$$K_o = (A')^{\frac{2 - q_l - r_j}{r}}$$

$$K_1 = 2b_j \left(\frac{A'}{B'}\right)^{\frac{r_j}{r}}$$

$$\beta_\alpha(u, v) = \int_0^\alpha t^{u-1} \cdot (1 - t)^{v-1}\, dt$$

$$u = \frac{1 - rj - r}{r}$$

$$v = \frac{q_l + rj - 2}{r}$$

$$u' = \frac{1 + r}{r}$$

$$v' = \frac{q_l - 2}{r}$$

$$\alpha_2 = \mathrm{Max}\left[0,\ 1 - A'E_{l+1}^{-r}\right]$$

$$\alpha_1 = \mathrm{Max}\left[0,\ 1 - A'E_l^{-r}\right]$$

E_l and E_{l+1} are specified by Equation 4-12.

The incomplete beta function is evaluated by:

$$\beta_\alpha(u, v) = \frac{\alpha^u}{u} \cdot F(u,\ 1 - v,\ u + 1,\ \alpha) \qquad (4\text{-}20)$$

for $0 < \alpha < 1$ with v negative and for $0 < \alpha \leq 1/2$ with v positive. If v is positive and $1/2 < \alpha < 1$,

$$\beta_\alpha(u, v) = \frac{\Gamma(u) \cdot \Gamma(v)}{\Gamma(u + v)} - \beta_{1-\alpha}(v, u). \qquad (4\text{-}21)$$

Here, F(a, b, c, x) is the hypergeometric series.

$$F(a, b, c, x) = 1 + \frac{a\,b}{c} \cdot x + \frac{a(a + 1)\,b(b + 1)}{c(c + 1)}\ \frac{x^2}{2!} + \ldots \qquad (4\text{-}22)$$

The hypergeometric series is truncated at a point where the last term does not contribute to the eighth significant figure.

For zero thickness shields or for high energy particles penetrating thin shields, Equation 4-18 takes the following form.

$$I_l (E_l^*, E_{l+1}^*) = \frac{B'}{a_j r_j} \int_{E_l^*}^{E_{l+1}^*} E^{1 - q_l - r_j} \cdot (1 + 2b_j E^{r_j}) \, dE \qquad (4\text{-}23)$$

The code evaluates analytical solutions of this equation for all values of the exponents.

The dose at the j^{th} detector is obtained by means of Equation 4-17, using 4-18 or 4-23 as appropriate.

4.2 ELECTRON DOSE CALCULATION

The expression for the electron physical dose or dose rate at a detector is given by:

$$D = K \sum_i \Omega_i \int_0^{\infty} \Phi (E^*) \, T(X, E^*) \, C_o \int_0^{E_u} S(E) \, E^{\beta} (E_u - E)^{\alpha} \, dE \, dE^* \qquad (4\text{-}24)$$

where

D = dose (rad) or dose rate at a detector (detector subscripts are omitted),

K = energy deposition-to-dose conversion factor,

Ω_i = i^{th} solid angle,

E^* = incident electron energy,

E = exit electron energy,

$\Phi (E^*)$ = incident electron flux - e/cm^2-MeV-ster-(sec),

X = shield thickness - gm/cm^2,

$T(X, E^*)$ = electron number transmission factor,

$S(E)$ = stopping power - MeV-cm^2/gm,

C_o = normalization factor, a function of X and E*,

E_u = upper energy of transmitted electron spectrum arising from electron with original energy E*, a function of X and E*, and

α, β = parameters defining shape of transmitted electron spectrum, functions of X and E*.

The transmitted electron spectrum, arising from incident electrons with energy E*, is assumed to have a shape given by the beta distribution, $E^{\beta}(E_u - E)^{\alpha}$.

For the purpose of electron transmission, multi-material shields are simulated by equivalent aluminum shields. The equivalent aluminum thickness is obtained by the following relation:

$$X_{Al\ eq.} = \sum_{k=1}^{L} X_k \frac{Z_k}{A_k} \frac{A_{Al}}{Z_{Al}},$$

where

$X_{Al\ eq.}$ equivalent aluminum thickness - gm/cm^2,
X_k thickness of k^{th} layer,
Z_k, A_k atomic number and weight of material in the k^{th} layer, and
Z_{Al}, A_{Al} atomic number and weight of aluminum.

The electron number transmission factor is computed using;

$$T(X, E) = \exp\left(-(C_1 E)^{C_2}\right) \qquad (4\text{-}25)$$

where

$C_1 = (.585 \cdot 13^{-.271}/X)^{.848}$, and
$C_2 = -14.5 \cdot 13^{-.48}$.

This empirical equation was derived by Mar[29] using Monte Carlo data. The equation assumes normally incident electrons in the energy range 0.1 to 10. MeV.

The electron stopping power in water (as an approximation to tissue) is expressed analytically by the relation:

$$S(E) = A \cdot E + B + C/E \qquad (4\text{-}26)$$

$A = .061729277,$

$B = 1.6119395,$ and

$C = .2460117.$

This expression is obtained, from Berger and Seltzer's data,[13] by a least squares fit of $E \cdot S(E)$ to $A \cdot E^2 + BE + C$. The maximum error of the analytic representation is 3.8% on the energy interval .025 to 10. MeV. A graph of $E \cdot S(E)$ versus E is shown in Figure 4-1.

An analytical expression for electron range in aluminum, obtained by application of the least squares technique to Berger and Seltzer's range data,[13] is given by the following relation:

$$R(E) = cE^{a \ln E + b} \qquad (4\text{-}27)$$

$a = -.09391135,$

$b = 1.2204666,$ and

$\ln c = -.60608292.$

The maximum error of this relation is 7.4 percent on the energy interval .02 to 10. MeV. The error curve is shown in Figure 4-2.

In the electron transport model, the assumption is made that the transmitted energy spectrum due to an incident electron with energy E* has the form of a beta distribution,

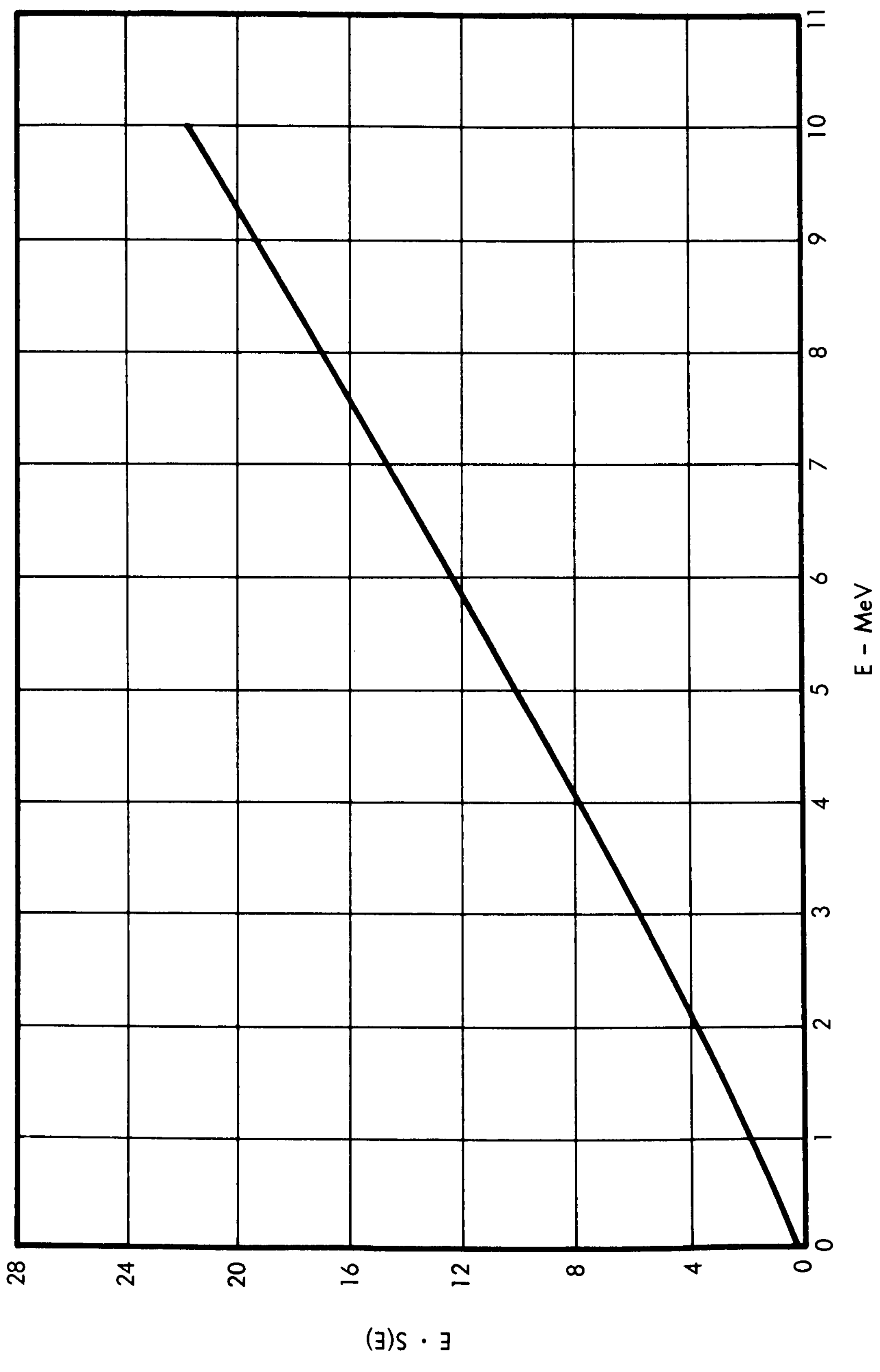

FIGURE 4-1 ENERGY TIMES ELECTRON STOPPING POWER FOR WATER VERSUS ENERGY

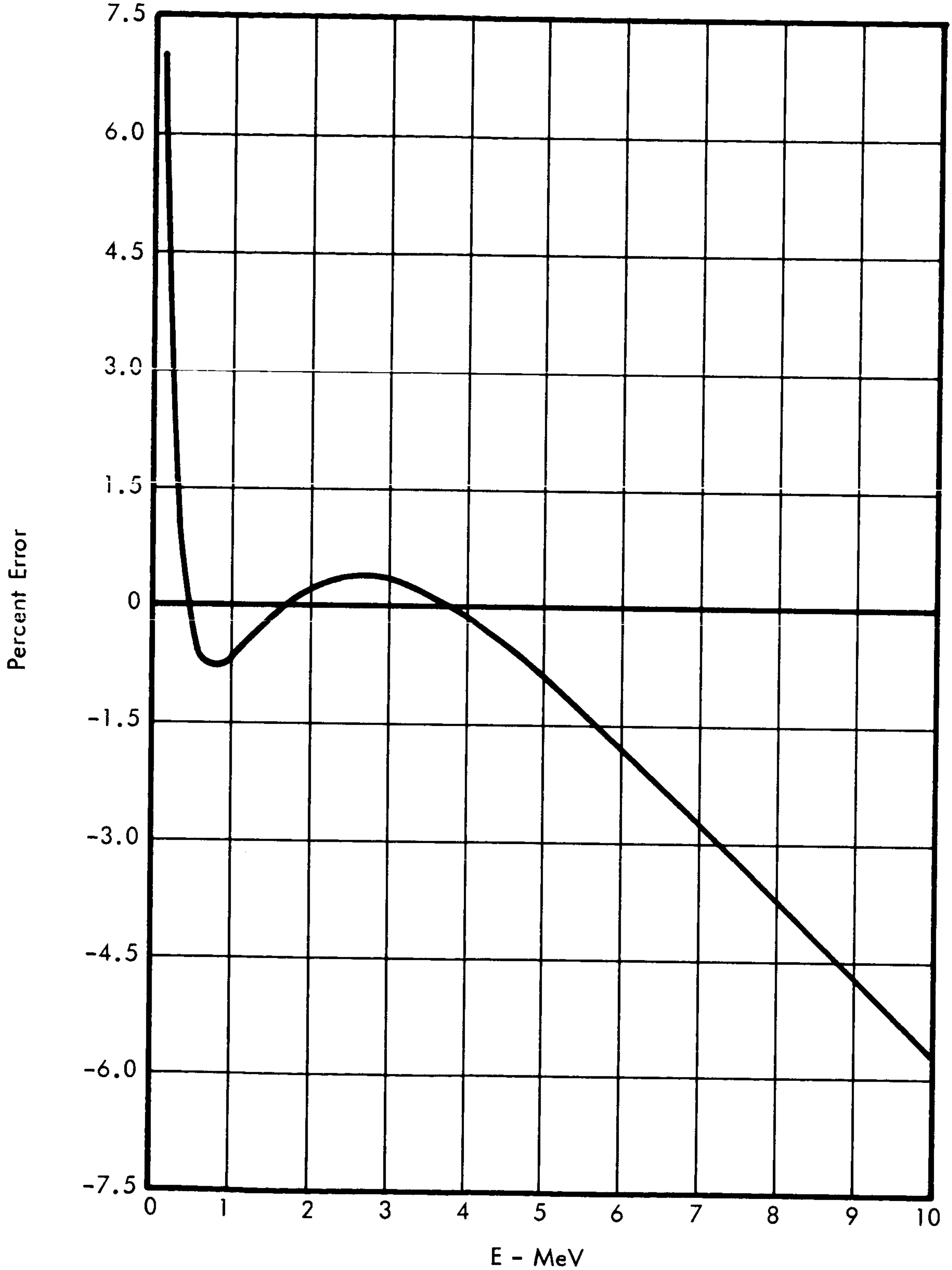

FIGURE 4-2 PERCENT ERROR IN ELECTRON RANGE FUNCTION FOR ALUMINUM

$$C_o E^{\beta}(E_u - E)^{\alpha} .$$

The upper energy limit, E_u, of the transmitted spectrum is defined by:

$$E_u = (2R^{-1}\left[R(E^*) - X\right] + E^*)/3; \qquad (4\text{-}28)$$

where

$R^{-1}(y)$ is the inverse range function.

The parameters α and β are determined by two conditions: the maximum value of the distribution occurs at the energy E_p, and the half-maximum value occurs at the energy $E_p - W$. These conditions lead to the relations:

$$\beta = -\ln(2)/\left[\ln\left(\frac{E_p - W}{E_p}\right) + \frac{E_u - E_p}{E_p} \cdot \ln\left(\frac{E_u - E_p + W}{E_u - E_p}\right)\right] \qquad (4\text{-}29)$$

and

$$\alpha = \frac{\beta(E_u - E_p)}{E_p} . \qquad (4\text{-}30)$$

E_p is obtained from the empirical formula,

$$E_p = (1 - g)^g \cdot (.99 + \frac{g}{10}) \cdot E_u ; \qquad (4\text{-}31)$$

and W is obtained from the empirical formula,

$$W = g^h \cdot E_p ; \qquad (4\text{-}32)$$

where

h = Min (1.85, 1.3 + 5.5g), and

g = X/R(E*).

Because the transmitted spectrum, $C_o E^{\beta} (E_u - E)^{\alpha}$, pertains to unit transmitted electron flux; then,

$$C_o \int_0^{E_u} E^{\beta} (E_u - E)^{\alpha} \, dE = 1, \qquad (4\text{-}33)$$

from which C_o may be determined.

Substituting Equation 4-26 and the value of C_o into Equation 4-24, the expression for the electron dose becomes:

$$D = K \sum_i \Omega_i \int_0^{\infty} \Phi(E^*) \cdot T(E^*, X) \cdot \left[\frac{A \cdot (\beta + 1) E_u}{\alpha + \beta + 2} + B + \frac{C \cdot (\alpha + \beta + 1)}{\beta \cdot E_u} \right] \cdot dE^*. \qquad (4\text{-}34)$$

Note that α, β, and E_u are functions of E^* and X. The Dose program evaluates Equation 4-34 for each detector.

The electron number transmission, $T(E^*, X)$, is compared with the Monte Carlo data of Berger and Seltzer. The comparison with sapphire (Al_2O_3)[11] is shown in Table 4-3; the comparison with aluminum[12] is shown in Table 4-4. The maximum difference is less than 10 percent. Thick shield data and data for materials other than aluminum and sapphire are not available for comparison. The calculated electron transmission spectrum, $C_o E^{\beta} (E_u - E)^{\alpha}$, is compared with the Monte Carlo results of Berger and Seltzer for aluminum[12] and sapphire[11] in Figures 4-3 through 4-8. Whereas Figures 4-3 through 4-8 exhibit the transmission of monoenergetic electron beams, Figure 4-9 illustrates the calculated transmission of a continuous electron spectrum through several thicknesses of aluminum.

TABLE 4-3 ELECTRON NUMBER TRANSMISSION - SAPPHIRE[11]

Energy MeV	0.1 gm/cm^2			0.2 gm/cm^2			0.3 gm/cm^2		
	LETS*	MC**	DIFF	LETS	MC	DIFF	LETS	MC	DIFF
1.	.991	.970	.021	.852	.776	.076	.433	.431	.002
2.	1.	.998	.002	.994	.987	.007	.970	.949	.021
2.954	1.	.999	.001	.999	.998	.001	.995	.992	.003
4.	1.	1.	.000	1.	.999	.001	.999	.998	.001
5.907	1.	1.	.000	1.	.999	.001	1.	.999	.001
8.	1.	1.	.000	1.	1.	.000	1.	1.	.000

*Present calculation

**Monte Carlo calculation of Berger and Seltzer

TABLE 4-4 ELECTRON NUMBER TRANSMISSION - ALUMINUM ONE MeV[12]

Thickness gm/cm^2	LETS	MC	DIFF
.055	.9975	.9877	.0098
.110	.9704	.9276	.0428
.165	.8790	.8134	.0656
.220	.6961	.6635	.0326

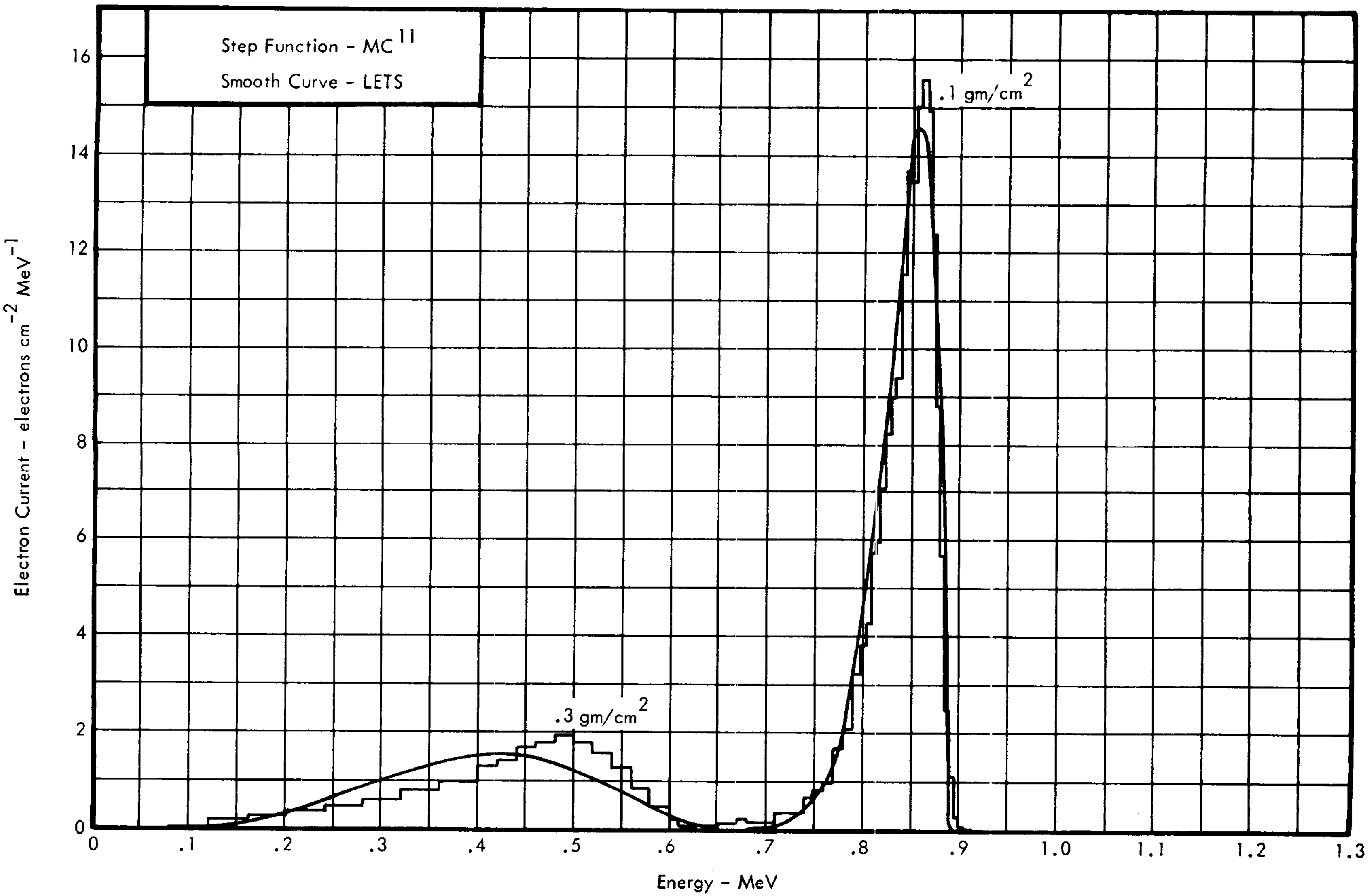

FIGURE 4-3 COMPARISON OF ELECTRON ENERGY SPECTRA THROUGH SAPPHIRE (Al_2O_3) — 1 MeV

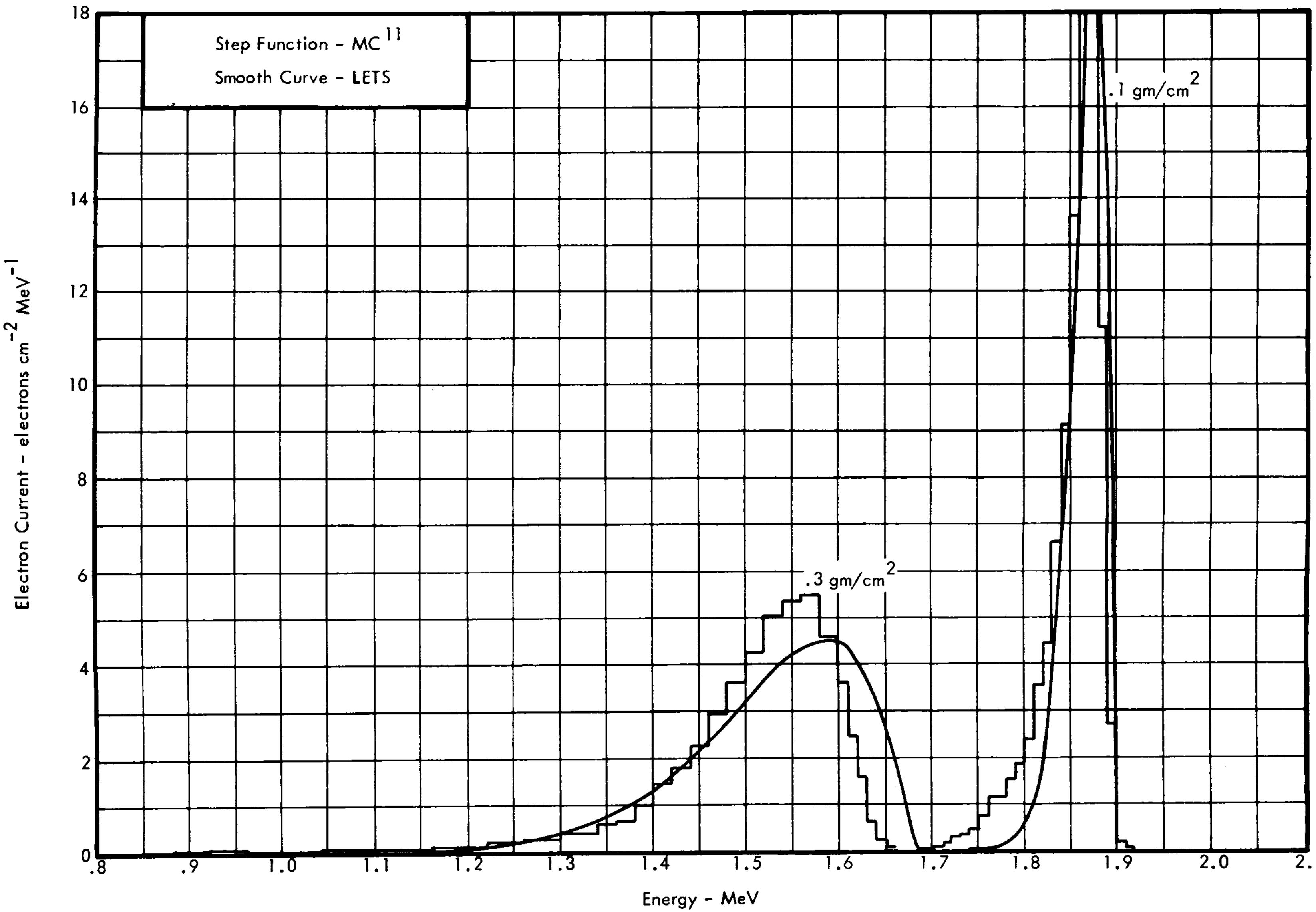

FIGURE 4-4 COMPARISON OF ELECTRON ENERGY SPECTRA THROUGH SAPPHIRE (Al_2O_3) — 2 MeV

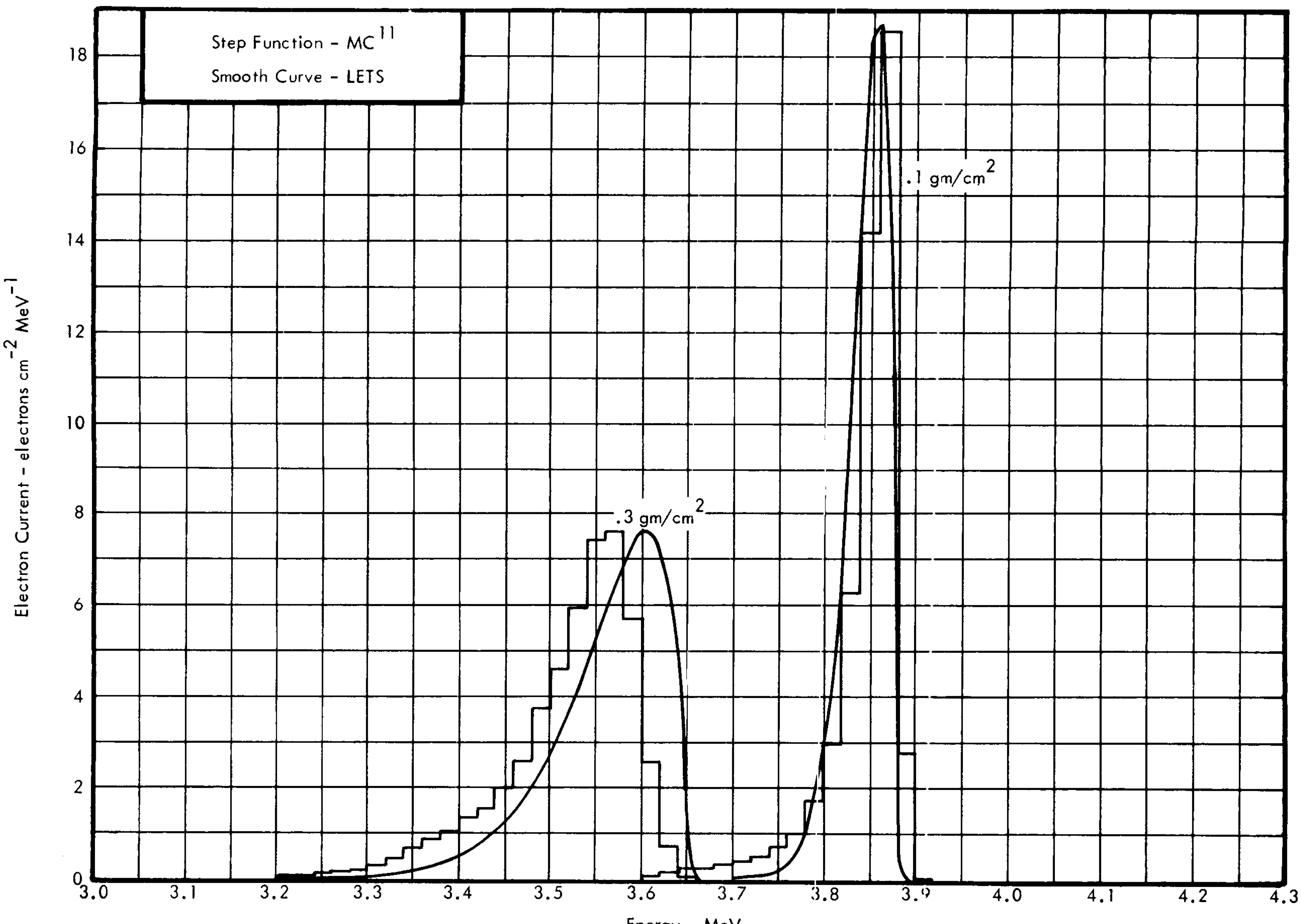

FIGURE 4-5 COMPARISON OF ELECTRON ENERGY SPECTRA THROUGH SAPPHIRE (Al_2O_3) — 4 MeV

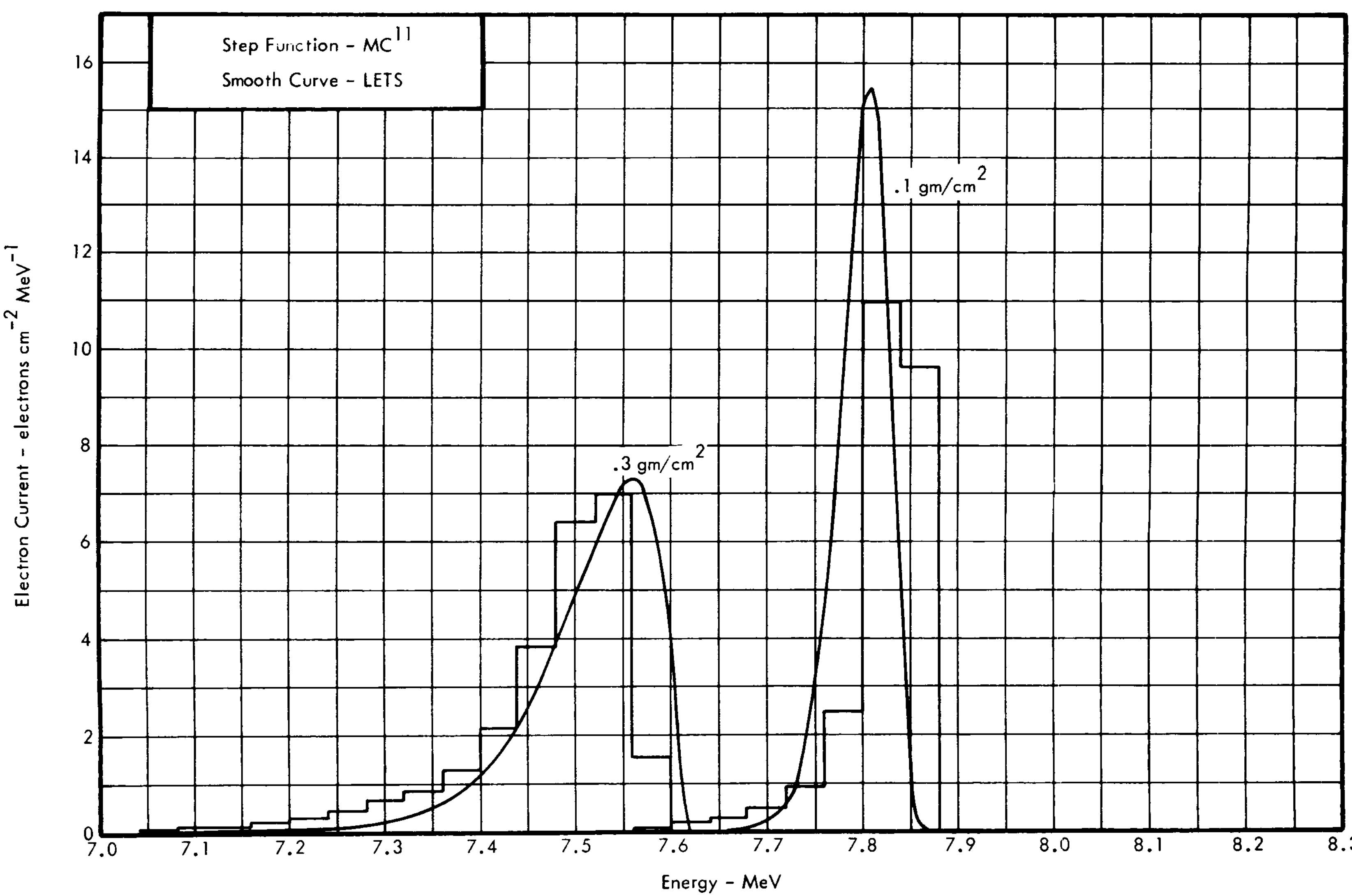

FIGURE 4-6 COMPARISON OF ELECTRON ENERGY SPECTRA THROUGH SAPPHIRE (Al_2O_3) – 8 MeV

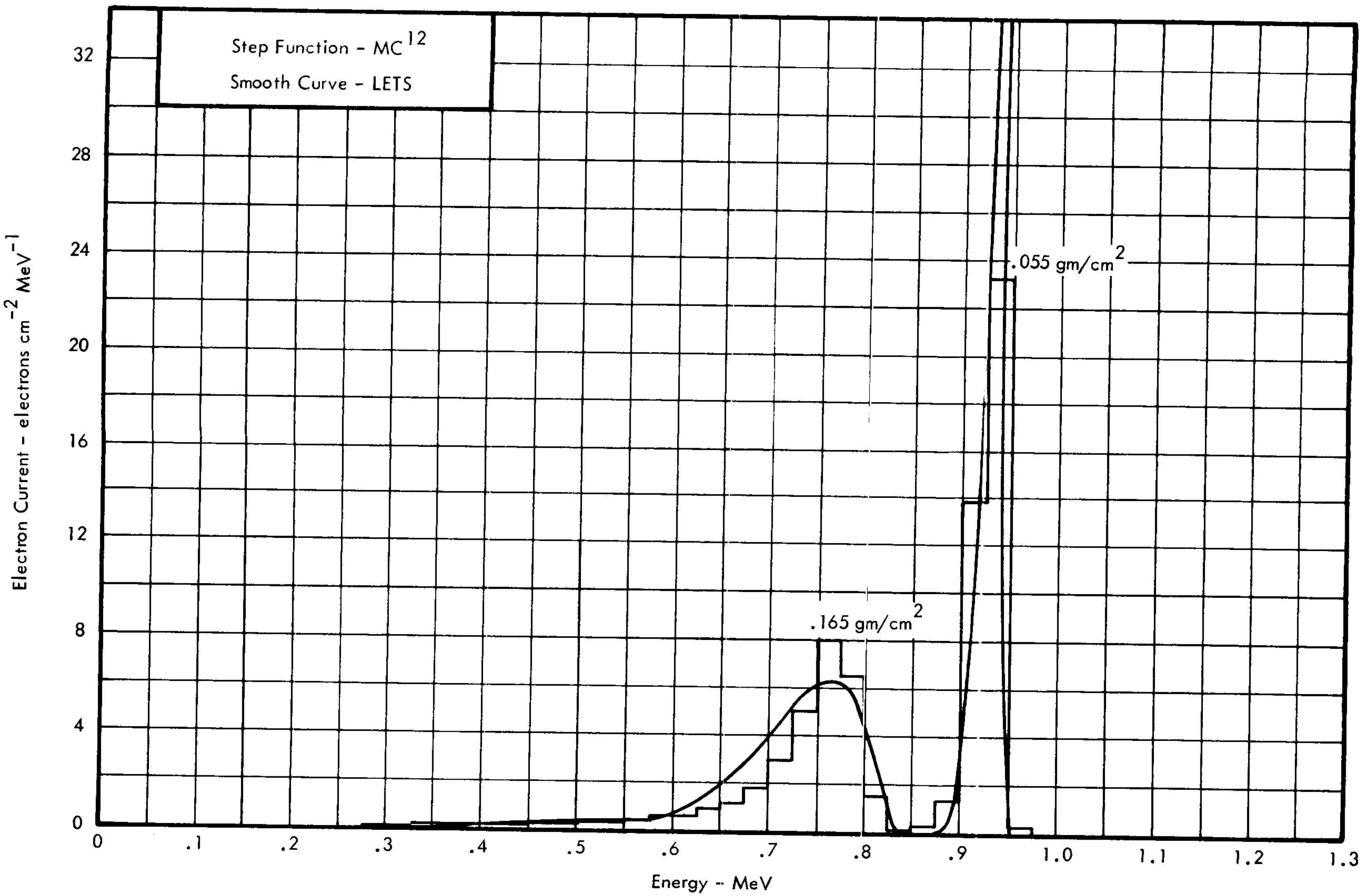

FIGURE 4-7 COMPARISON OF ELECTRON ENERGY SPECTRA THROJGH ALUMINUM - 1 MeV

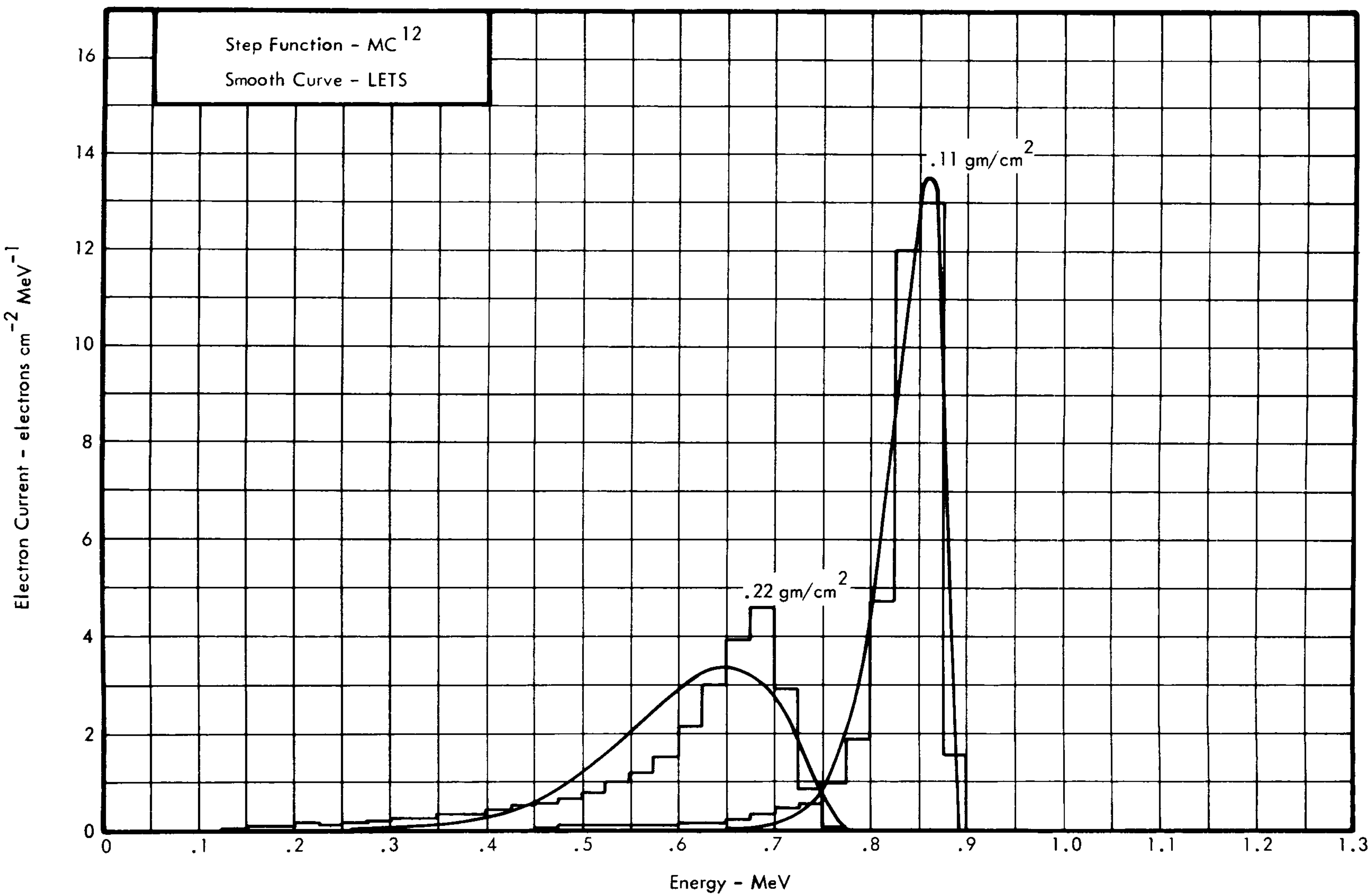

FIGURE 4-8 COMPARISON OF ELECTRON ENERGY SPECTRA THROUGH ALUMINUM - 1 MeV

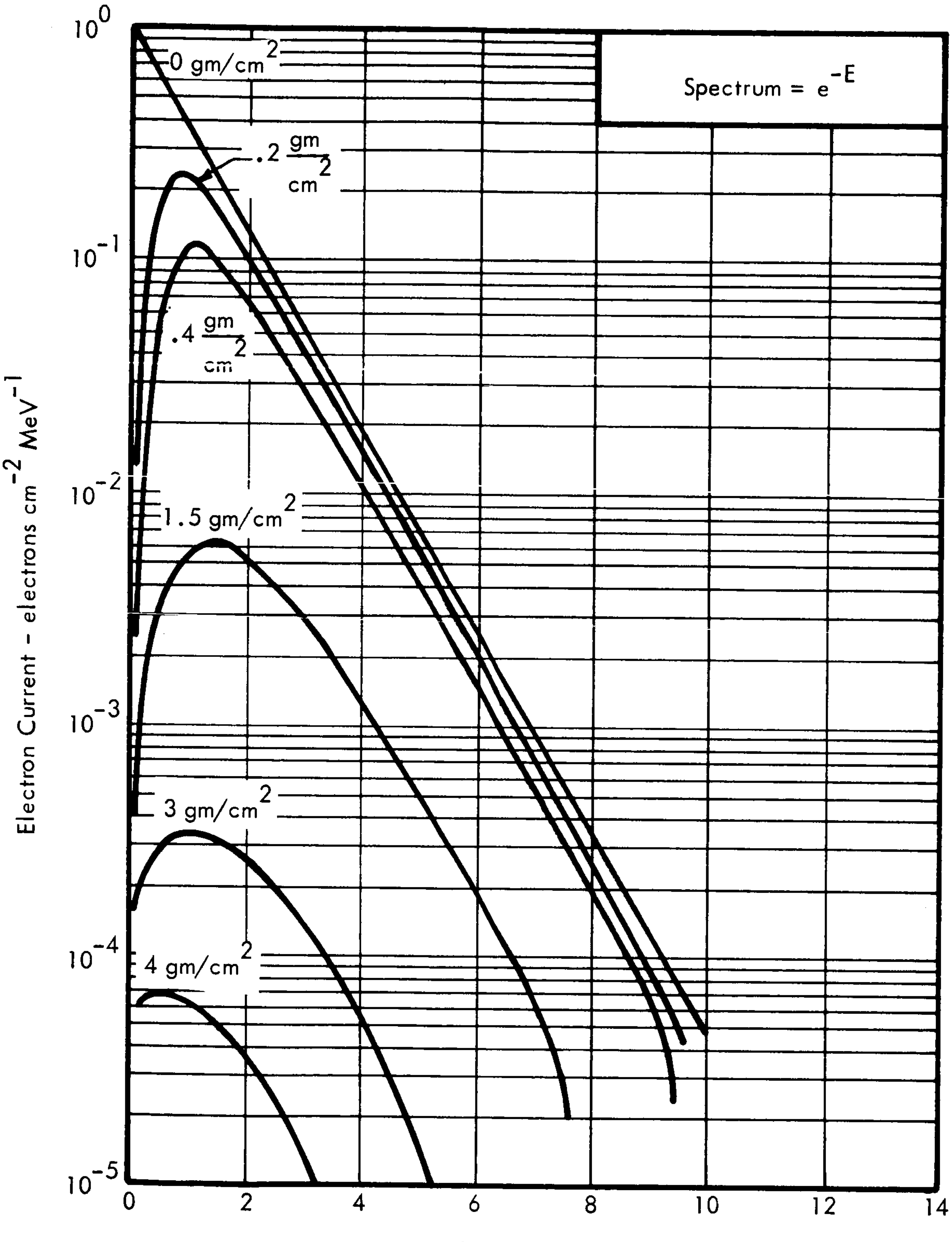

FIGURE 4-9 ELECTRON SPECTRA THROUGH ALUMINUM SHIELD

4.3 SPECIAL FEATURES

The Dose code treats an unrestricted number of detectors. The only limitation is imposed by the number of detector positions prepared by the Geometry code which also treats an unrestricted number of detectors. The Dose code may be instructed to ignore some of the detectors on the geometry tape and to rewind the geometry tape in order to process the detectors again, possibly with a different input spectrum.

The detector dose calculations are performed vector by vector; therefore, the dose may be tallied into solid angle regions specified by the user. The solid angle regions may be discrete, nested, or partially overlapped. This feature permits the user to check the relative importance of shield sections and determine the effect of streaming.

The Dose code is designed to facilitate parametric studies. Material densities may be changed, even zeroed, with the "FF" values. This procedure effectively changes material penetration thicknesses. The range parameters associated with material numbers may be altered. These two features permit changes in shield materials and thicknesses without preparing a new geometry tape. In this context, the term "shield" refers to any set of volume elements in the configuration. These features, in conjunction with the capability of changing the input spectrum and rewinding the geometry tape, permit extensive parametric investigations with one access to the computer.

4.4 DOSE PROGRAM DATA INPUT PREPARATION

In the following, the column headed "FORMAT" gives the DIP format control under which this data is to be read, the column headed "NAME" gives the name of the data array, the column headed "DIMENSION" indicates the number of words available in fast storage for the named array, and the column headed "DEFINITION" is an attempt to describe the named data array.

The NAME card for the following data set must be:

N31, PHI, E, MAT, SA, SB, R1, HEAD, NPHI, NM, N2, ND, BIN, FDC, UNITS, FF, AT, EE, NE, FI, CA, CB, Z, AW, CC, NDM, AA, AB, AR1, EA, PHA, NPHA.

(See the description of the DIP program - Appendix A.1, Volume II)

FORMAT	NAME	DIMENSION	DEFINITION
3	PHI	(100)	Free field proton flux (P/cm^2-MeV-ster.)
3	E	(100)	Energies (MeV) associated with the tabulated proton flux (PHI).

NOTE: PHI and E must be tabulated in order of increasing energy.

FORMAT	NAME	DIMENSION	DEFINITION
4	MAT	(100)	Material numbers (an identification number); these numbers MUST match the material numbers (MVX) in the Geometry program. This list should contain a material number only once for each shield material number regardless of the number of times the material number appears in the geometric configuration. The list should also include the material number of each detector; however, if more than one detector is of the same material, the number need only be entered once. Detector material numbers MUST be last in the list.
3	SA	(100)	Parameters associated with the proton range
3	SB	(100)	equation: $R(E) = \frac{a}{2b} \ln (1 + 2b E^r)$, SA = a,

FORMAT	NAME	DIMENSION	DEFINITION
			(Continued)
3	R1	(100)	SB = b, and R1 = r. Table A5, Appendix A, Volume I. The number of each of the parameters must equal the number of MAT's and must be ordered to correspond to the materials in the MAT list. All the R1's must be equal, except those that pertain to detector materials.
5	HEAD	(20)	Any set of alphanumeric and special character information to identify the particular case at hand.
4	NPHI	(1)	The number of entries in the PHI-table (proton flux).
4	NM	(1)	The number of entries in the MAT-table.
4	N2	(1)	The logical number of the tape unit upon which the geometry tape is to be mounted.
4	ND	(1)	The number of detectors associated with this particular geometry tape. (If ND is zero, the program ends immediately with a memory dump; if ND is negative, the program ends with no dump. One of these methods should be used to cease the calculations.)

FORMAT	NAME	DIMENSION	DEFINITION
5	BIN	(1)	Hollerith information indicating the storage location of the geometry tape.
3	FDC	(1)	Energy deposition-to-dose conversion factor.
5	UNITS	(3)	Hollerith information consistent with FDC. (Usually RAD/HR or RAD).
3	FF	(100)	A factor, associated with each material, for adjusting the density (or thickness-gm/cm^2) of the material. The FF's must be in the same "order" as the MAT's. A value of unity preserves the penetration thicknesses computed by the Geometry program.
3	AT	(100)	A factor for adjusting buildup; this value should approximate the atomic mass number of the volume element with which it is associated. AT should equal zero if buildup is not needed. The AT's must be in the same "order" as the MAT's. (See Equation 5-2)
3	EE	(100)	Energies (MeV) associated with the tabulated electron flux (FI).
4	NE	(1)	The number of entries in the FI-table.
3	FI	(100)	Free field electron flux (e/cm^2-MeV-ster.).

FORMAT	NAME	DIMENSION	DEFINITION
3	CA	(10)	Coefficients associated with the electron stopping power equation: $S(E) = A \cdot E + B + C/E$. CA = A, CB = B, and CC = C. (See Equation 4-26, Section 4.2). These coefficients apply to the detector material.
3	CB	(10)	
3	CC	(10)	
3	Z	(100)	The "Z numbers" of the materials in the materials list (MAT). These numbers MUST be in the same order as the materials in the list (MAT).
3	AW	(100)	The "atomic weight" of the materials in the materials list (MAT). These numbers MUST be in the same order as the materials in the list (MAT).
4	NDM	(1)	The number of detector materials.
3	AA	(100)	Parameters associated with the alpha range equation: $R(E) = \frac{a}{2b} \ln(1 + 2b E^r)$; AA = a; AB = b; and AR1 = r. Table A6, Appendix A, Volume I. The number of each of the parameters must be equal to the number of MAT's and must be ordered to correspond to the materials in the MAT list. All the AR1's must be equal, except those that pertain to detector materials.
3	AB	(100)	
3	AR1	(100)	

FORMAT	NAME	DIMENSION	DEFINITION
3	EA	(100)	Energies (MeV) associated with the tabulated alpha flux (PHA).
3	PHA	(100)	Free field alpha flux (A/cm^2-MeV-ster.).
4	NPHA	(1)	The number of entries in the PHA-table.

Control must be returned to the program after the above data are read.

The following data are input in a do-loop over the number of detectors, ND. The NAME card associated with this data set is:

N4, NAR, POLA, AZIM, NSKIP

FORMAT	NAME	DIMENSION	DEFINITION
4	NAR	(1)	Number of angular regions. This indicates the number of partial solid angle regions into which the dose is to be tallied for the detector of current interest. If the sum of the mutually exclusive partial solid angular regions is less than 4π, the dose in the remaining solid angle is also tallied. The total dose at the detector is calculated whether NAR is zero or not. NAR must not be greater than 150.
3	POLA	(300)	The polar angle limits of the angular region - two polar angles per region.

FORMAT	NAME	DIMENSION	DEFINITION
3	AZIM	(300)	The azimuthal angle limits of the angular region - two azimuthal angles per region.

NOTE: All angles are in degrees and are positive; the lower limit must be the first of the pair. The polar angles must lie between 0° (positive z-axis of configuration) and 180° (negative z-axis of configuration) inclusive. The polar angle lower limit must be less than the upper limit. The azimuthal angles are measured counter clock-wise from the configuration positive x-axis. The azimuthal angles must lie between 0° and 360° inclusive. The azimuthal angle lower limit need not be less than the upper limit. For example, the data card to define two angular regions - (1), the first octant, and (2), a special region defined by the polar angles 20° to 160°, and the azimuthal angles - 45° to 45°, will have the following format:

4NAR, 2, $3POLA, 0, 90, 20, 160, AZIM, 0, 90, 315, 45

FORMAT	NAME	DIMENSION	DEFINITION
4	NSKIP	(1)	If this value is greater than zero, the current detector is processed; if this value is less than or equal to zero the current detector is skipped.

Control must be returned to the program for each detector. After ND detectors are processed and/or skipped, control returns to the first calling sequence which expects a new NAME card and case data.

See sample input data listing in Appendix H.

4.5 DOSE PROGRAM OUTPUT

A sample Dose program output is presented in Appendix H. On the first page of output, much of the input data is listed. First is a list of the shield materials, by material number (MAT), and their associated parameters: SA, SB, R1, AA, AB, AR1, FF, AT, Z, and AW (See Section 4.4 for explanations of all input parameters). Next, a list of detector materials, by material number (MAT), and their associated parameters, SA, SB, R1, AA, AB, AR1, CA, CB, and CC are presented. Following the detector materials list is the geometry tape storage location (BIN) and the energy deposition-to-flux conversion factor (FDC). The units of FDC in this example are rad-gm/MeV-ster because the units of flux are particles/MeV-cm^2-mission for all spectra. Next, the alpha, proton, and electron spectra are displayed. For each spectrum, the energy and particle flux, differential in energy, is listed: alpha (EA(I) and PHA(I)), proton (E(I) and PHI(I)), and electron (EE(I) and FI(I)). Associated with the alpha and proton spectra are the respective power law parameters H_i and Q_i for the expression $H_i E^{-Q_i}$.

The results of the dose calculations are printed on a separate page for each detector considered. The heading information from the input data HEAD is printed at the top of the page. Below the heading is detector data from the geometry tape; this includes DHED (information input to the Geometry program), the detector coordinates (XD, YD, and ZD), and the detector material number. Next, the detector identification number and dose units are displayed. The remainder of the page contains the total proton dose, the total alpha dose, the total electron dose, and the total bremsstrahlung dose (at present, there is no bremsstrahlung calculation); also the doses, and their associated "weight fractions", are exhibited for each angular region and the region (REMAINDER) not contained in any angular region. A "weight fraction" is defined by:

$$\text{weight fraction} = \frac{\Delta D/D}{\Delta\Omega/4\pi}$$

where

ΔD = the partial dose for the radiation type in the angular region,

D = total dose for the radiation type, and

$\Delta\Omega$ = solid angle subtended by the angular region.

APPENDIX A

Compilation Of PCA Events During The Nineteenth Solar Activity Cycle

TABLE A1 COMPILATION OF SOLAR FLUX EVENTS[8,28]
1954 - 1963

Date Of Event	Protons/cm^2 > 30 MeV	Duration Of PCA (Days)	Date Of Event	Protons/cm^2 > 30 MeV	Duration Of PCA (Days)
1/17/55		2	9/2/57	5 + 7	1 1/2
2/23/56	1 + 9*	3	9/12/57	6 + 6	1 1/2
3/11 56		4	9/21/57	1.15 + 8	2
4/27/56		2	9/26/57		1
8/31/56	2.5 + 7	2 1/2	10/20/57	5 + 7	1
11/13/56	1 + 8	2	11/4/57	9 + 6	
1/20/57	2 + 8	2 1/2	12/17/57		
2/21/57			2/9/58	1 + 7	1
4/3/57	5 + 7	2 1/2	3/14/58		
4/6/57			3/23/58	2.5 + 8	1 1/2
4/11/57			3/25/58	6 + 8	4 1/2
5/19/57		1/2	3/30/58		
6/19/57			4/10/58	5 + 7	2
6/21/57	1.5 + 8	3	6/6/58		
7/3/57	2 + 7	2	7/7/58	2.5 + 8	4
7/24/57	7.5 + 6	1/2	7/29/58	8.5 + 6	1
8/9/57	1.5 + 6	1	8/16/58	4 + 7	2 1/2
8/29/57		1/2	8/22/58	7 + 7	3 1/2
8/29/57	1.5 + 8	2	8/26/58	1.1 + 8	3
8/31/57	8 + 7	2	9/22/58	8.5 + 7	3 1/2

*The Sign And Digit Following Each Number Represent The Power Of Ten Multiplying That Number.

TABLE A1 COMPILATION OF SOLAR FLUX EVENTS[8,28]
1954 – 1963 (Continued)

Date Of Event	Protons/cm^2 > 30 MeV	Duration Of PCA (Days)
1/26/59		
2/12/59		
5/10/59	9.6 + 8	7
6/13/59	8.5 + 7	> 2
7/10/59	1 + 9	4
7/14/59	1.3 + 9	3
7/17/59	9.1 + 8	7
8/18/59	1.8 + 6	
9/2/59	1.15 + 7	2
10/6/59		
1/11/60	6 + 6	4
3/29/60	6 + 6	1
3/30/60	6 + 6	1
4/1/60	5 + 6	2
4/5/60	1.1 + 6	4
4/28/60	2.5 + 7	1
4/29/60	1.75 + 8	5
5/4/60	6 + 6	2
5/6/60	4 + 6	2
5/13/60	5 + 7	2

Date Of Event	Protons/cm^2 > 30 MeV	Duration Of PCA (Days)
9/3/60	3.5 + 7	14
11/12/60	1.3 + 9	2
11/15/60	7.2 + 8	4
11/20/60	4.5 + 7	15
7/11/61	3 + 6	
7/12/61	4 + 7	1
7/13/61		2 1/2
7/15/61	1.25 + 7	3
7/18/61	3 + 8	2 1/2
7/20/61	5 + 6	
7/28/61	4.4 + 6	
9/8/61	3 + 6	
9/10/61	3.75 + 7	
9/28/61	6 + 6	
11/10/61		
2/4/62		1
10/23/62	1.2 + 5	
4/15/63		
9/21/63		
9/26/63		

APPENDIX B

Compilation Of Small Solar Flux Events During 1960, Unaccompanied By PCA

PRECEDING PAGE BLANK NOT FILMED.

TABLE B1 COMPILATION OF SMALL SOLAR FLUX EVENTS[21] DURING 1960, UNACCOMPANIED BY PCA

Date Of Event
1/15/60
2/7/60
2/15/60
2/29/60
3/10/60
3/17/60
4/15/60
5/9/60
5/17/60
5/26/60
6/1/60
6/15/60
6/25/60

Date Of Event
6/27/60
6/28/60
8/11/60
8/26/60
9/25/60
10/3/60
10/29/60
11/10/60
11/11/60
11/14/60
11/19/60
12/5/60

APPENDIX C

Julian Day Number, 1950 - 2000 A.D.

TABLE C1

JULIAN DAY NUMBER

DAYS ELAPSED AT GREENWICH NOON, A. D. 1950–2000

Year	Jan. 0	Feb. 0	Mar. 0	Apr. 0	May 0	June 0	July 0	Aug. 0	Sept. 0	Oct. 0	Nov. 0	Dec. 0
1950	243 3282	3313	3341	3372	3402	3433	3463	3494	3525	3555	3586	3616
1951	3647	3678	3706	3737	3767	3798	3828	3859	3890	3920	3951	3981
1952	4012	4043	4072	4103	4133	4164	4194	4225	4256	4286	4317	4347
1953	4378	4409	4437	4468	4498	4529	4559	4590	4621	4651	4682	4712
1954	4743	4774	4802	4833	4863	4894	4924	4955	4986	5016	5047	5077
1955	243 5108	5139	5167	5198	5228	5259	5289	5320	5351	5381	5412	5442
1956	5473	5504	5533	5564	5594	5625	5655	5686	5717	5747	5778	5808
1957	5839	5870	5898	5929	5959	5990	6020	6051	6082	6112	6143	6173
1958	6204	6235	6263	6294	6324	6355	6385	6416	6447	6477	6508	6538
1959	6569	6600	6628	6659	6689	6720	6750	6781	6812	6842	6873	6903
1960	243 6934	6965	6994	7025	7055	7086	7116	7147	7178	7208	7239	7269
1961	7300	7331	7359	7390	7420	7451	7481	7512	7543	7573	7604	7634
1962	7665	7696	7724	7755	7785	7816	7846	7877	7908	7938	7969	7999
1963	8030	8061	8089	8120	8150	8181	8211	8242	8273	8303	8334	8364
1964	8395	8426	8455	8486	8516	8547	8577	8608	8639	8669	8700	8730
1965	243 8761	8792	8820	8851	8881	8912	8942	8973	9004	9034	9065	9095
1966	9126	9157	9185	9216	9246	9277	9307	9338	9369	9399	9430	9460
1967	9491	9522	9550	9581	9611	9642	9672	9703	9734	9764	9795	9825
1968	9856	9887	9916	9947	9977	*0008	*0038	*0069	*0100	*0130	*0161	*0191
1969	244 0222	0253	0281	0312	0342	0373	0403	0434	0465	0495	0526	0556
1970	244 0587	0618	0646	0677	0707	0738	0768	0799	0830	0860	0891	0921
1971	0952	0983	1011	1042	1072	1103	1133	1164	1195	1225	1256	1286
1972	1317	1348	1377	1408	1438	1469	1499	1530	1561	1591	1622	1652
1973	1683	1714	1742	1773	1803	1834	1864	1895	1926	1956	1987	2017
1974	2048	2079	2107	2138	2168	2199	2229	2260	2291	2321	2352	2382
1975	244 2413	2444	2472	2503	2533	2564	2594	2625	2656	2686	2717	2747
1976	2778	2809	2838	2869	2899	2930	2960	2991	3022	3052	3083	3113
1977	3144	3175	3203	3234	3264	3295	3325	3356	3387	3417	3448	3478
1978	3509	3540	3568	3599	3629	3660	3690	3721	3752	3782	3813	3843
1979	3874	3905	3933	3964	3994	4025	4055	4086	4117	4147	4178	4208
1980	244 4239	4270	4299	4330	4360	4391	4421	4452	4483	4513	4544	4574
1981	4605	4636	4664	4695	4725	4756	4786	4817	4848	4878	4909	4939
1982	4970	5001	5029	5060	5090	5121	5151	5182	5213	5243	5274	5304
1983	5335	5366	5394	5425	5455	5486	5516	5547	5578	5608	5639	5669
1984	5700	5731	5760	5791	5821	5852	5882	5913	5944	5974	6005	6035
1985	244 6066	6097	6125	6156	6186	6217	6247	6278	6309	6339	6370	6400
1986	6431	6462	6490	6521	6551	6582	6612	6643	6674	6704	6735	6765
1987	6796	6827	6855	6886	6916	6947	6977	7008	7039	7069	7100	7130
1988	7161	7192	7221	7252	7282	7313	7343	7374	7405	7435	7466	7496
1989	7527	7558	7586	7617	7647	7678	7708	7739	7770	7800	7831	7861
1990	244 7892	7923	7951	7982	8012	8043	8073	8104	8135	8165	8196	8226
1991	8257	8288	8316	8347	8377	8408	8438	8469	8500	8530	8561	8591
1992	8622	8653	8682	8713	8743	8774	8804	8835	8866	8896	8927	8957
1993	8988	9019	9047	9078	9108	9139	9169	9200	9231	9261	9292	9322
1994	9353	9384	9412	9443	9473	9504	9534	9565	9596	9626	9657	9687
1995	244 9718	9749	9777	9808	9838	9869	9899	9930	9961	9991	*0022	*0052
1996	245 0083	0114	0143	0174	0204	0235	0265	0296	0327	0357	0388	0418
1997	0449	0480	0508	0539	0569	0600	0630	0661	0692	0722	0753	0783
1998	0814	0845	0873	0904	0934	0965	0995	1026	1057	1087	1118	1148
1999	1179	1210	1238	1269	1299	1330	1360	1391	1422	1452	1483	1513
2000	245 1544	1575	1604	1635	1665	1696	1726	1757	1788	1818	1849	1879

APPENDIX D

The proton, alpha, and electron spectra for the missions described in Section 2.0 are tabulated in this appendix.

For the Mars and Lunar missions, the units are particles per square centimeter-MeV-mission. The heading above each spectrum indicates the probability, in percent, of encountering a flux larger than that shown, arising from solar flux events.

For the Earth orbit missions, the units are particles per square centimeter-MeV-day. The proton data are derived from the Vette integral flux orbital integrations[37] of proton map AP3. The electron data are derived from the Vette integral flux orbital integrations[37] of the projected 1968 electron environment.

TABLE D1 MARS MISSION SPECTRA

October 9, 1977

E(MeV)	Proton				Alpha			
	0.1%	1.0%	10.0%	50.0%	0.1%	1.0%	10.0%	50.0%
10	2.53 + 11*	8.28 + 10	3.10 + 9	1.72 + 8	5.02 + 11	5.01 + 10	2.89 + 9	1.26 + 8
30	2.18 + 10	5.49 + 9	6.44 + 8	2.12 + 7	2.49 + 10	4.98 + 9	3.89 + 8	1.43 + 7
50	6.46 + 9	1.34 + 9	1.77 + 8	6.45 + 6	4.77 + 9	1.12 + 9	9.68 + 7	3.54 + 6
100	1.23 + 9	2.09 + 8	2.21 + 7	8.64 + 5	3.83 + 8	1.13 + 8	1.12 + 7	4.49 + 5
200	2.07 + 8	2.97 + 7	1.99 + 6	7.54 + 4	2.74 + 7	8.46 + 6	7.64 + 5	3.06 + 4
400	3.74 + 7	3.18 + 6	1.10 + 5	4.32 + 3	1.84 + 6	4.56 + 5	4.13 + 4	1.31 + 3
1000	1.38 + 6	5.80 + 4	1.74 + 3	2.95 + 1	4.67 + 4	7.35 + 3	2.96 + 2	8.29 + 0
1500	1.72 + 5	4.35 + 3	8.77 + 1	1.31 + 0	9.85 + 3	7.62 + 2	1.90 + 1	5.75 - 1

*The Sign And Digit(s) Following Each Number Represent The Power Of Ten Multiplying That Number.

TABLE D1 MARS MISSION SPECTRA
(Continued)
December 28, 1981

E(MeV)	Proton				Alpha			
	0.1%	1.0%	10.0%	50.0%	0.1%	1.0%	10.0%	50.0%
10	1.78 + 11	7.46 + 10	9.44 + 9	1.10 + 9	4.26 + 11	7.19 + 10	9.00 + 9	5.67 + 8
30	1.79 + 10	5.24 + 9	1.34 + 9	8.45 + 7	1.95 + 10	6.05 + 9	8.93 + 8	5.84 + 7
50	6.15 + 9	1.44 + 9	3.63 + 8	2.05 + 7	3.62 + 9	1.41 + 9	2.21 + 8	1.40 + 7
100	1.48 + 9	2.59 + 8	4.38 + 7	2.97 + 6	3.28 + 8	1.38 + 8	2.31 + 7	1.50 + 6
200	3.12 + 8	3.92 + 7	4.35 + 6	3.55 + 5	2.61 + 7	1.03 + 7	1.84 + 6	1.12 + 5
400	5.68 + 7	7.71 + 6	2.46 + 5	1.88 + 4	1.95 + 6	6.21 + 5	8.11 + 4	4.47 + 3
1000	4.28 + 6	4.31 + 4	3.05 + 3	7.87 + 1	6.07 + 4	1.26 + 4	6.67 + 2	3.75 + 1
1500	6.08 + 5	3.66 + 3	2.53 + 2	4.39 + 0	1.27 + 4	2.18 + 3	5.49 + 1	2.45 + 0

TABLE D1 MARS MISSION SPECTRA
(Continued)
April 16, 1986**

E(MeV)	Proton				Alpha			
	0.1%	1.0%	10.0%	50.0%	0.1%	1.0%	10.0%	50.0%
10	3.40 + 10	4.22 + 9	5.39 + 7	1.24 + 6	9.60 + 10	2.73 + 9	2.76 + 7	6.17 + 5
30	3.19 + 9	3.87 + 8	8.25 + 6	1.22 + 5	1.66 + 10	4.35 + 8	5.11 + 6	9.87 + 4
50	9.88 + 8	1.08 + 8	2.65 + 6	3.84 + 4	4.97 + 9	1.16 + 8	1.36 + 6	2.82 + 4
100	2.09 + 8	2.11 + 7	3.50 + 5	5.90 + 3	5.90 + 8	1.31 + 7	1.56 + 5	3.03 + 3
200	2.69 + 7	2.29 + 6	2.34 + 4	5.06 + 2	3.50 + 7	7.55 + 5	1.06 + 4	1.82 + 2
400	2.40 + 6	1.35 + 5	8.58 + 2	1.25 + 1	1.12 + 6	2.59 + 4	4.95 + 2	6.33 + 0
1000	2.61 + 4	7.23 + 2	6.56 + 0	3.63 - 2	9.38 + 3	1.75 + 2	3.70 + 0	4.43 - 2
1500	1.55 + 3	4.02 + 1	2.89 - 1	2.88 - 3	5.54 + 2	1.71 + 1	1.85 - 1	4.28 - 3

**19.6 Percent Of Missions Encountered No Flux Events

TABLE D2 LUNAR MISSION SPECTRA

June 1, 1969*

E(MeV)	Proton				Alpha			
	0.1%	1.0%	10.0%	50.0%	0.1%	1.0%	10.0%	50.0%
10	6.64 + 10	7.50 + 9	8.38 + 7	1.20 + 6	5.34 + 10	3.58 + 9	7.12 + 7	7.66 + 5
30	6.73 + 9	5.67 + 8	9.06 + 6	1.33 + 5	5.98 + 9	4.82 + 8	5.85 + 6	9.67 + 4
50	1.74 + 9	1.75 + 8	2.71 + 6	3.86 + 4	9.47 + 8	1.17 + 8	1.67 + 6	2.46 + 4
100	2.34 + 8	2.62 + 7	3.79 + 5	5.26 + 3	9.95 + 7	1.31 + 7	1.92 + 5	2.70 + 3
200	3.10 + 7	2.10 + 6	3.15 + 4	4.46 + 2	6.65 + 6	8.62 + 5	1.33 + 4	1.91 + 2
400	3.46 + 6	1.77 + 5	1.53 + 3	1.84 + 1	4.05 + 5	4.81 + 4	5.14 + 2	6.80 + 0
1000	5.57 + 4	1.10 + 3	9.75 + 0	1.08 - 1	7.10 + 3	3.05 + 2	3.18 + 0	5.38 - 2
1500	3.84 + 3	5.67 + 1	4.54 - 1	7.93 - 3	6.58 + 2	2.20 + 1	2.05 - 1	3.93 - 3

*14.56 Percent Of Missions Encountered No Flux Events

TABLE D2 LUNAR MISSION SPECTRA
(Continued)
January 1, 1970**

E(MeV)	Proton				Alpha			
	0.1%	1.0%	10.0%	50.0%	0.1%	1.0%	10.0%	50.0%
10	2.51 + 10	5.23 + 8	4.74 + 6	——	2.68 + 10	8.58 + 8	3.02 + 6	——
30	2.10 + 9	9.83 + 7	5.12 + 5	——	2.18 + 9	5.43 + 7	3.67 + 5	——
50	4.88 + 8	2.56 + 7	1.44 + 5	——	4.56 + 8	1.59 + 7	9.38 + 4	——
100	6.63 + 7	3.99 + 6	1.88 + 4	——	4.14 + 7	2.12 + 6	1.03 + 4	——
200	5.97 + 6	2.85 + 5	1.73 + 3	——	2.69 + 6	1.23 + 5	7.01 + 2	——
400	3.76 + 5	1.69 + 4	8.58 + 1	——	1.01 + 5	5.06 + 3	2.91 + 1	——
1000	3.62 + 3	1.27 + 2	3.97 - 1	——	8.07 + 2	3.04 + 1	1.60 - 1	——
1500	2.21 + 2	4.93 + 0	1.56 - 2	——	6.91 + 1	2.21 + 0	1.03 - 2	——

**58.49 Percent Of Missions Encountered No Flux Events

TABLE D2 LUNAR MISSION SPECTRA
(Continued)
June 1, 1971***

E(MeV)	Proton				Alpha			
	0.1%	1.0%	10.0%	50.0%	0.1%	1.0%	10.0%	50.0%
10	2.31 + 10	2.13 + 9	4.21 + 7	3.41 + 5	2.28 + 10	1.55 + 9	1.94 + 7	2.23 + 5
30	4.85 + 9	3.97 + 8	3.79 + 6	5.82 + 4	5.25 + 9	2.48 + 8	3.36 + 6	3.93 + 4
50	9.04 + 8	1.04 + 8	1.18 + 6	1.56 + 4	8.53 + 8	5.62 + 7	8.09 + 5	9.48 + 3
100	9.57 + 7	1.43 + 7	1.29 + 5	2.02 + 3	7.13 + 7	7.67 + 6	7.60 + 4	1.04 + 3
200	2.16 + 7	1.22 + 6	1.63 + 4	1.64 + 2	5.31 + 6	4.78 + 5	5.64 + 3	7.33 + 1
400	2.79 + 6	5.77 + 4	6.53 + 2	3.59 + 0	3.09 + 5	2.38 + 4	2.41 + 2	2.88 + 0
1000	4.12 + 4	5.51 + 2	4.39 + 0	1.25 - 2	6.04 + 3	1.72 + 2	1.23 + 0	8.09 - 3
1500	2.80 + 3	3.14 + 1	1.86 - 1	8.21 - 4	6.08 + 2	1.27 + 1	8.40 - 2	4.25 - 4

***25.69 Percent Of Missions Encountered No Flux Events

TABLE D3 EARTH ORBIT SPECTRA - PROTONS, AP3

E(MeV)	150 Nautical Miles			300 Nautical Miles			600 Nautical Miles		
	0°	30°	90°	0°	30°	90°	0°	30°	90°
10	———	6.46 + 3	6.55 + 3	8.62 + 2	5.71 + 4	4.28 + 4	1.48 + 5	3.53 + 5	1.73 + 5
50	———	4.06 + 3	3.64 + 3	5.77 + 2	3.78 + 4	2.59 + 4	1.25 + 5	2.66 + 5	1.28 + 5
100	———	2.28 + 3	1.75 + 3	3.50 + 2	2.25 + 4	1.38 + 4	1.01 + 5	1.86 + 5	8.85 + 4
200	———	7.15 + 2	4.03 + 2	1.28 + 2	8.03 + 3	3.95 + 3	6.59 + 4	9.10 + 4	4.20 + 4
400	———	7.06 + 1	2.14 + 1	1.73 + 1	1.02 + 3	3.21 + 2	2.81 + 4	2.18 + 4	9.45 + 3
1000	———	6.77 - 2	3.20 - 3	4.23 - 2	2.08 + 0	1.73 - 1	2.18 + 3	3.02 + 2	1.08 + 2

E(MeV)	1000 Nautical Miles			2000 Nautical Miles			3000 Nautical Miles		
	0°	30°	90°	0°	30°	90°	0°	30°	90°
10	1.03 + 6	1.97 + 6	8.05 + 5	4.48 + 6	3.72 + 6	1.64 + 6	1.28 + 7	1.28 + 7	5.61 + 6
50	8.86 + 5	1.47 + 6	6.04 + 5	3.11 + 6	2.36 + 6	1.05 + 6	3.30 + 6	3.09 + 6	1.36 + 6
100	7.31 + 5	1.01 + 6	4.21 + 5	1.96 + 6	1.34 + 6	5.99 + 5	6.07 + 5	5.22 + 5	2.31 + 5
200	4.98 + 5	4.79 + 5	2.05 + 5	7.86 + 5	4.31 + 5	1.95 + 5	2.05 + 4	1.49 + 4	6.70 + 3
400	2.31 + 5	1.08 + 5	4.87 + 4	1.26 + 5	4.45 + 4	2.07 + 4	2.33 + 1	1.21 + 1	5.61 + 0
1000	2.29 + 4	1.23 + 3	6.51 + 2	5.15 + 2	4.91 + 1	2.48 + 1	3.45 - 8	6.44 - 9	3.30 - 9

E(MeV)	5000 Nautical Miles		
	0°	30°	90°
10	5.20 + 8	3.68 + 8	1.73 + 8
50	1.56 + 6	1.12 + 6	5.20 + 5
100	1.09 + 3	7.85 + 2	3.68 + 2
200	5.30 - 4	3.94 - 4	1.84 - 4
400	1.26 - 16	9.90 - 17	4.56 - 17
1000	1.63 - 54	1.56 - 54	7.00 - 54

TABLE D4 EARTH ORBIT SPECTRA -- ELECTRONS, 1968

E(MeV)	150 Nautical Miles			300 Nautical Miles			600 Nautical Miles		
	0°	30°	90°	0°	30°	90°	0°	30°	90°
0.5	———	1.99 + 8	6.68 + 9	1.65 + 6	1.32 + 10	1.76 + 10	1.71 + 11	3.62 + 11	1.88 + 11
1.0	———	4.77 + 6	1.47 + 9	8.99 + 4	3.16 + 8	2.71 + 9	7.40 + 9	9.27 + 9	1.57 + 10
2.0	———	2.89 + 4	1.39 + 8	6.25 + 2	1.92 + 6	2.48 + 8	4.05 + 7	5.40 + 7	1.14 + 9
4.0	———	1.89 + 4	1.72 + 6	4.75 + 1	1.26 + 6	3.65 + 6	1.25 + 7	3.43 + 7	2.81 + 7
6.0	———	1.09 + 4	7.47 + 4	3.07 + 0	7.63 + 5	5.36 + 5	4.72 + 6	2.00 + 7	8.48 + 6
8.0	———	6.43 + 3	2.15 + 4	1.74 - 1	4.54 + 5	2.62 + 5	1.88 + 6	1.12 + 7	4.39 + 6
10.0	———	4.23 + 3	1.18 + 4	1.21 - 2	2.77 + 5	1.54 + 5	8.47 + 5	6.73 + 6	2.34 + 6

E(MeV)	1000 Nautical Miles			2000 Nautical Miles			3000 Nautical Miles		
	0°	30°	90°	0°	30°	90°	0°	30°	90°
0.5	6.25 + 12	4.49 + 12	1.84 + 12	1.06 + 13	4.36 + 12	2.21 + 12	9.89 + 11	5.55 + 11	7.15 + 11
1.0	1.69 + 11	8.50 + 10	6.56 + 10	1.18 + 11	4.86 + 10	1.11 + 11	7.42 + 9	3.48 + 10	1.33 + 11
2.0	9.27 + 8	5.72 + 8	2.83 + 9	1.37 + 9	8.28 + 8	8.27 + 9	5.03 + 8	5.79 + 9	1.52 + 10
4.0	6.22 + 8	4.51 + 8	2.08 + 8	1.20 + 9	5.29 + 8	3.66 + 8	2.26 + 8	3.45 + 8	3.54 + 8
6.0	3.43 + 8	2.81 + 8	1.04 + 8	8.16 + 8	3.30 + 8	1.64 + 8	1.05 + 8	6.89 + 7	3.60 + 7
8.0	1.82 + 8	1.71 + 8	6.06 + 7	5.27 + 8	2.13 + 8	1.03 + 8	4.82 + 7	2.44 + 7	1.14 + 7
10.0	1.03 + 8	1.12 + 8	3.91 + 7	3.53 + 8	1.54 + 8	6.64 + 7	2.35 + 7	1.03 + 7	4.66 + 6

TABLE D4 EARTH ORBIT SPECTRA - ELECTRONS, 1968
(Continued)

E(MeV)	5000 Nautical Miles			7000 Nautical Miles			10,000 Nautical Miles		
	0°	30°	90°	0°	30°	90°	0°	30°	90°
0.5	2.11 + 12	2.56 + 12	1.58 + 12	4.08 + 12	4.32 + 12	2.16 + 12	5.54 + 12	4.57 + 12	1.97 + 12
1.0	1.23 + 11	4.88 + 11	3.14 + 11	1.04 + 12	1.20 + 12	5.55 + 11	1.38 + 12	9.99 + 11	4.25 + 11
2.0	1.65 + 10	7.30 + 10	4.01 + 10	2.00 + 11	1.84 + 11	7.79 + 10	1.52 + 11	8.20 + 10	3.49 + 10
4.0	1.80 + 9	2.77 + 9	1.26 + 9	6.36 + 9	4.47 + 9	1.85 + 9	1.74 + 9	7.46 + 8	3.31 + 8
6.0	1.96 + 8	1.74 + 8	6.97 + 7	2.02 + 8	1.16 + 8	4.24 + 7	1.94 + 7	7.76 + 6	3.51 + 6
8.0	2.07 + 7	1.45 + 7	5.95 + 6	6.13 + 6	3.06 + 6	2.10 + 6	2.33 + 5	9.01 + 4	3.90 + 4
10.0	2.37 + 6	1.27 + 6	6.33 + 5	1.90 + 5	8.07 + 4	3.50 + 4	4.28 + 3	1.70 + 3	7.24 + 2

E(MeV)	15,000 Nautical Miles		
	0°	30°	90°
0.5	3.71 + 12	2.01 + 12	8.39 + 11
1.0	4.32 + 11	2.15 + 11	9.09 + 10
2.0	7.40 + 9	3.22 + 9	1.41 + 9
4.0	2.09 + 6	8.06 + 5	3.62 + 5
6.0	5.88 + 2	2.36 + 2	1.03 + 2
8.0	1.39 - 1	3.25 - 2	2.23 - 2
10.0	3.98 - 5	1.18 - 4	1.02 - 4

APPENDIX E

This appendix contains the results of a parametric study of space radiation hazards for the Mars, Lunar, and Earth orbital missions described in Section 2.0. The flux spectra upon which these results are based are tabulated in Appendix D. For specified risk levels and radiation exposure dose limits this appendix may be used to estimate shield requirements.

Table E1 contains a summary of design dosages[14] recommended by NASA and reviewed by the Working Group on Radiation Problems, Man In Space Committee, National Academy of Sciences Space Science Board. Figures E1 through E12 present eye and abdomen dose within aluminum and polyethylene vehicles for three Mars missions; Figures E13 through E24 present similar data for three Lunar missions. The percents associated with each curve represent the probability of exceeding the indicated doses. Figures E25 through E28 present eye and abdomen proton dose rate within an aluminum vehicle for orbital missions at several altitudes and angles of inclination. Figures E29 and E30 present eye electron dose rate, within an aluminum vehicle as a function of altitude and angle of inclination. The dashed portions of the latter figures indicate a region where dose rate is changing rapidly; further calculations are required to accurately define these values.

TABLE E1 PROTON RADIATION EXPOSURE DOSE LIMITS[14]

Critical Organ	Maximum Permissible Integrated Dose rem	Proton RBE rem/rad	Average Yearly Dose rad	Maximum Permissible Single Acute Emergency Exposure rad
Skin Of Whole Body	1600	1.4 (Approximately)	250	[a] 500
Blood-forming - - - - - - -	270	1.0	55	200
Feet, Ankles, And Hands	4000	1.4	550	[b] 700
Eyes - - - - - - - - - - - - -	270	[c] 2	27	100

[a] Based on skin erythema level.

[b] Based on skin erythema level but these appendages are believed to be less radiosensitive.

[c] Slightly higher RBE assumed since eyes are believed more radiosensitive.

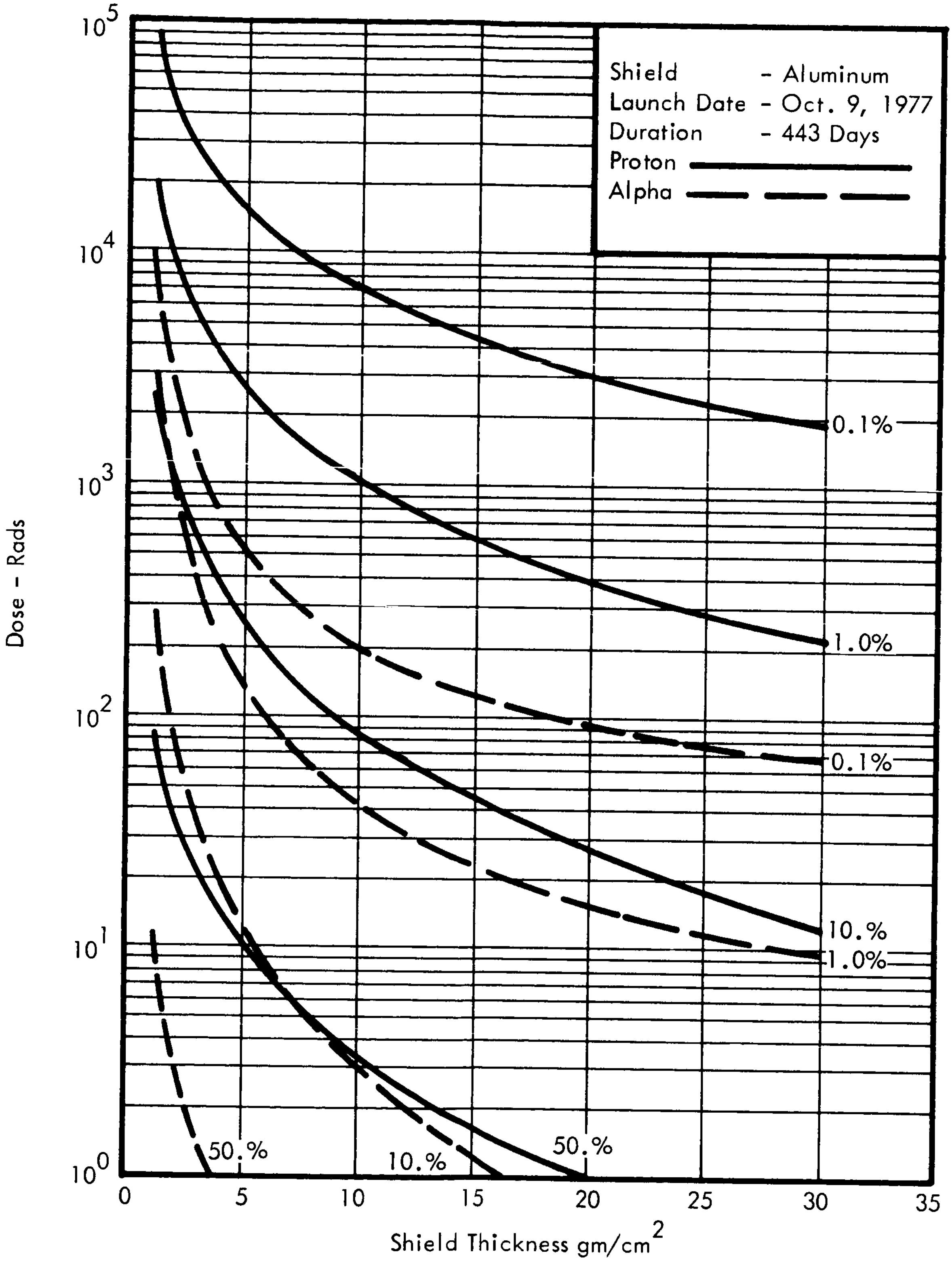

FIGURE E1 EYE DOSE VERSUS ALUMINUM SHIELD THICKNESS FOR A MARS MISSION

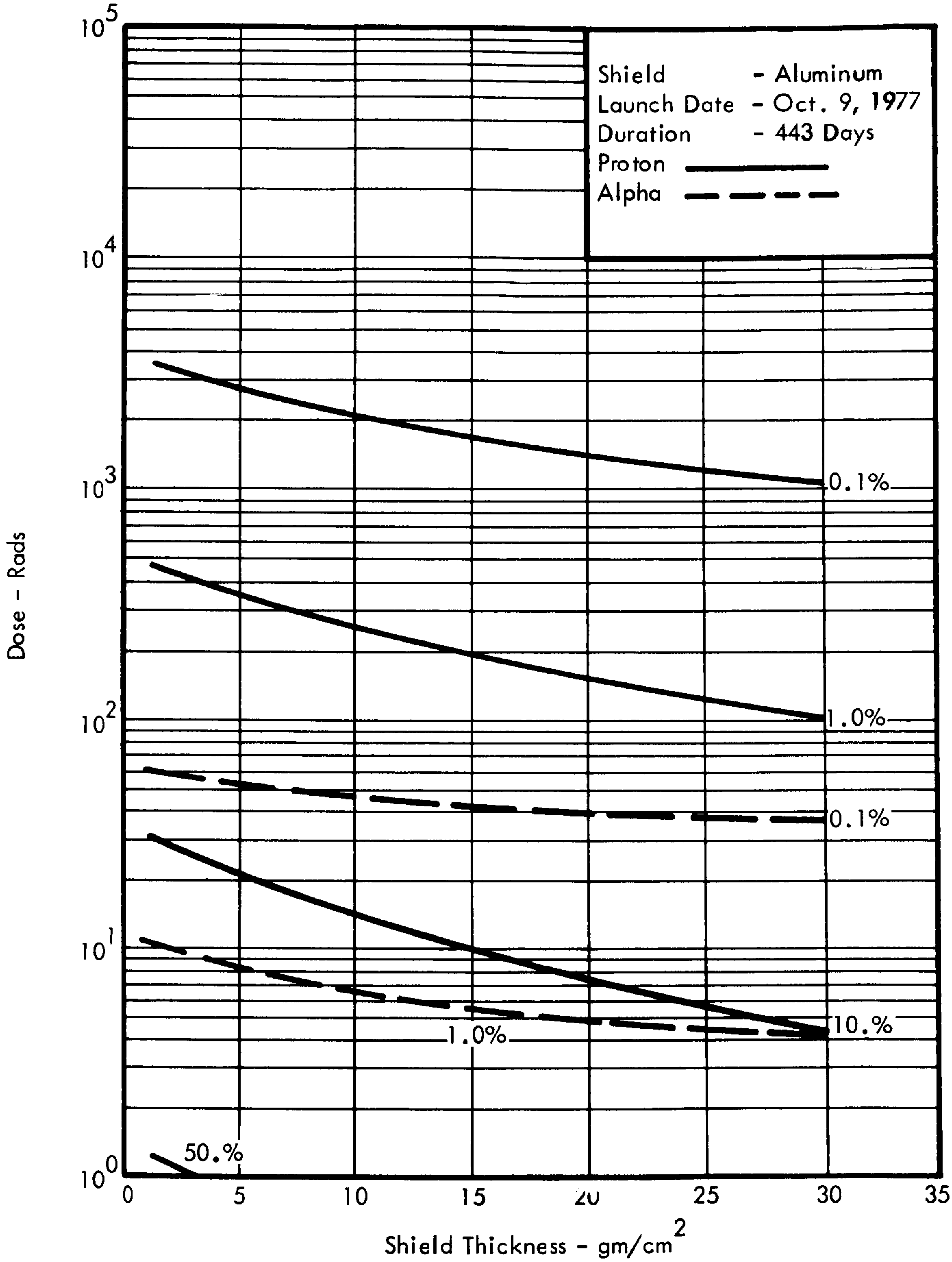

FIGURE E2 ABDOMEN DOSE VERSUS ALUMINUM SHIELD THICKNESS FOR A MARS MISSION

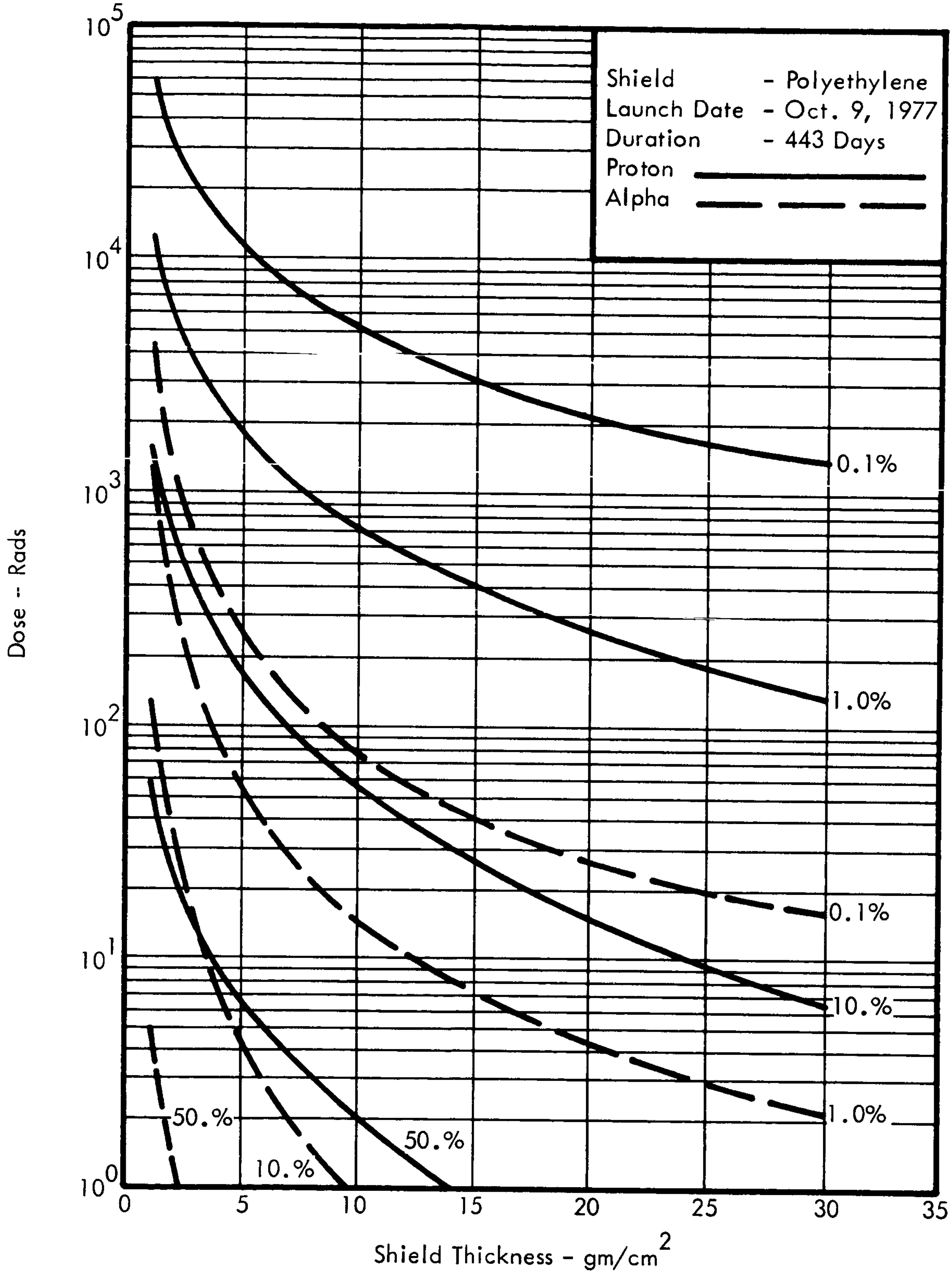

FIGURE E3 EYE DOSE VERSUS POLYETHYLENE SHIELD THICKNESS FOR A MARS MISSION

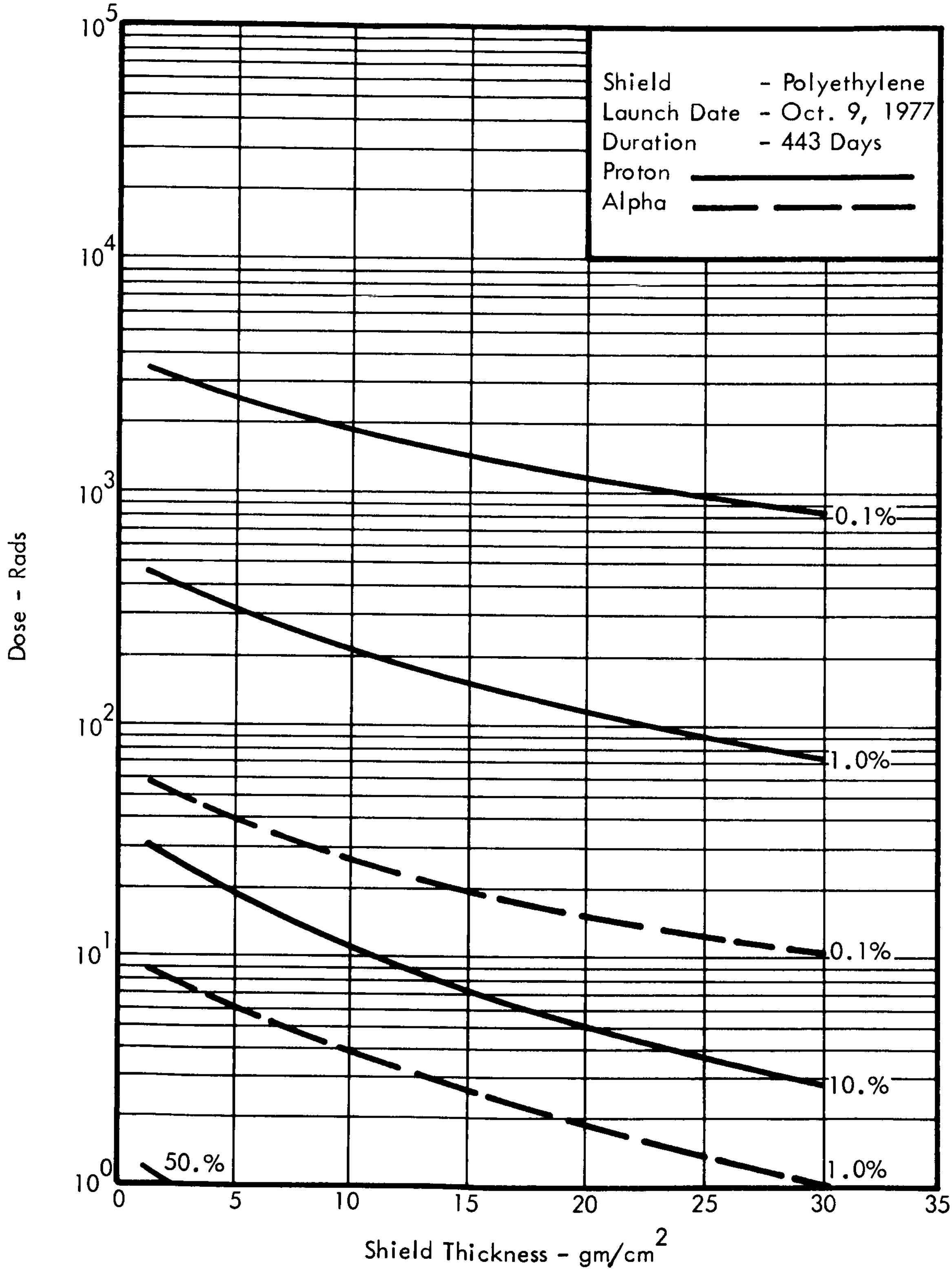

FIGURE E4 ABDOMEN DOSE VERSUS POLYETHYLENE SHIELD THICKNESS FOR A MARS MISSION

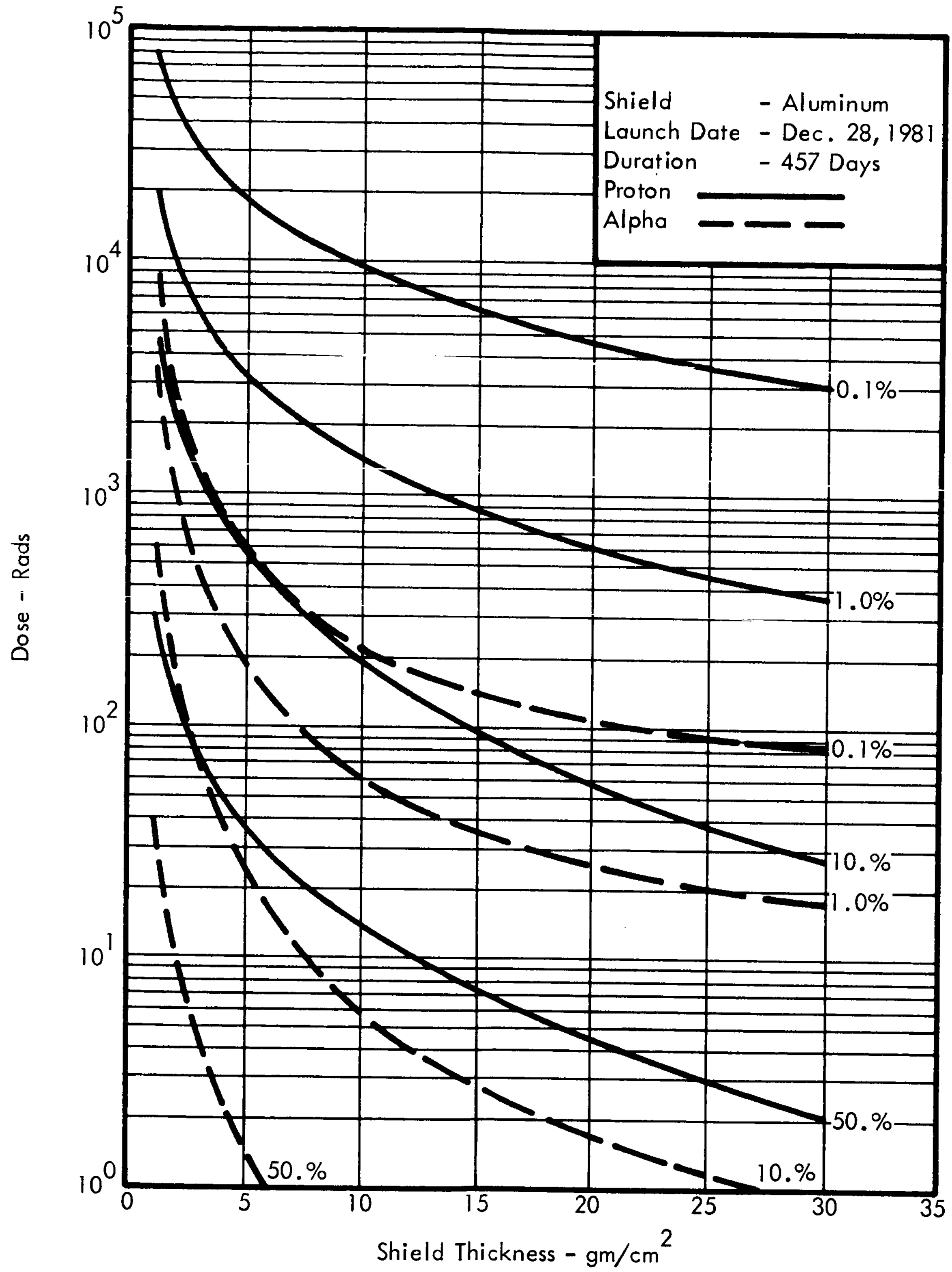

FIGURE E5 EYE DOSE VERSUS ALUMINUM SHIELD THICKNESS FOR A MARS MISSION

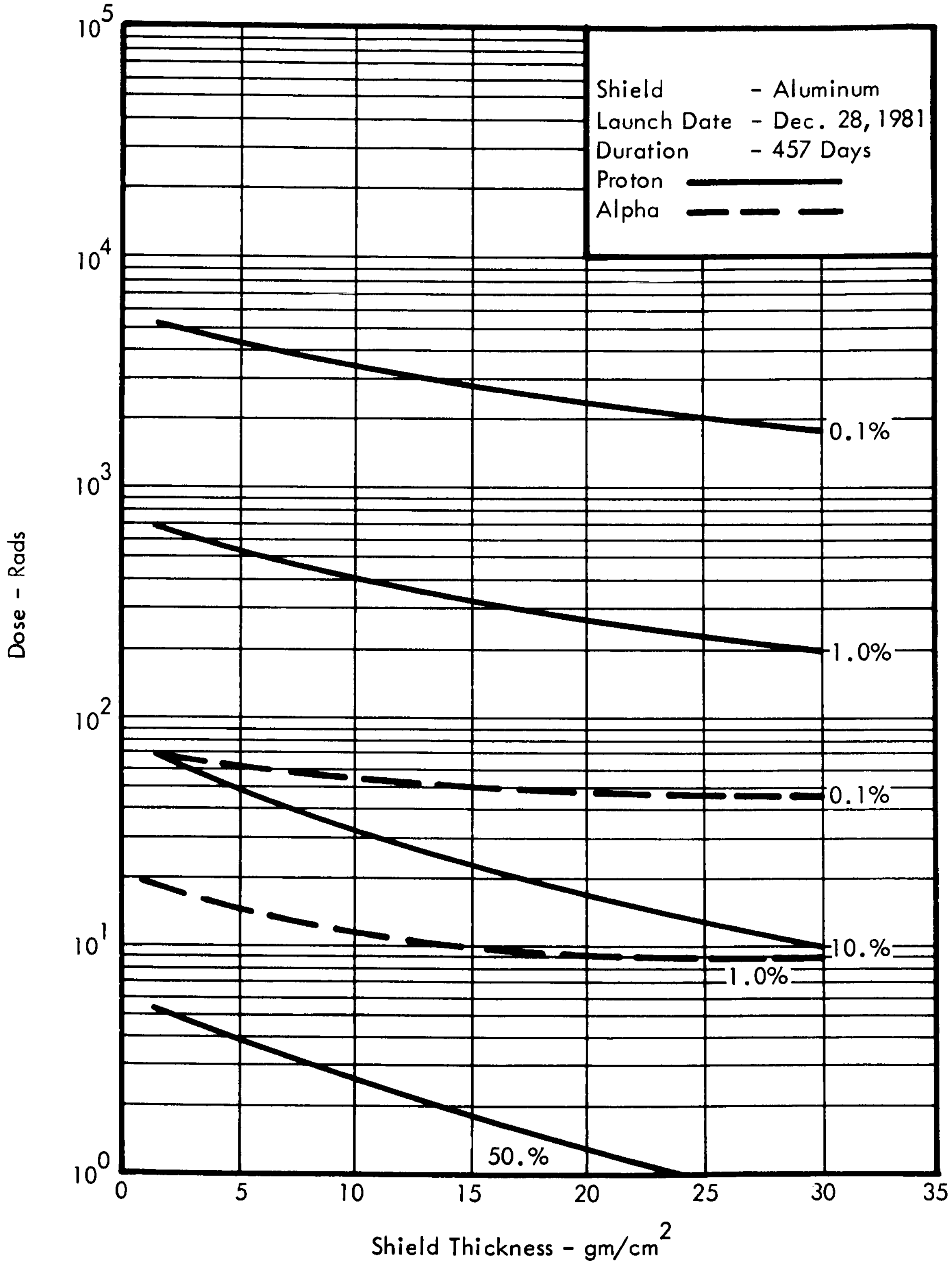

FIGURE E6 ABDOMEN DOSE VERSUS ALUMINUM SHIELD THICKNESS FOR A MARS MISSION

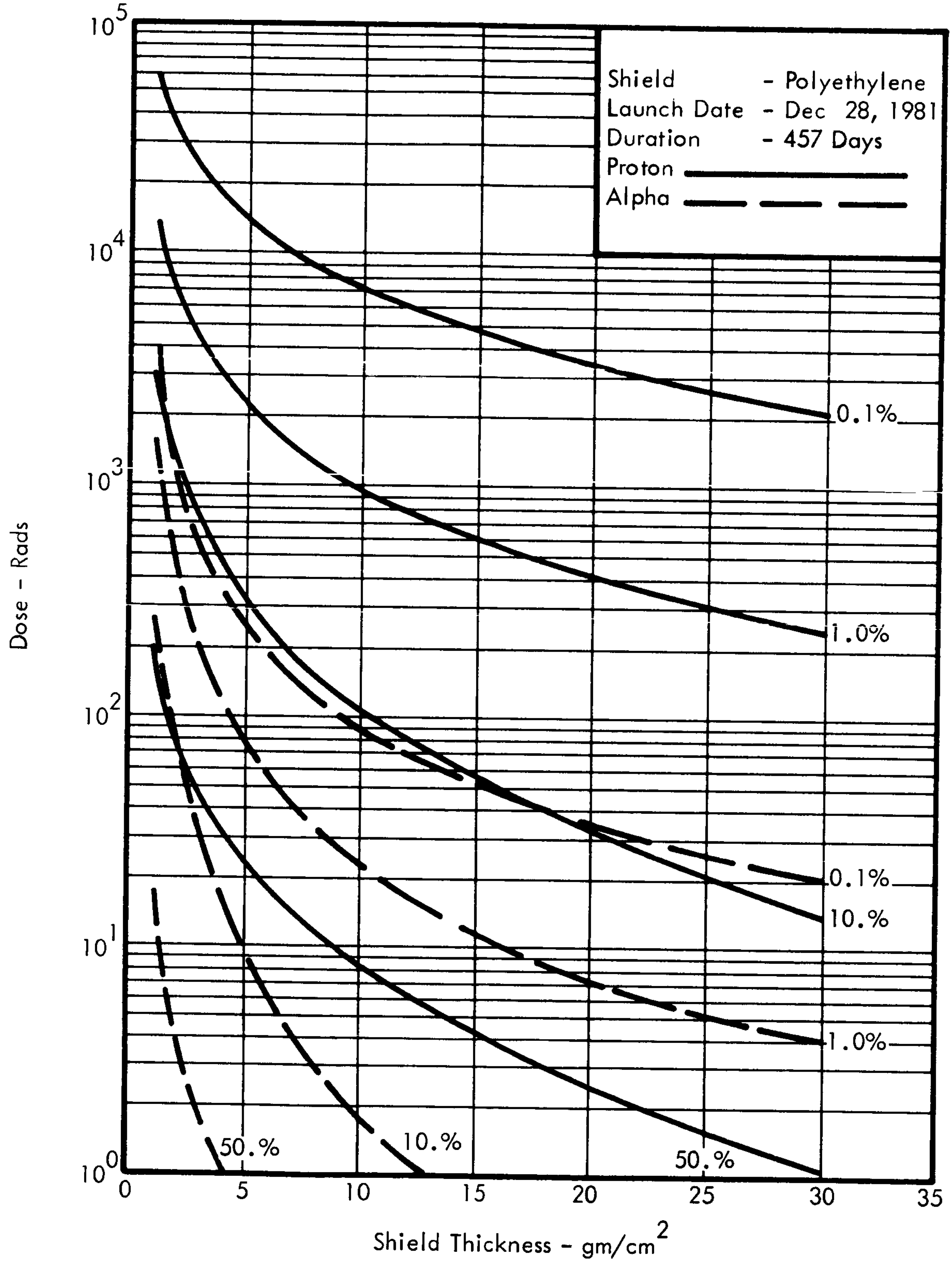

FIGURE E7 EYE DOSE VERSUS POLYETHYLENE SHIELD THICKNESS FOR A MARS MISSION

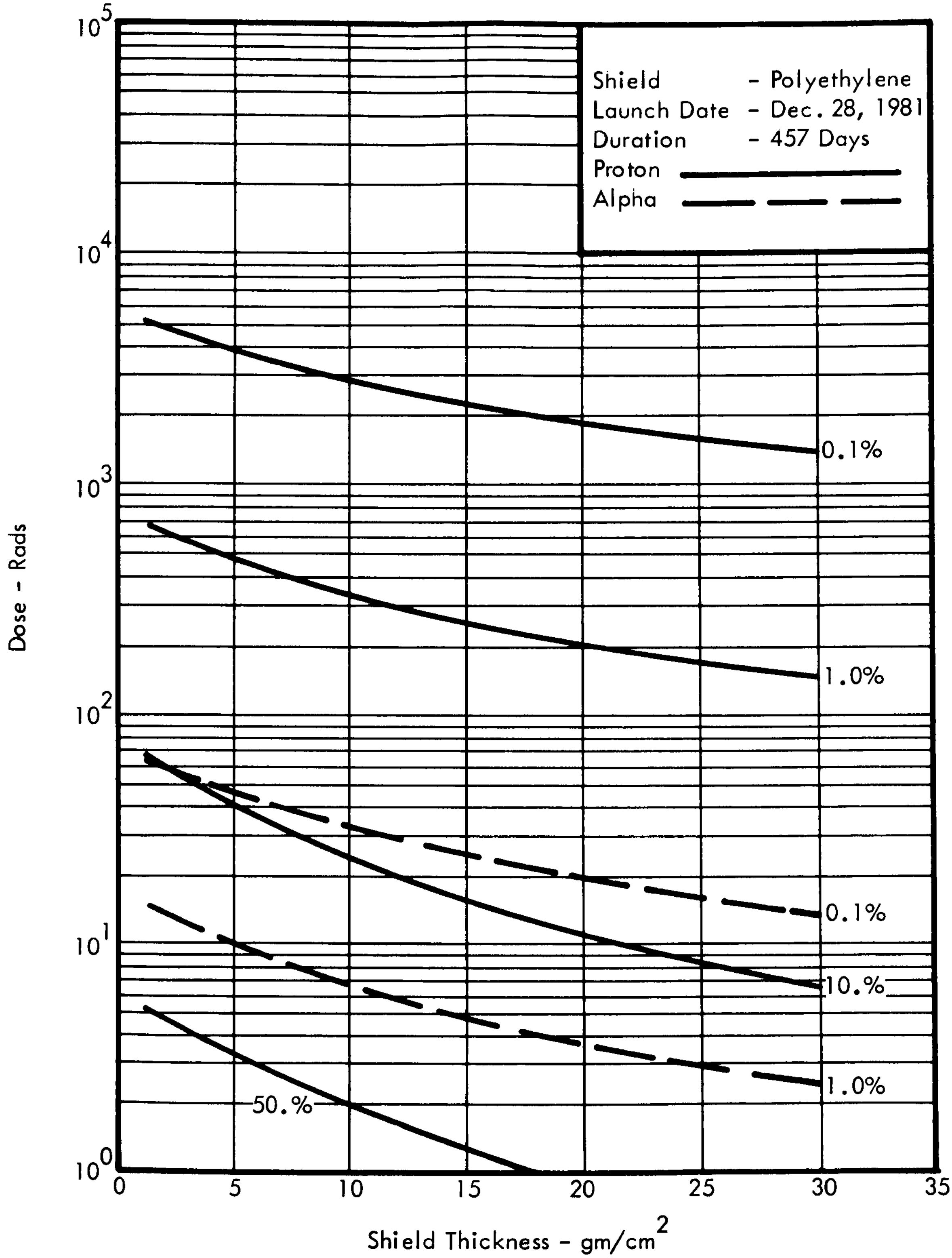

FIGURE E8 ABDOMEN DOSE VERSUS POLYETHYLENE SHIELD THICKNESS FOR A MARS MISSION

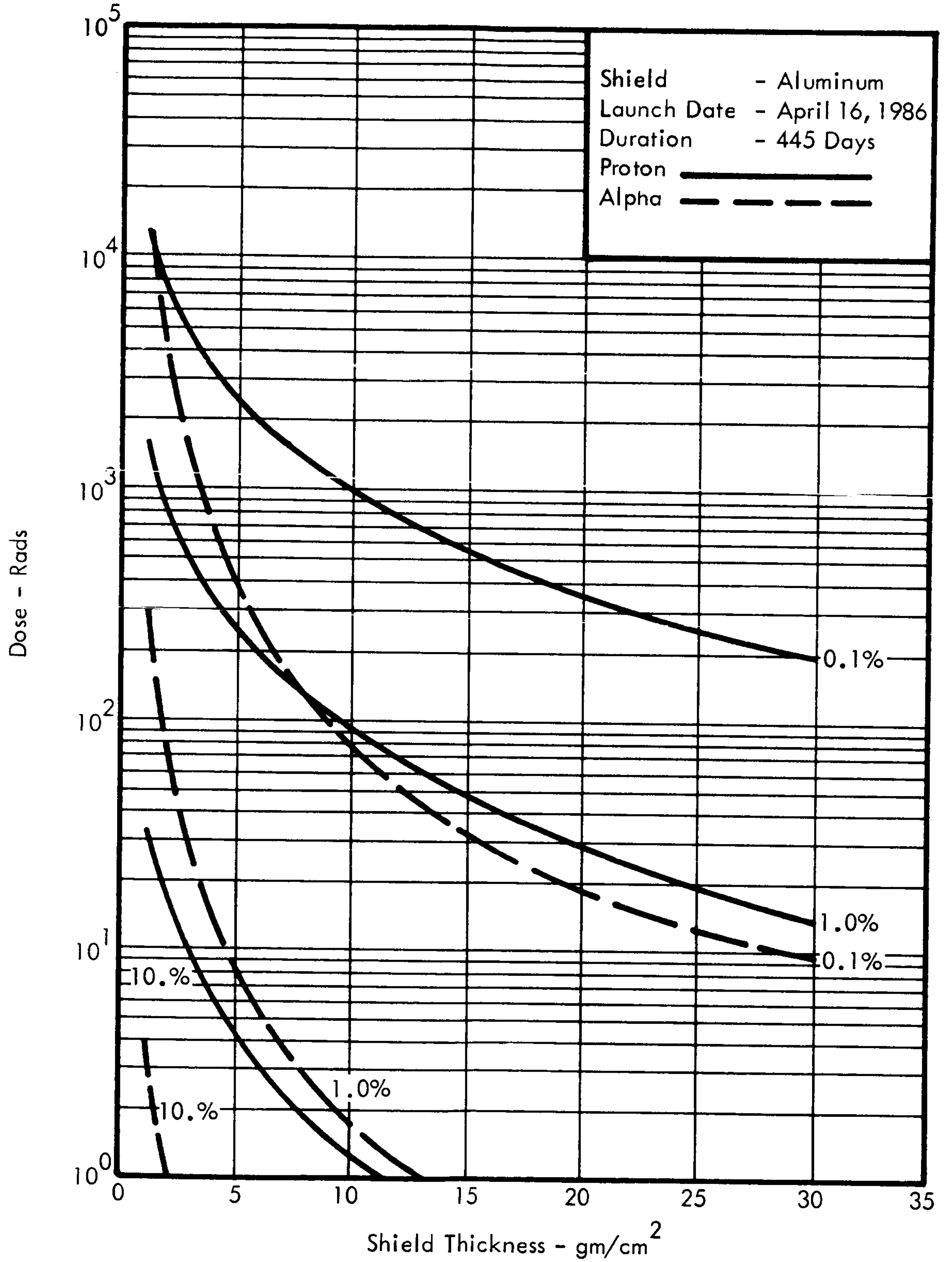

FIGURE E9 EYE DOSE VERSUS ALUMINUM SHIELD THICKNESS FOR A MARS MISSION

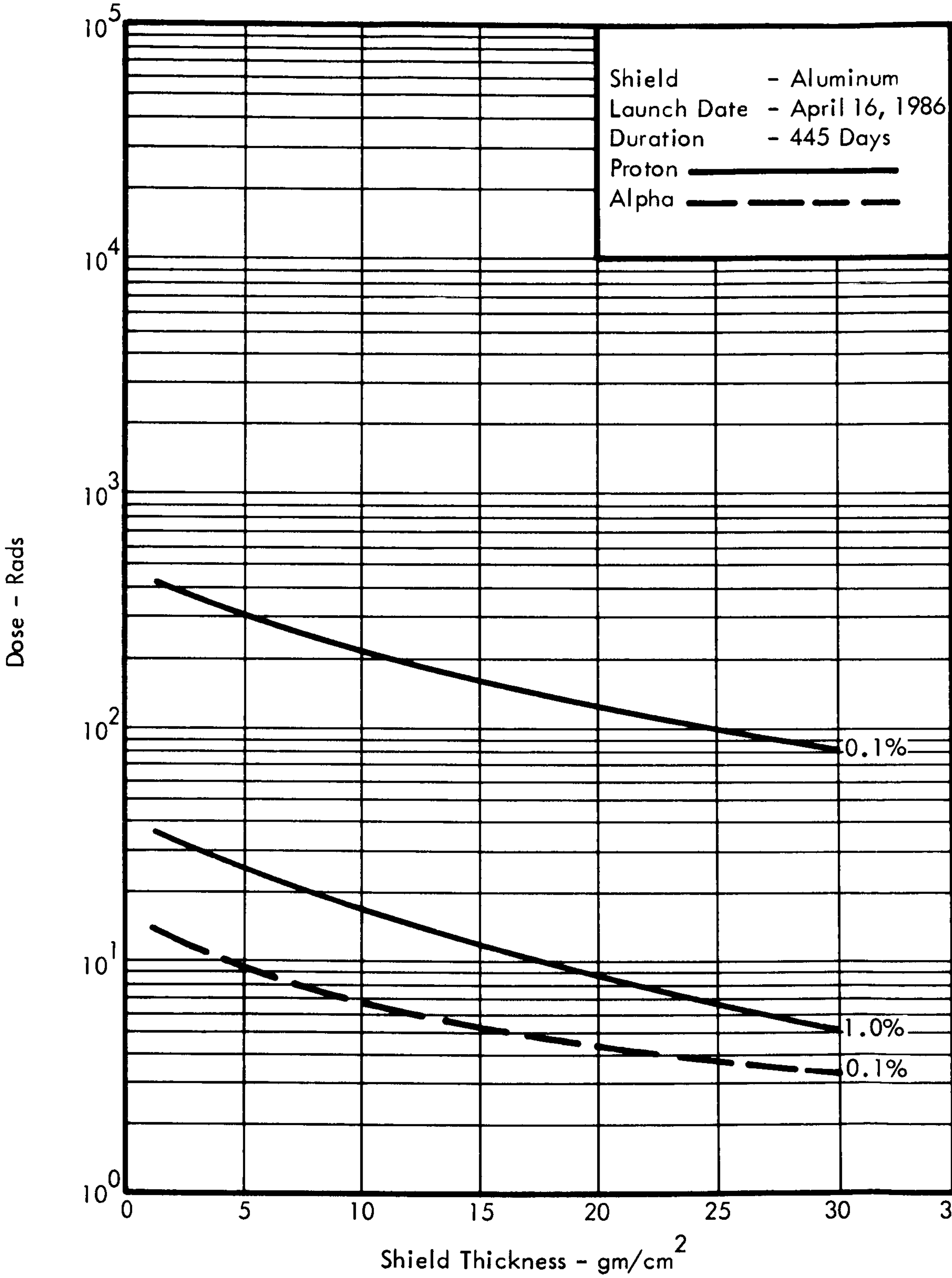

FIGURE E10 ABDOMEN DOSE VERSUS ALUMINUM SHIELD THICKNESS FOR A MARS MISSION

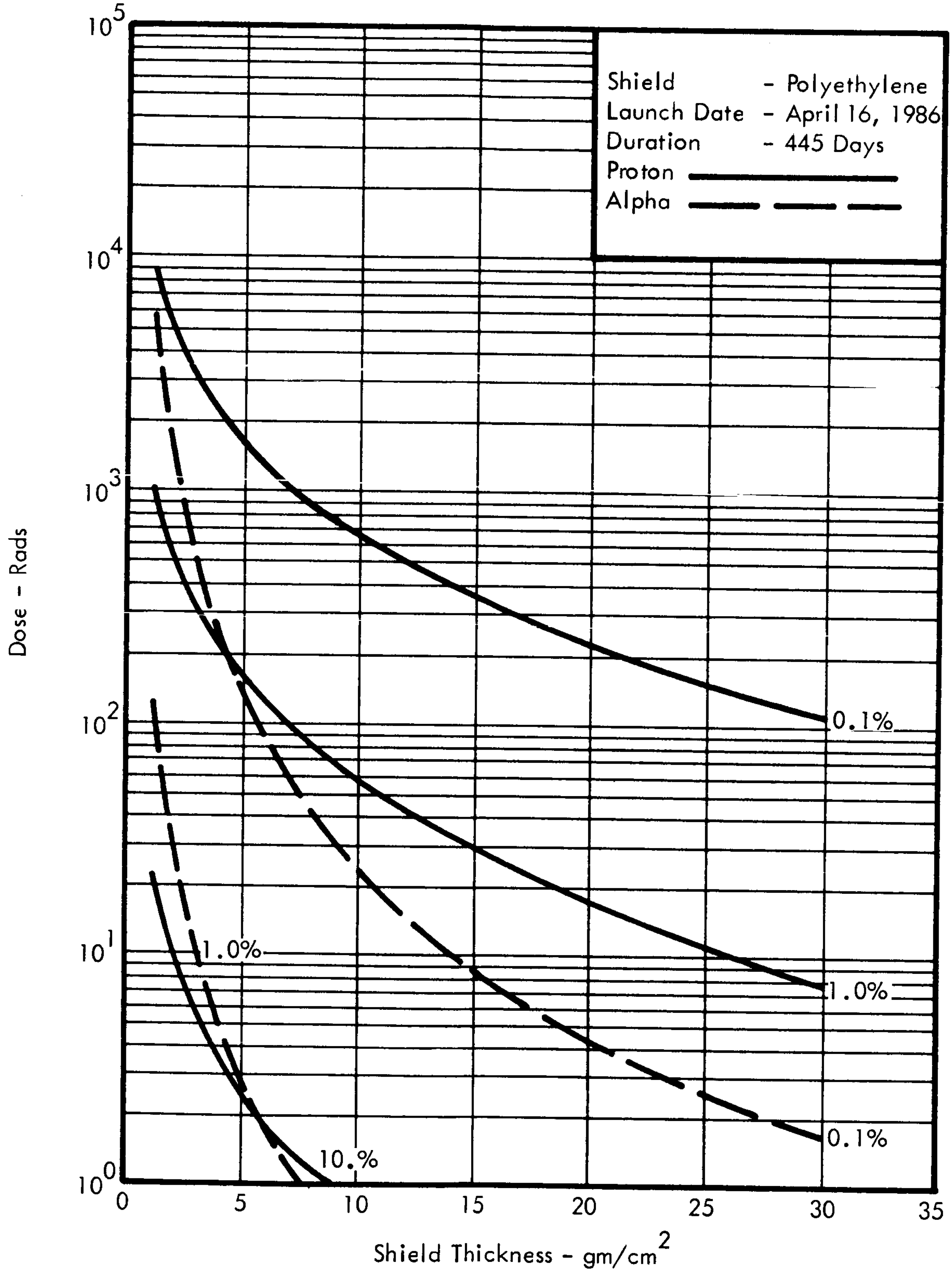

FIGURE E11 EYE DOSE VERSUS POLYETHYLENE SHIELD THICKNESS FOR A MARS MISSION

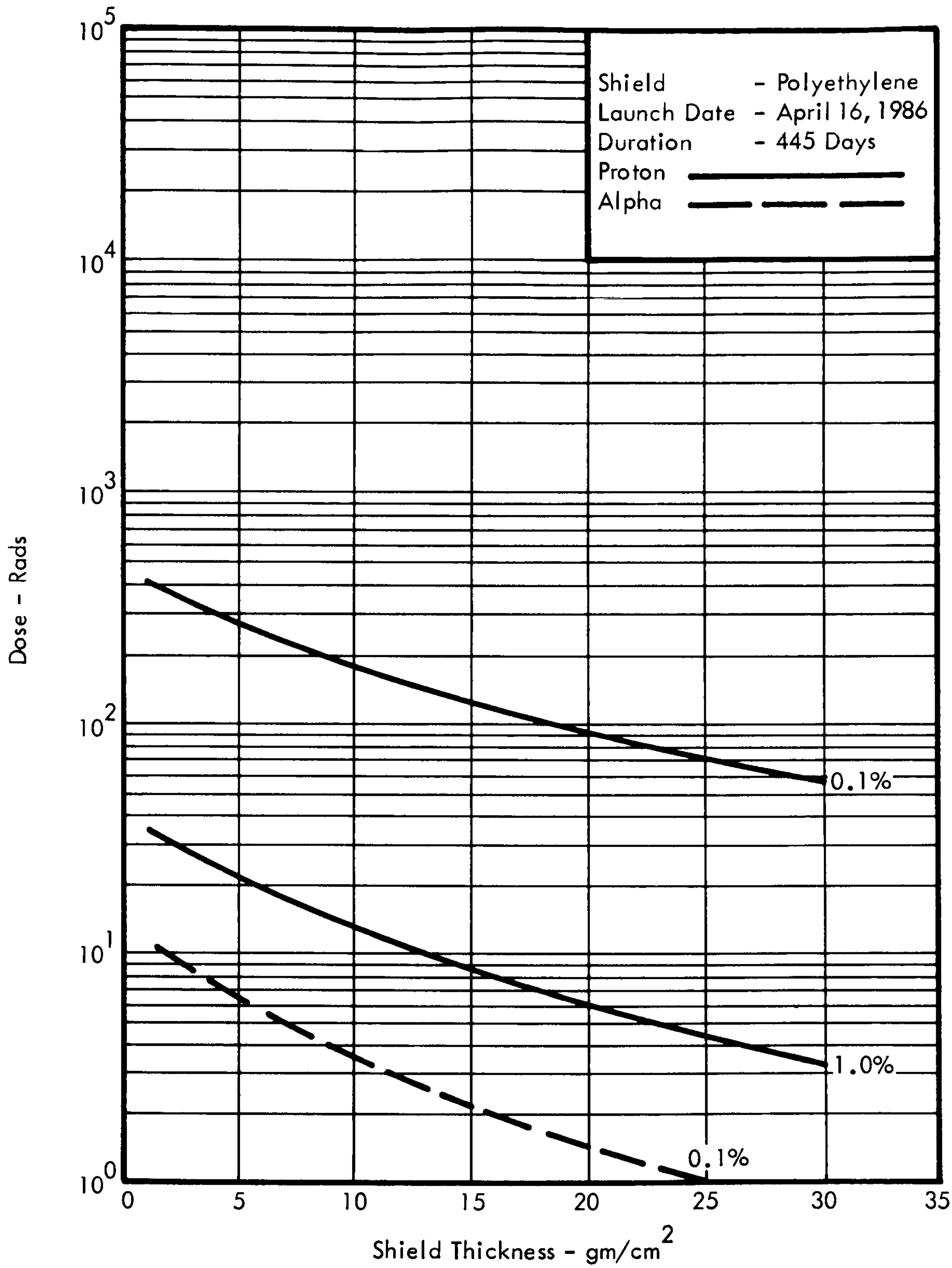

FIGURE E12 ABDOMEN DOSE VERSUS POLYETHYLENE SHIELD THICKNESS FOR A MARS MISSION

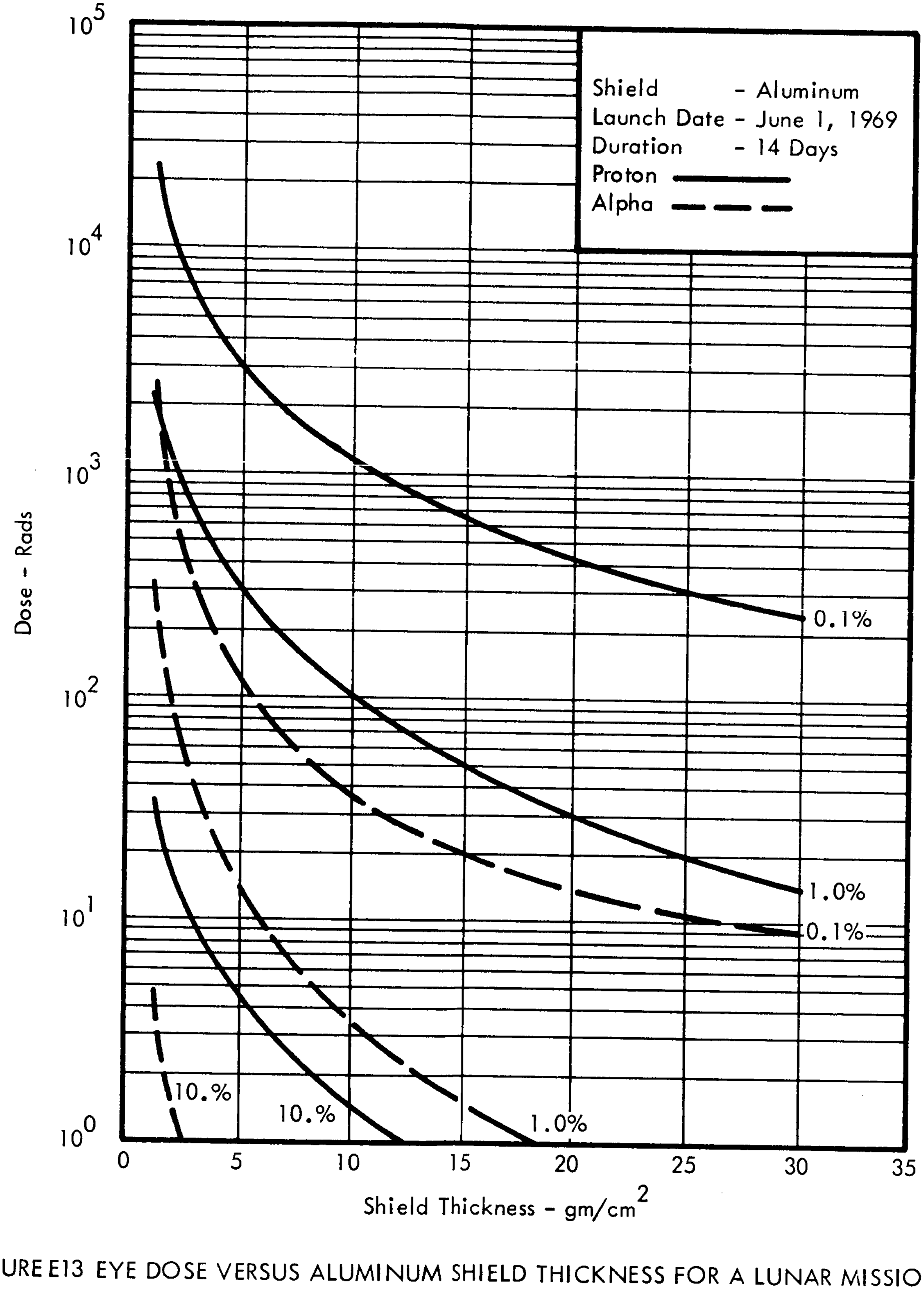

FIGURE E13 EYE DOSE VERSUS ALUMINUM SHIELD THICKNESS FOR A LUNAR MISSION

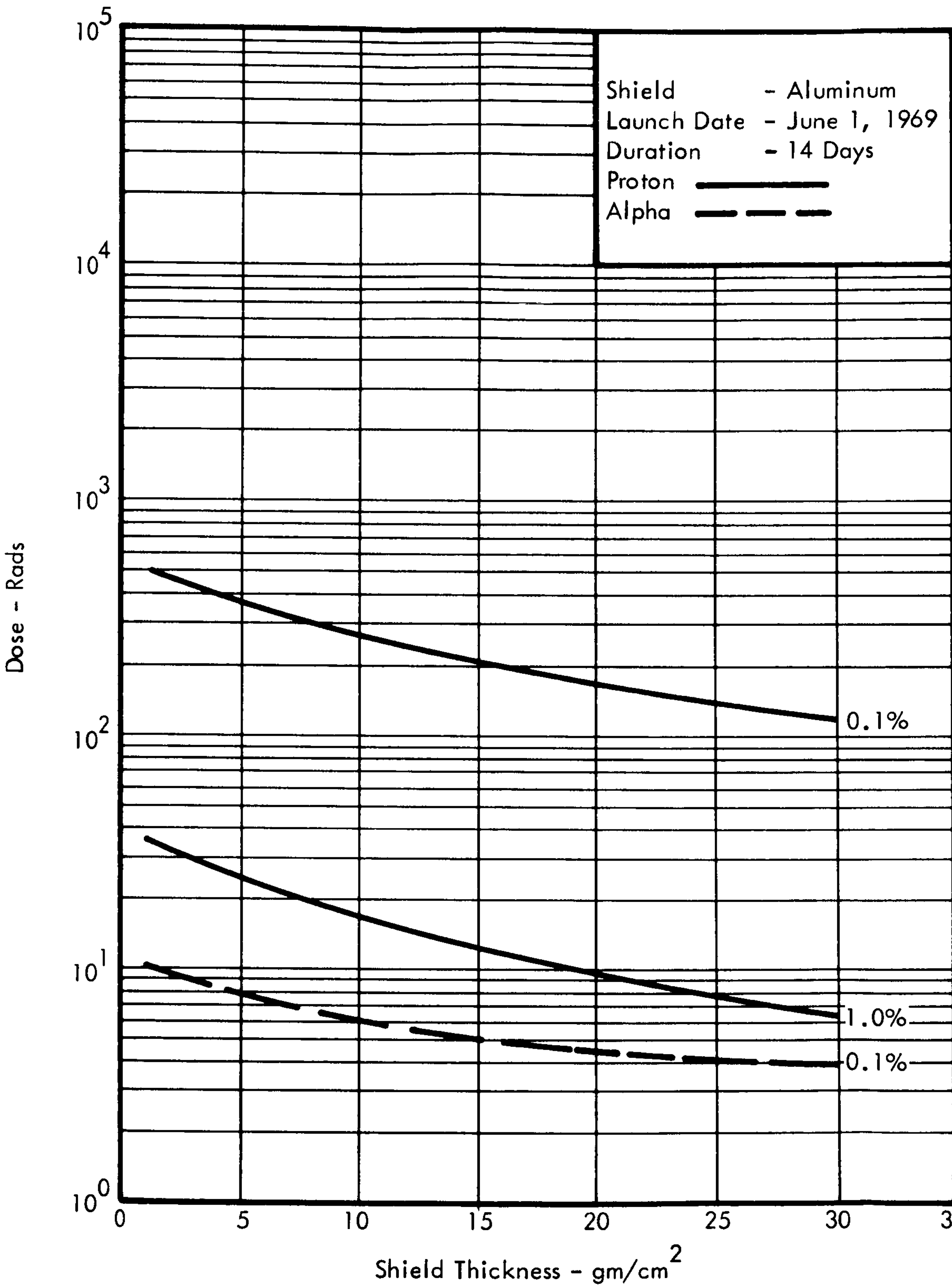

FIGURE E14 ABDOMEN DOSE VERSUS ALUMINUM SHIELD THICKNESS FOR A LUNAR MISSION

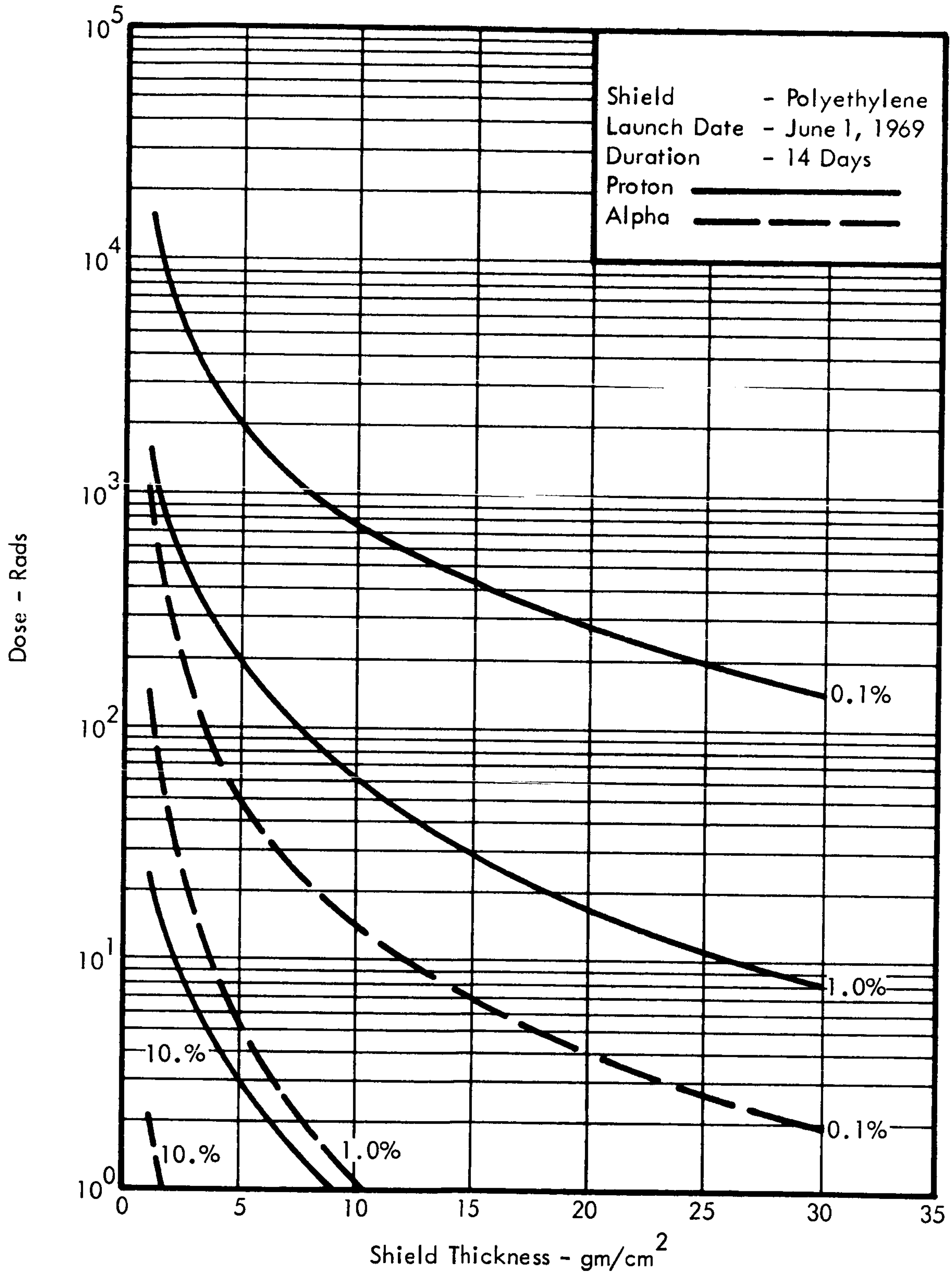

FIGURE E15 EYE DOSE VERSUS POLYETHYLENE SHIELD THICKNESS FOR A LUNAR MISSION

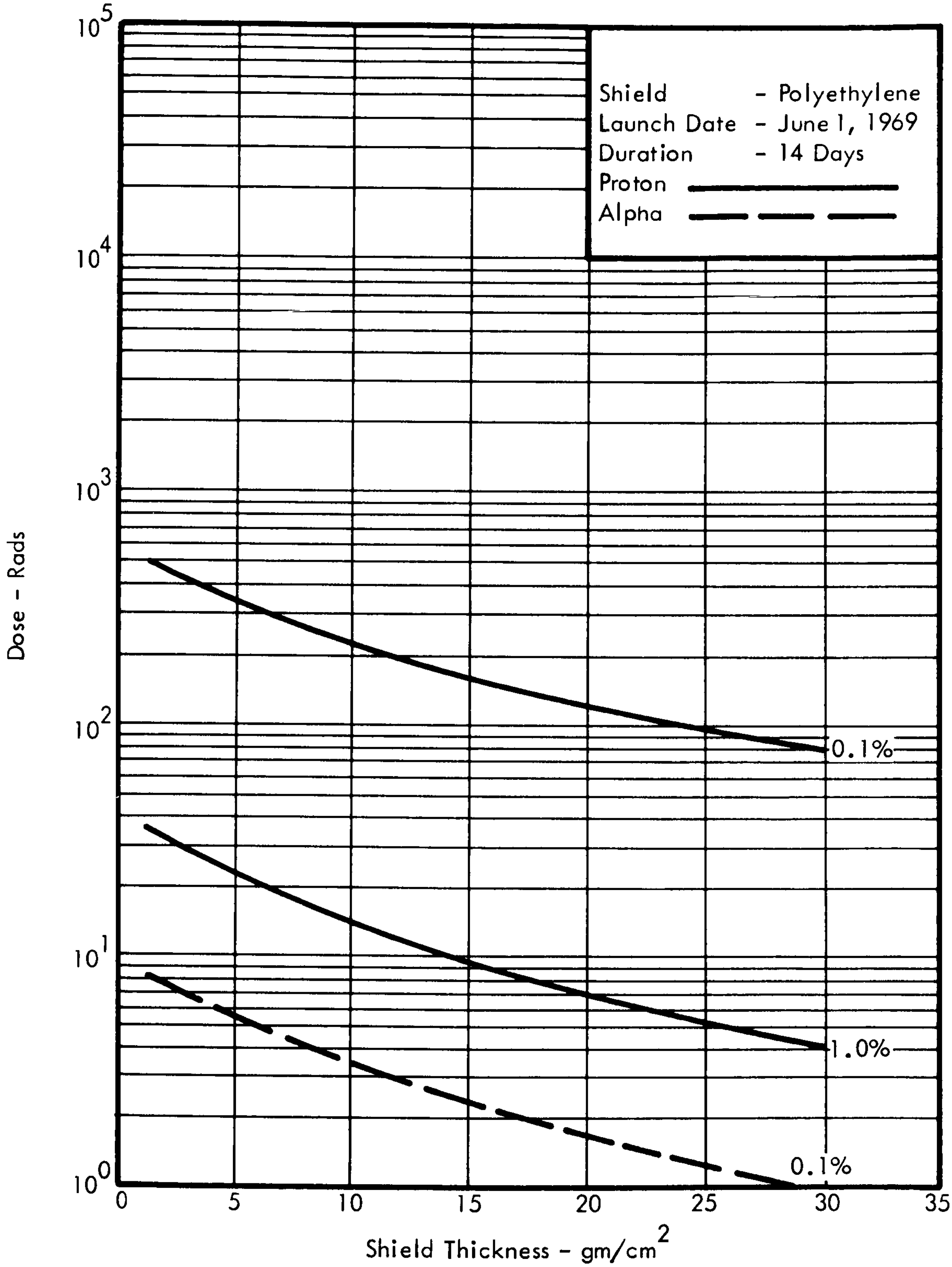

FIGURE E16 ABDOMEN DOSE VERSUS POLYETHYLENE SHIELD THICKNESS FOR A LUNAR MISSION

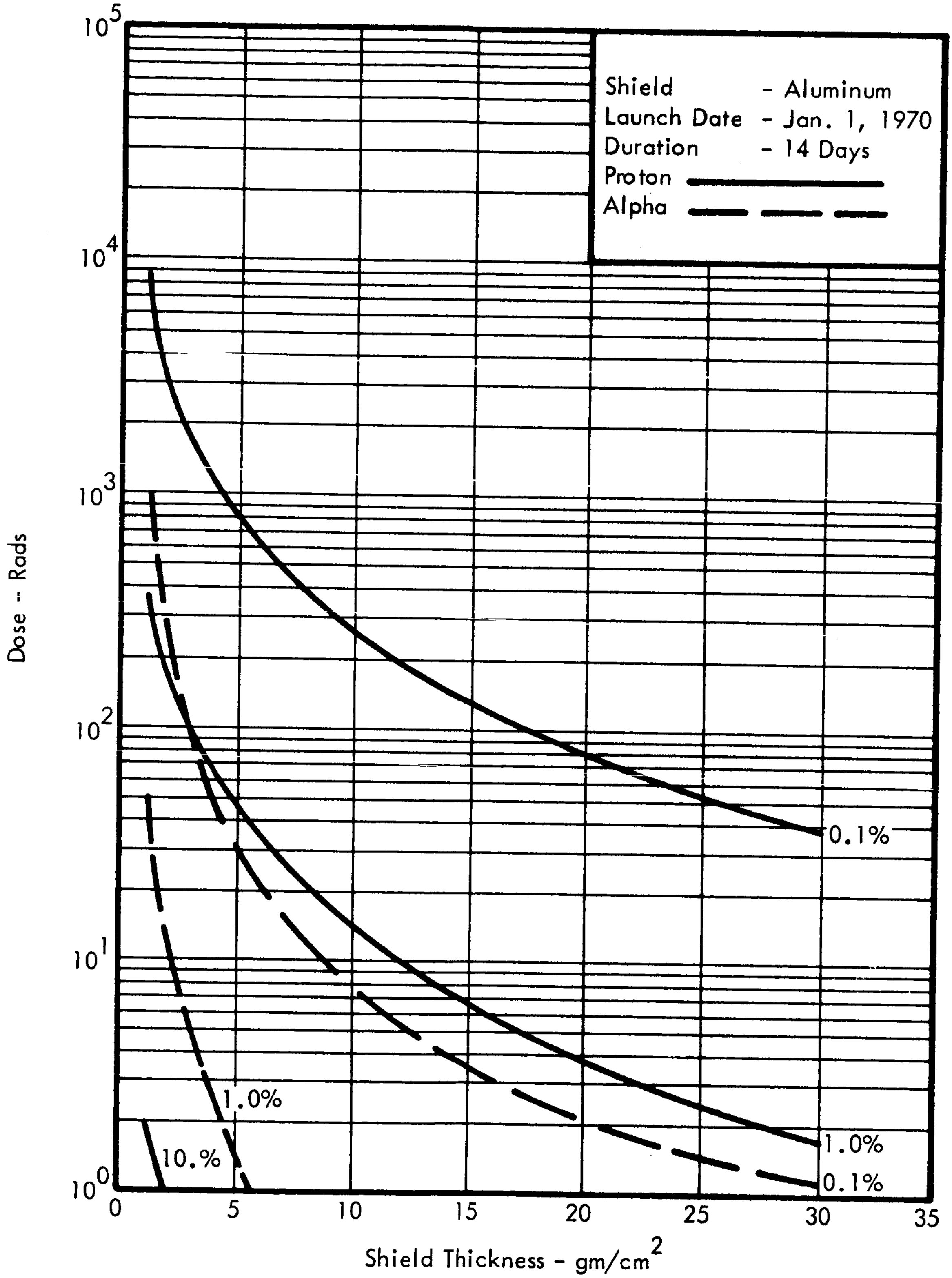

FIGURE E17 EYE DOSE VERSUS ALUMINUM SHIELD THICKNESS FOR A LUNAR MISSION

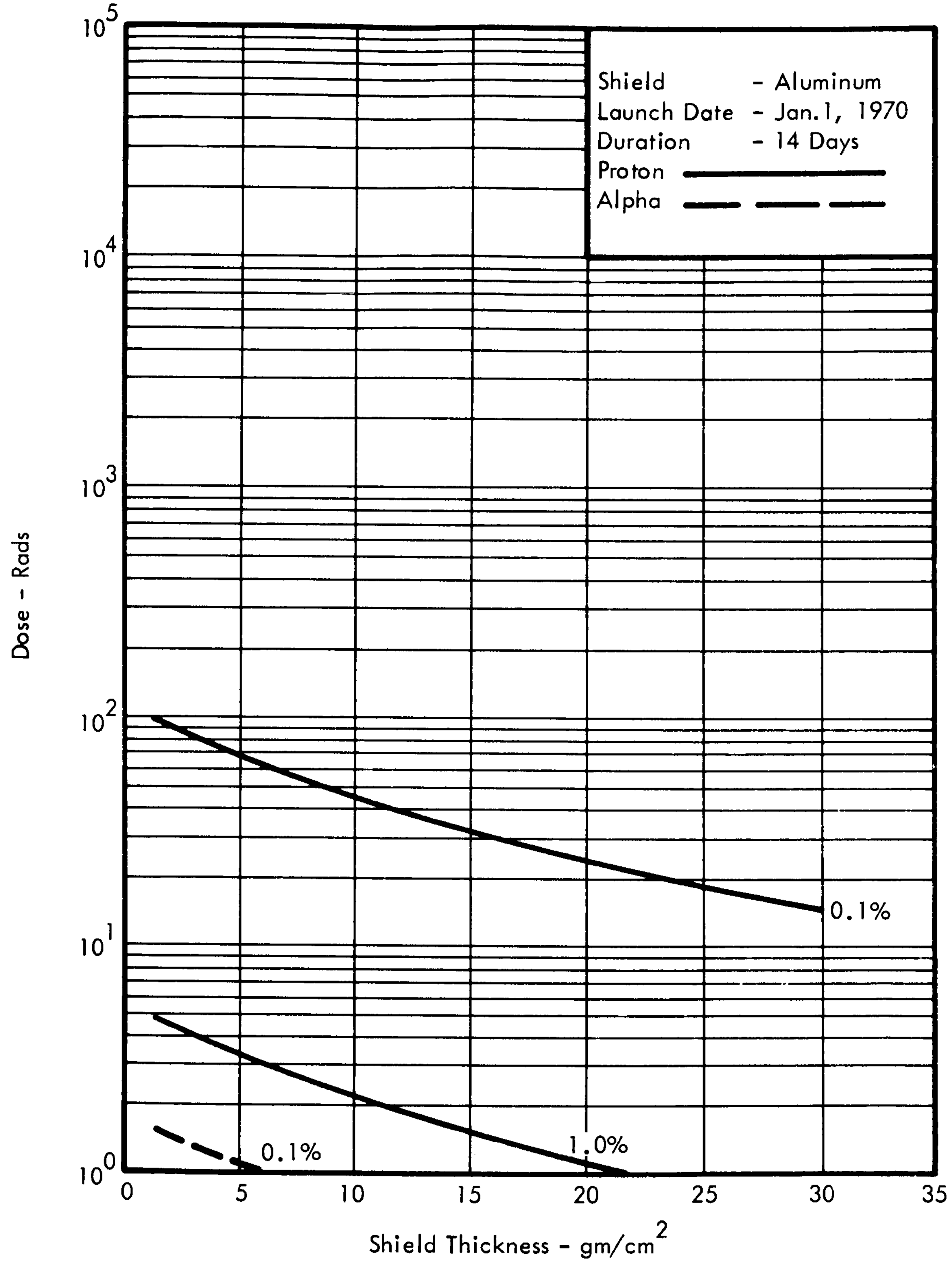

FIGURE E18 ABDOMEN DOSE VERSUS ALUMINUM SHIELD THICKNESS FOR A LUNAR MISSION

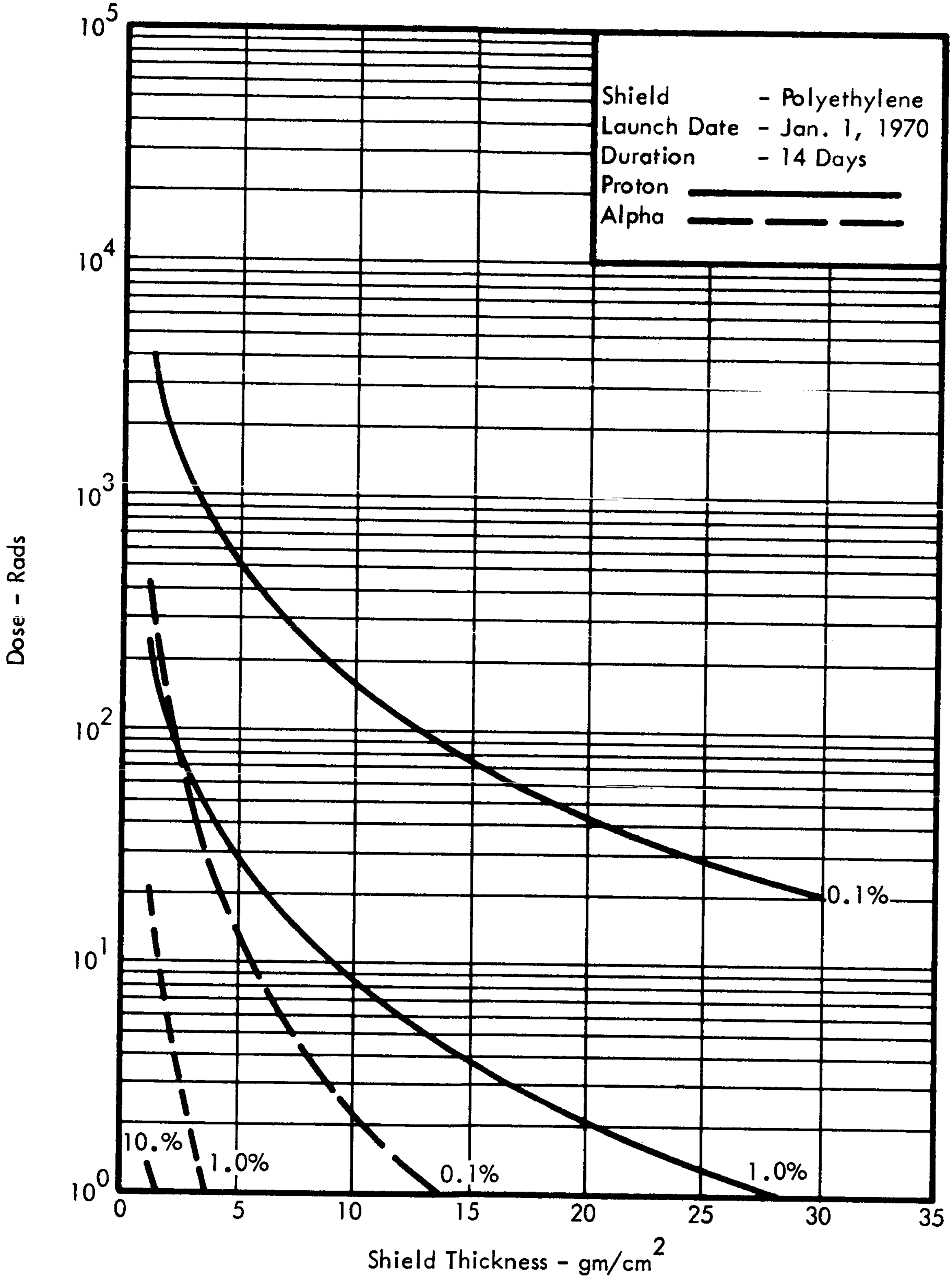

FIGURE E19 EYE DOSE VERSUS POLYETHYLENE SHIELD THICKNESS FOR A LUNAR MISSION

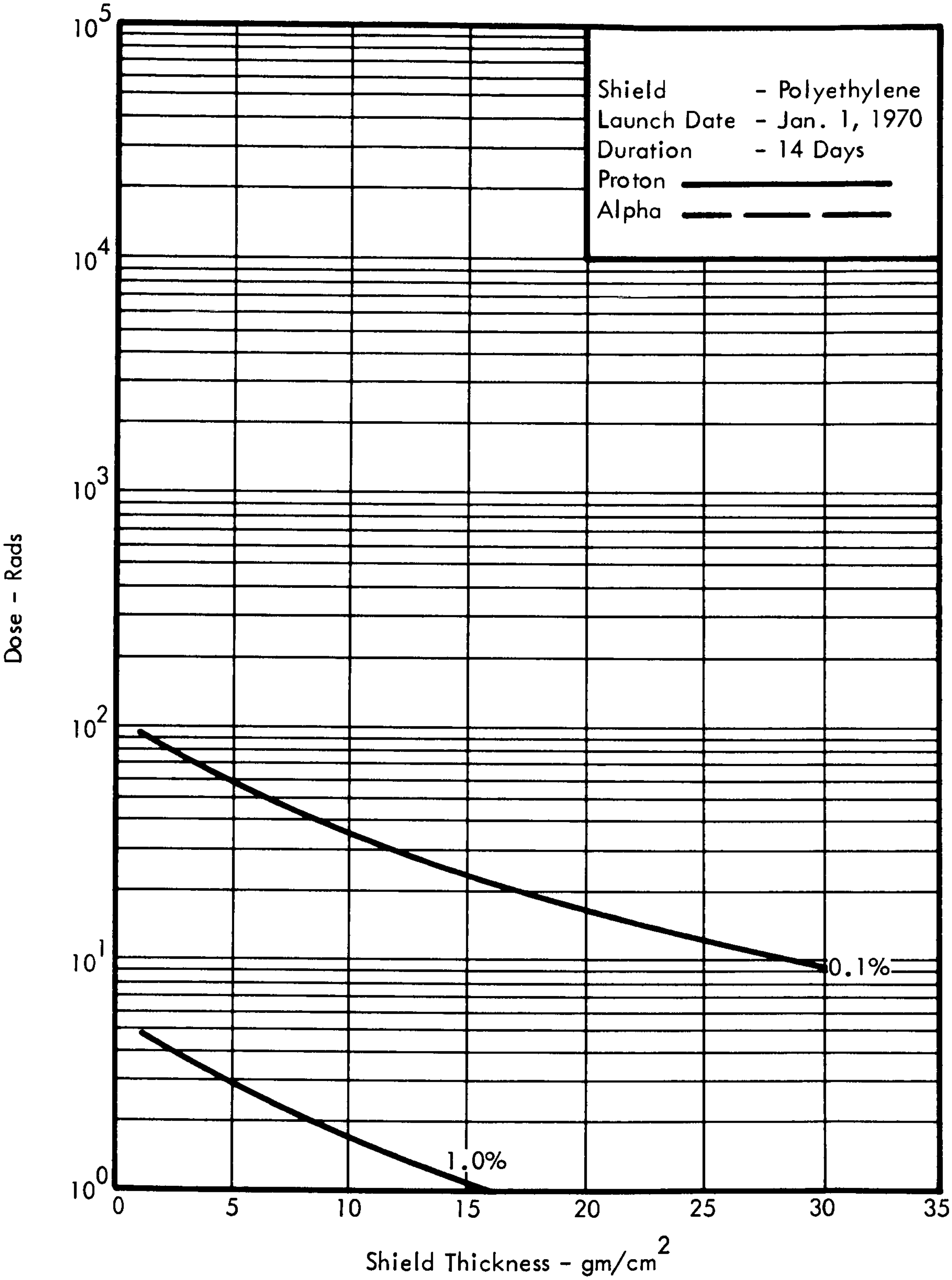

FIGURE E20 ABDOMEN DOSE VERSUS POLYETHYLENE SHIELD THICKNESS FOR A LUNAR MISSION

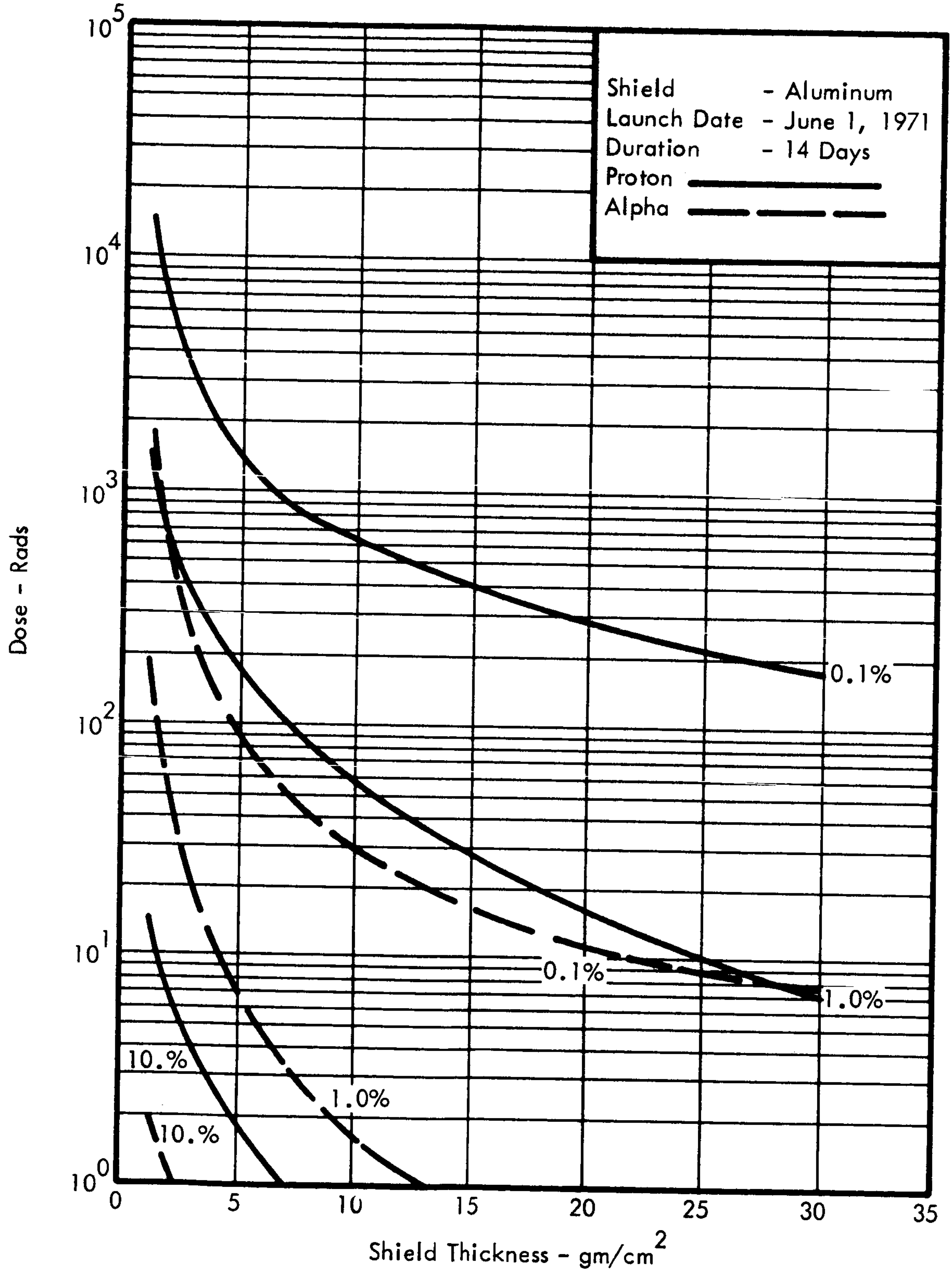

FIGURE E21 EYE DOSE VERSUS ALUMINUM SHIELD THICKNESS FOR A LUNAR MISSION

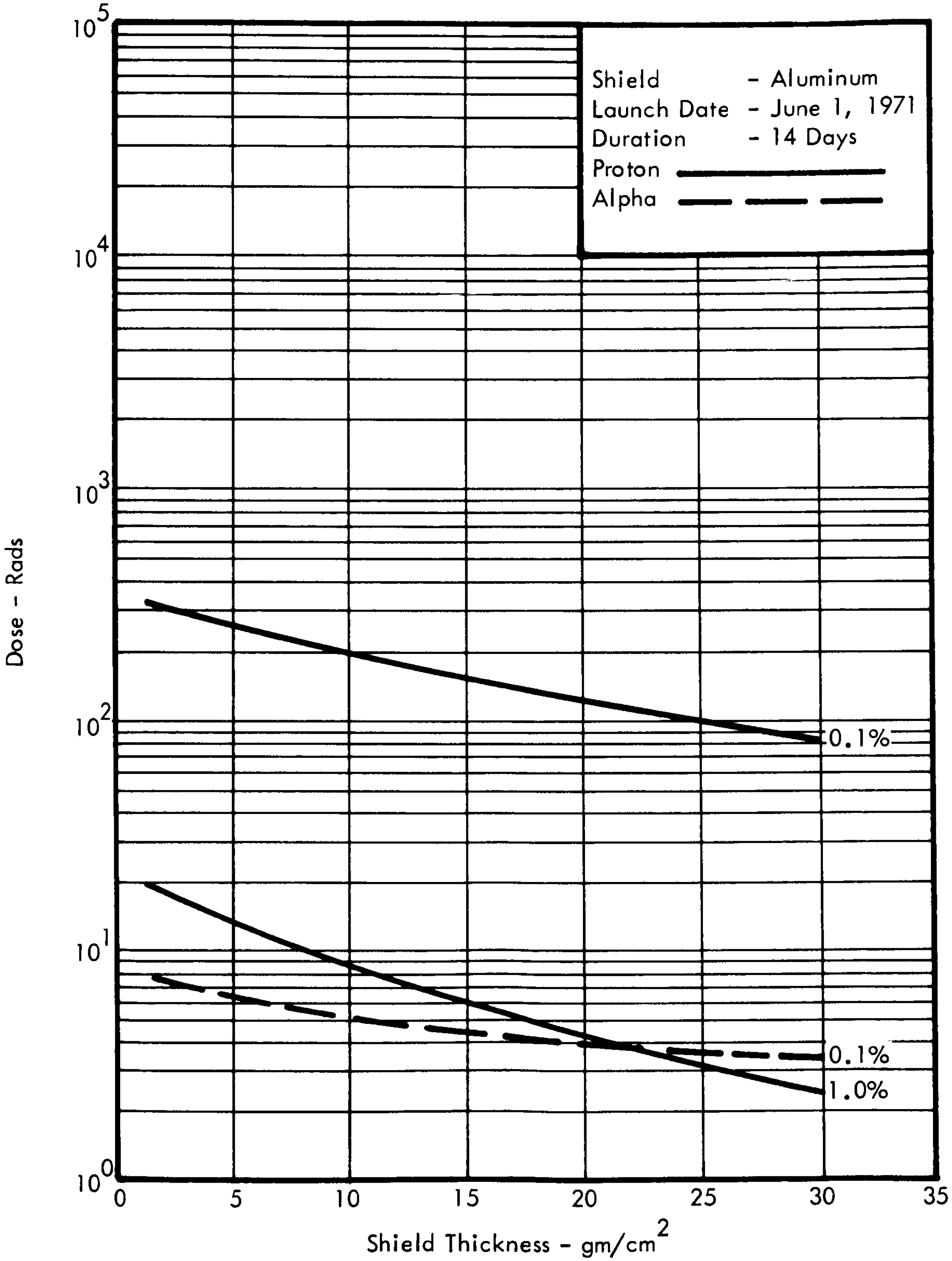

FIGURE E22 ABDOMEN DOSE VERSUS ALUMINUM SHIELD THICKNESS FOR A LUNAR MISSION

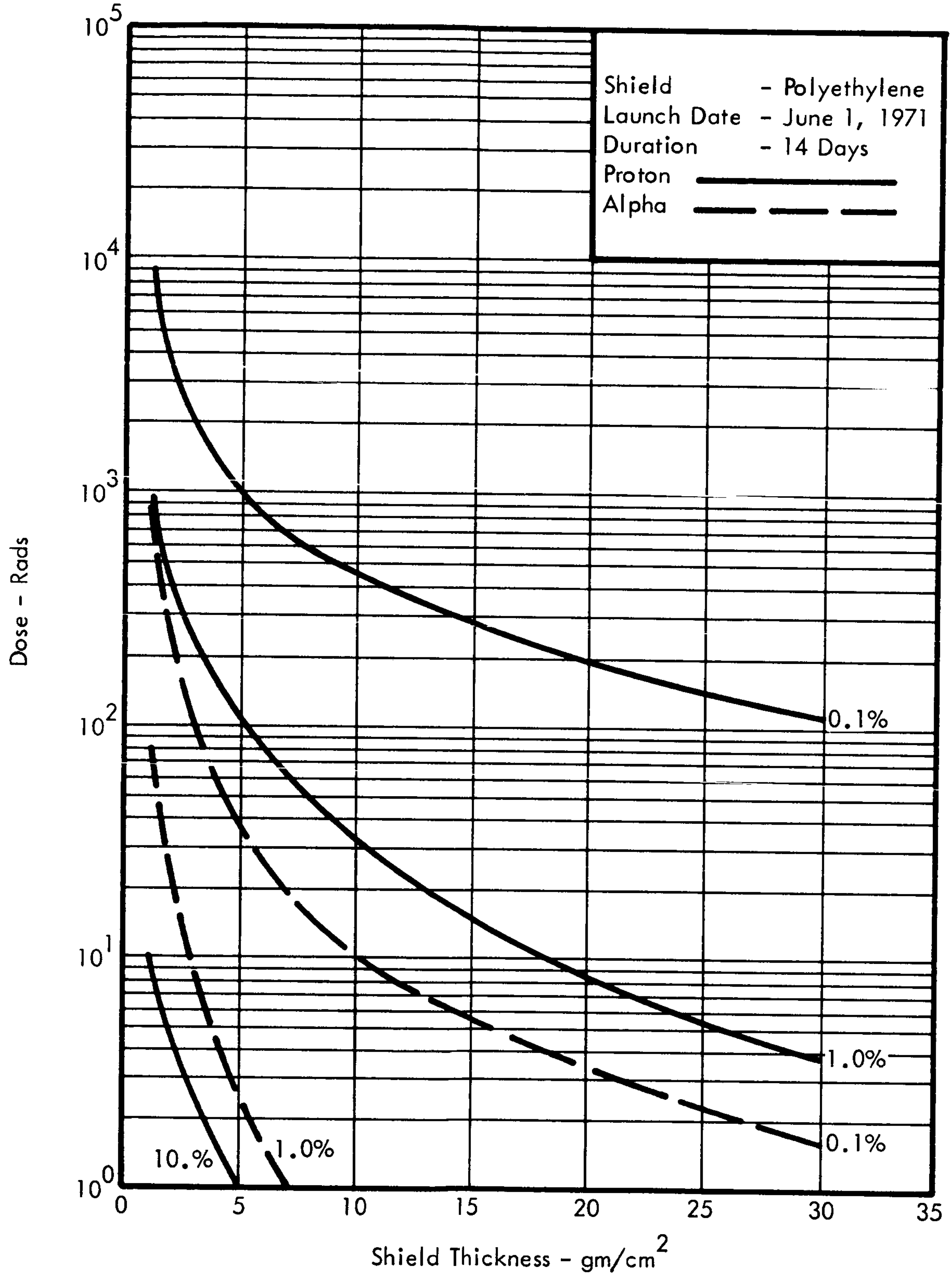

FIGURE E23 EYE DOSE VERSUS POLYETHYLENE SHIELD THICKNESS FOR A LUNAR MISSION

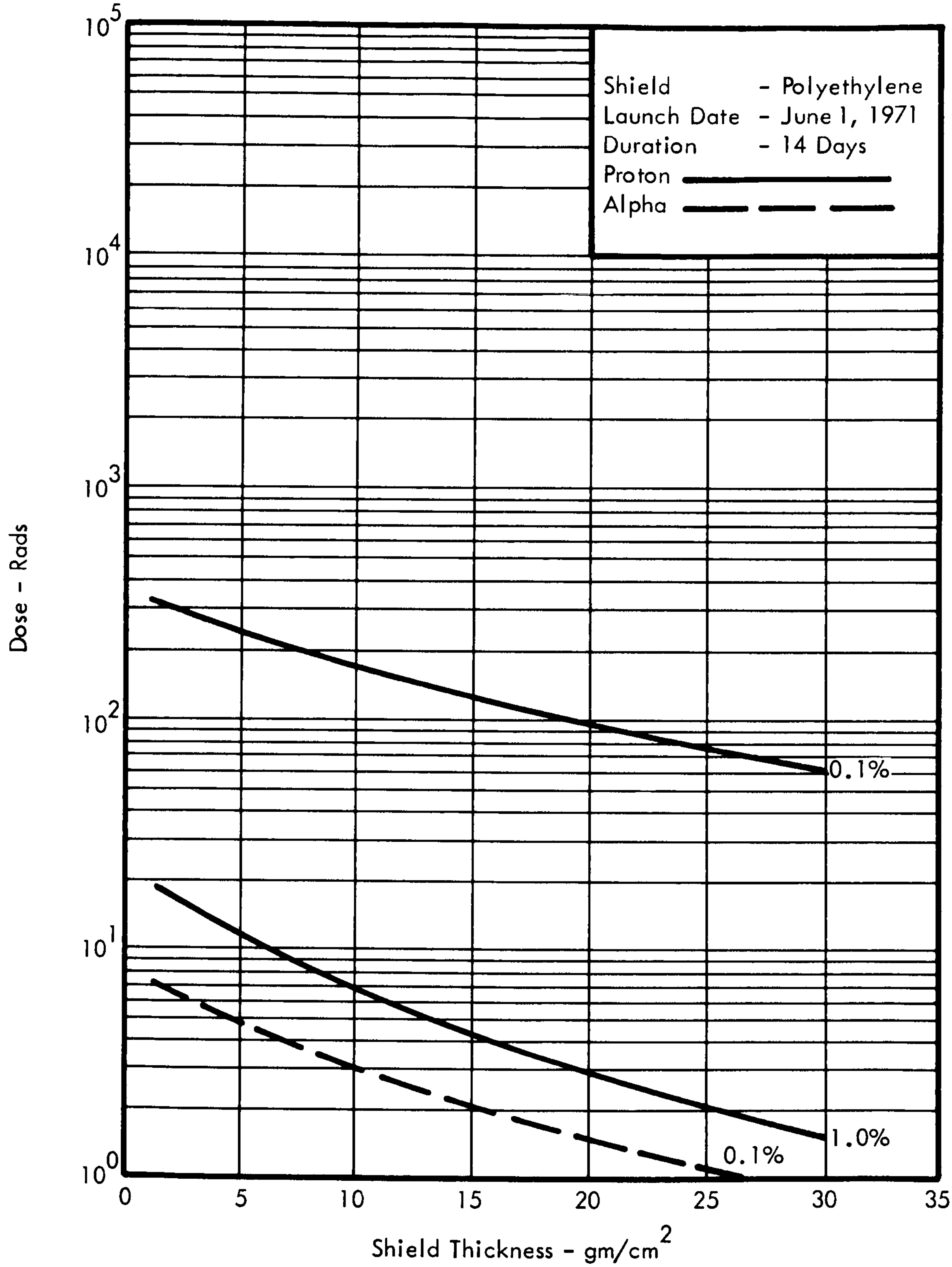

FIGURE E24 ABDOMEN DOSE VERSUS POLYETHYLENE SHIELD THICKNESS FOR A LUNAR MISSION

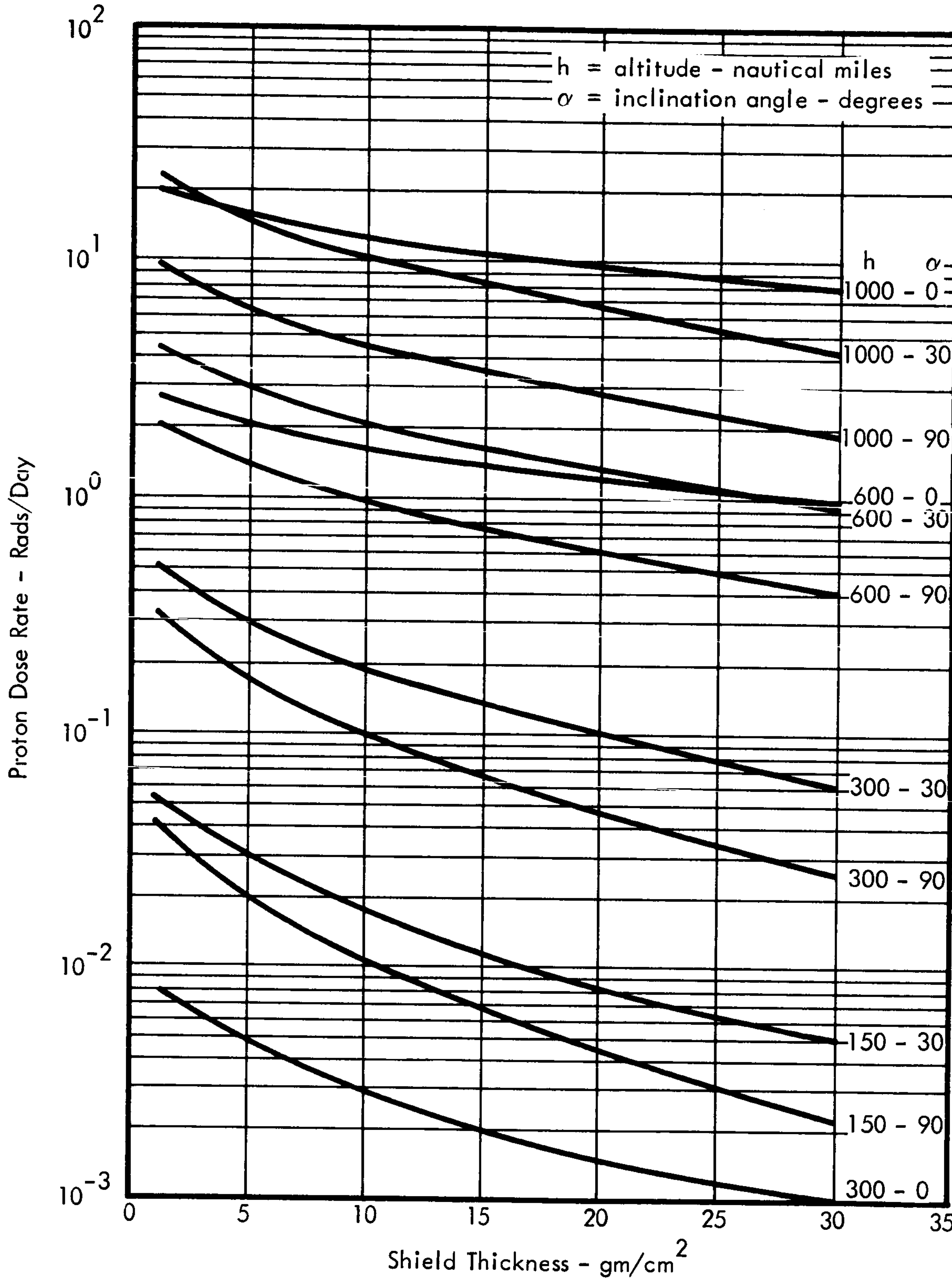

FIGURE E25 EYE DOSE RATE VERSUS ALUMINUM SHIELD THICKNESS FOR CIRCULAR ORBITS IN THE TRAPPED RADIATION BELTS - AP3

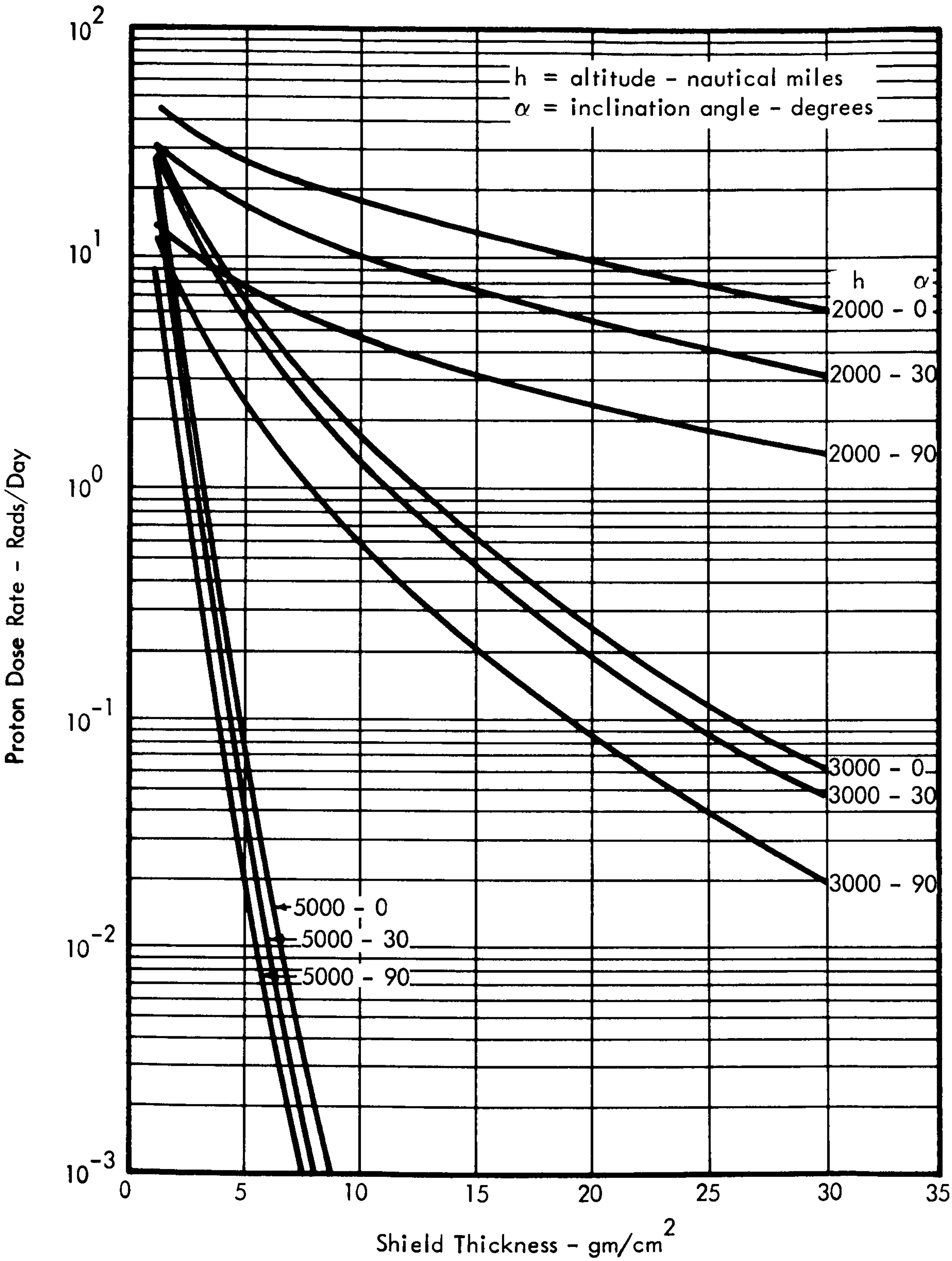

FIGURE E26 EYE DOSE RATE VERSUS ALUMINUM SHIELD THICKNESS FOR CIRCULAR ORBITS IN THE TRAPPED RADIATION BELTS - AP3

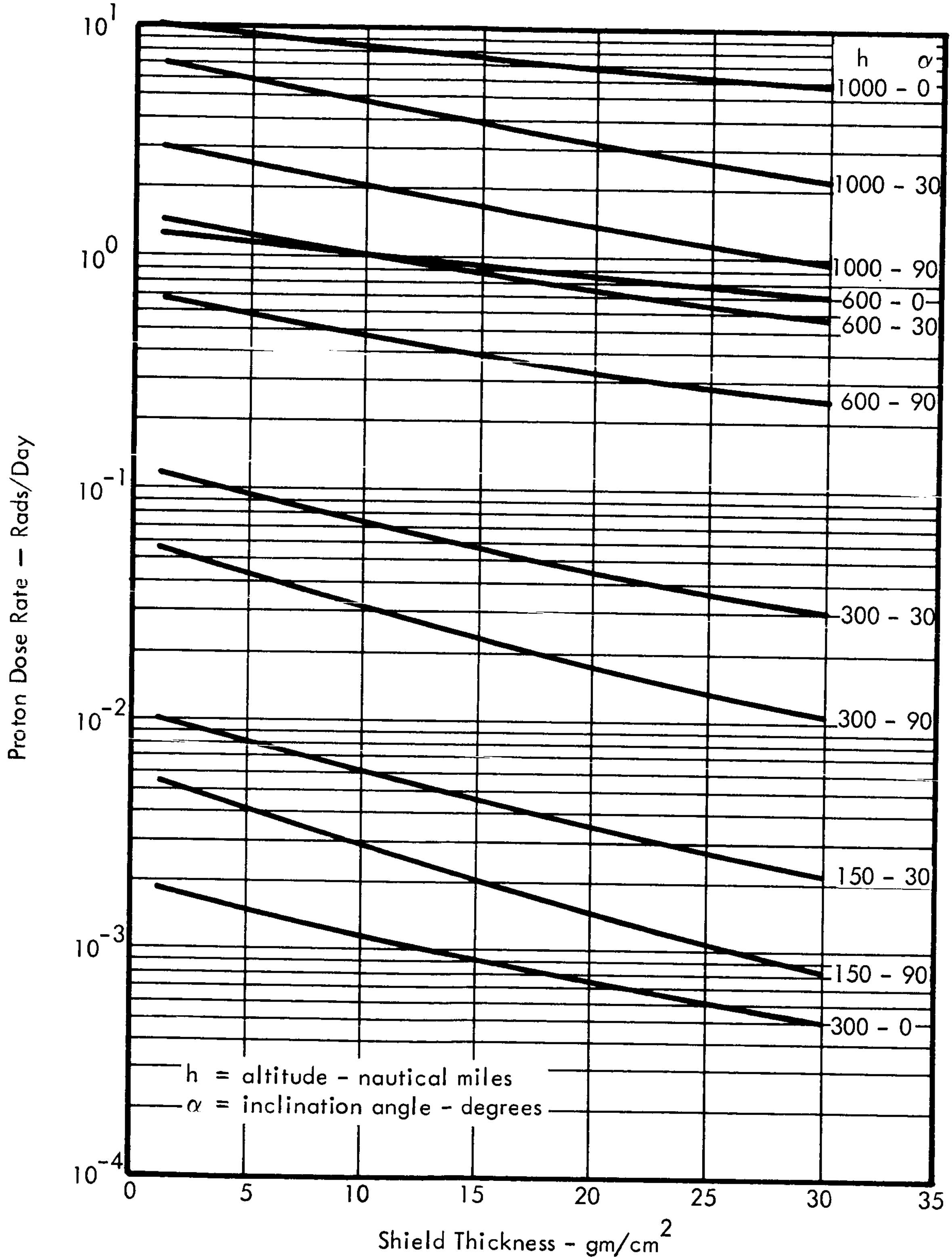

FIGURE E27 ABDOMEN DOSE RATE VERSUS ALUMINUM SHIELD THICKNESS FOR CIRCULAR ORBITS IN THE TRAPPED RADIATION BELTS - AP3

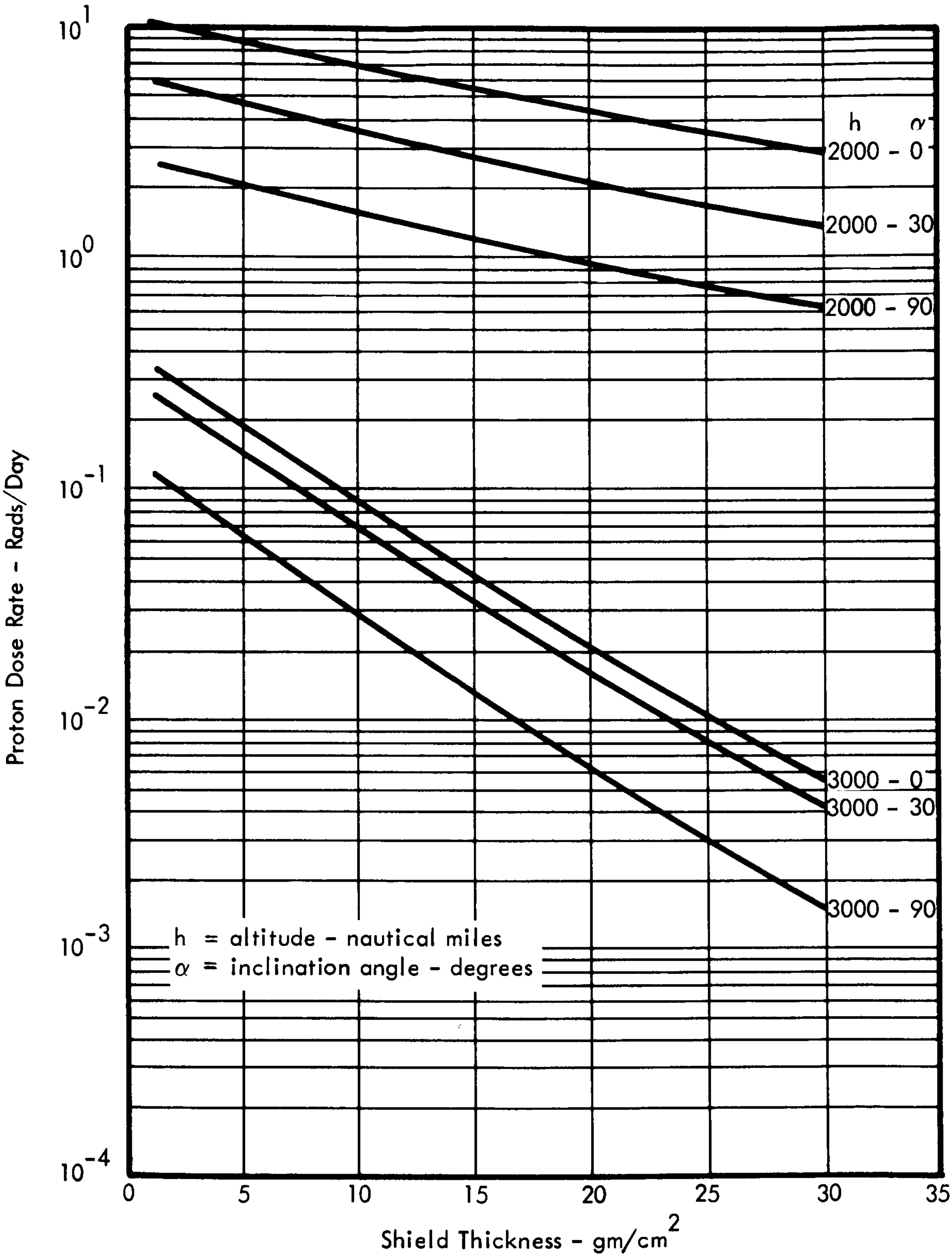

FIGURE E28 ABDOMEN DOSE RATE VERSUS ALUMINUM SHIELD THICKNESS FOR CIRCULAR ORBITS IN THE TRAPPED RADIATION BELTS - AP3

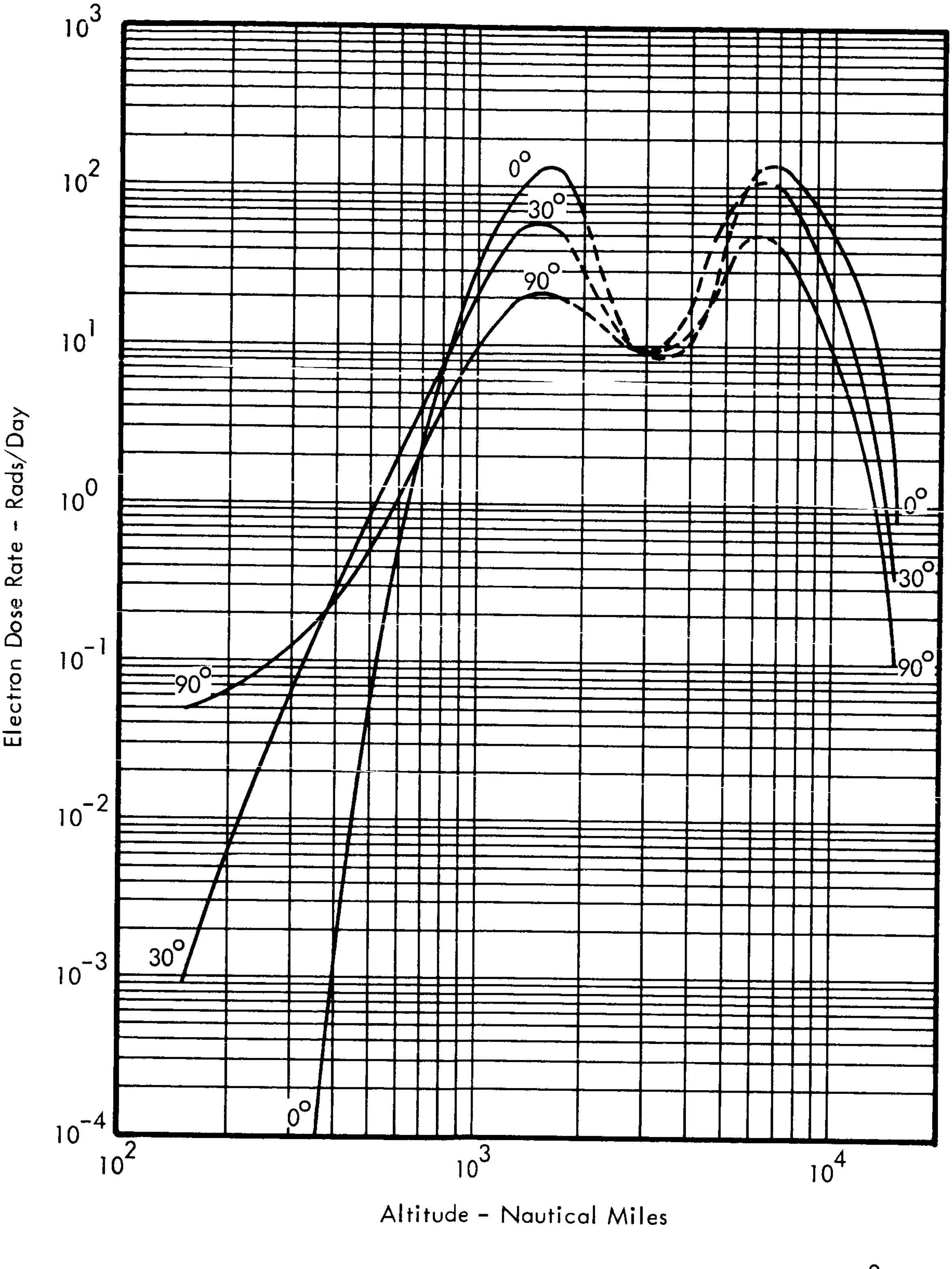

FIGURE E29 EYE DOSE RATE VERSUS ALTITUDE BEHIND ONE gm/cm^2 ALUMINUM SHIELD FOR CIRCULAR ORBITS IN THE TRAPPED RADIATION BELTS - 1968 ELECTRON ENVIRONMENT

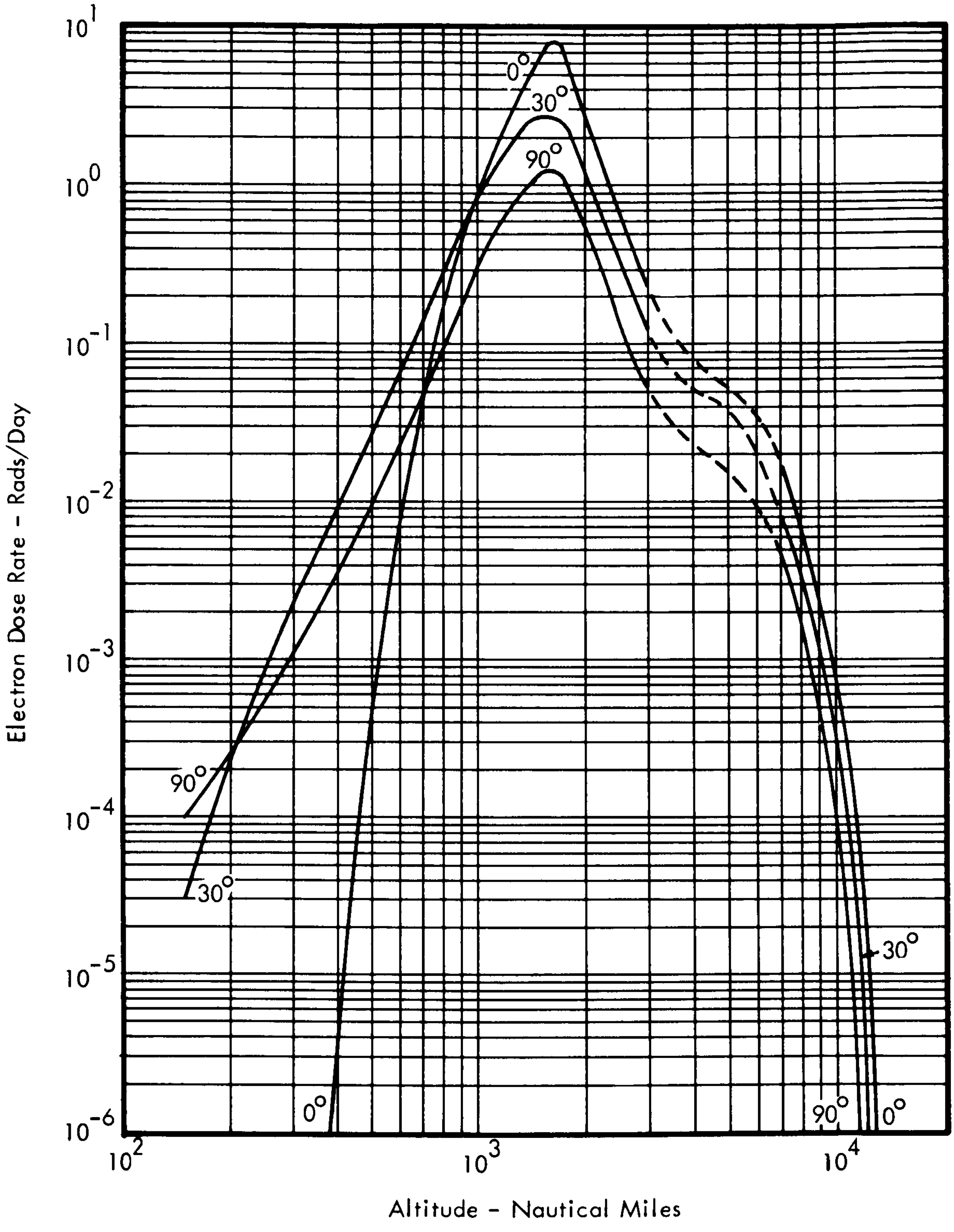

FIGURE E30 EYE DOSE RATE VERSUS ALTITUDE BEHIND FOUR gm/cm^2 ALUMINUM SHIELD FOR CIRCULAR ORBITS IN THE TRAPPED RADIATION BELTS - 1968 ELECTRON ENVIRONMENT

APPENDIX F

Charged Particle Reaction Cross Sections

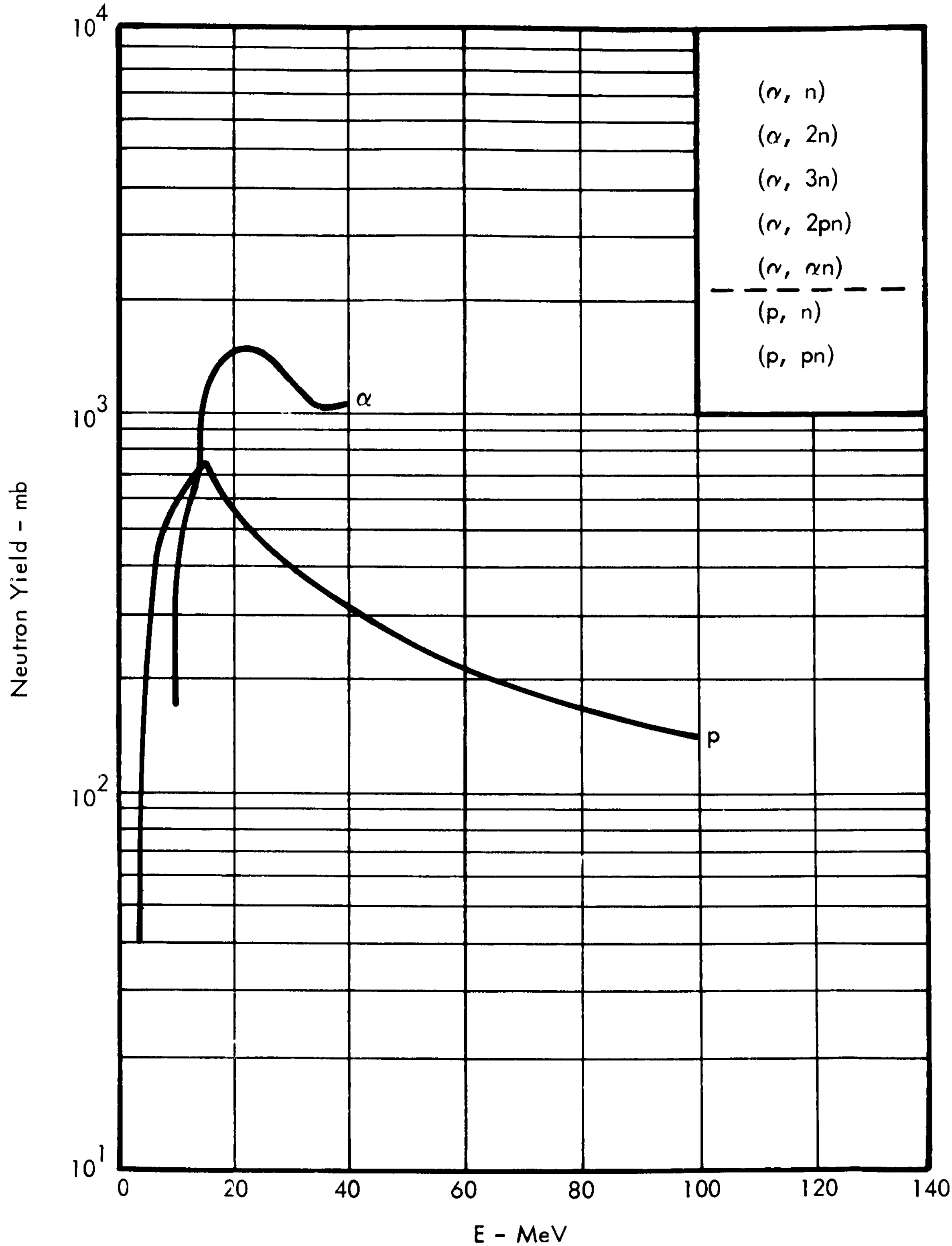

FIGURE F1 NEUTRON YIELD FROM MANGANESE - 55[30]

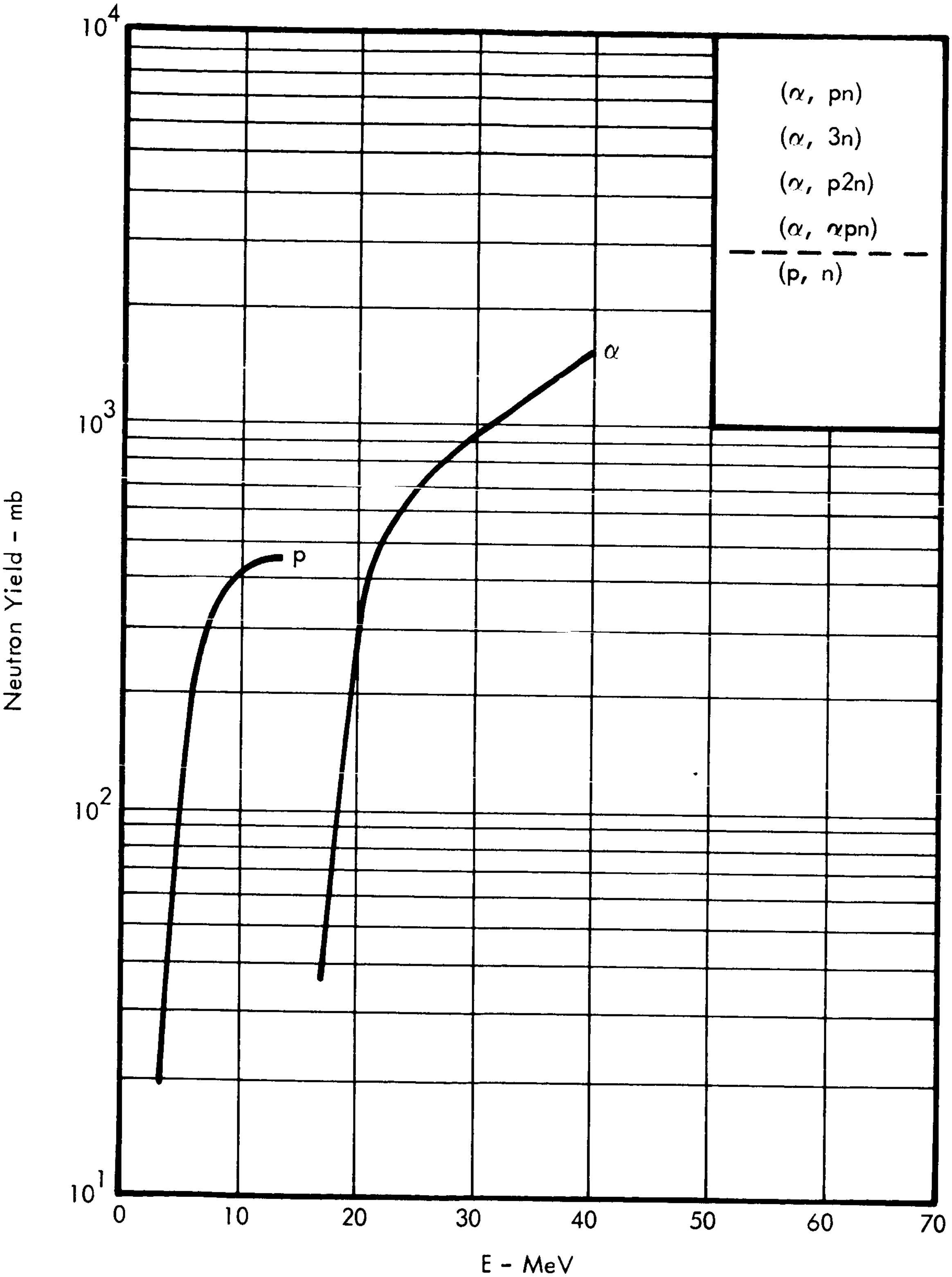

FIGURE F2 NEUTRON YIELD FROM IRON - 56[30]

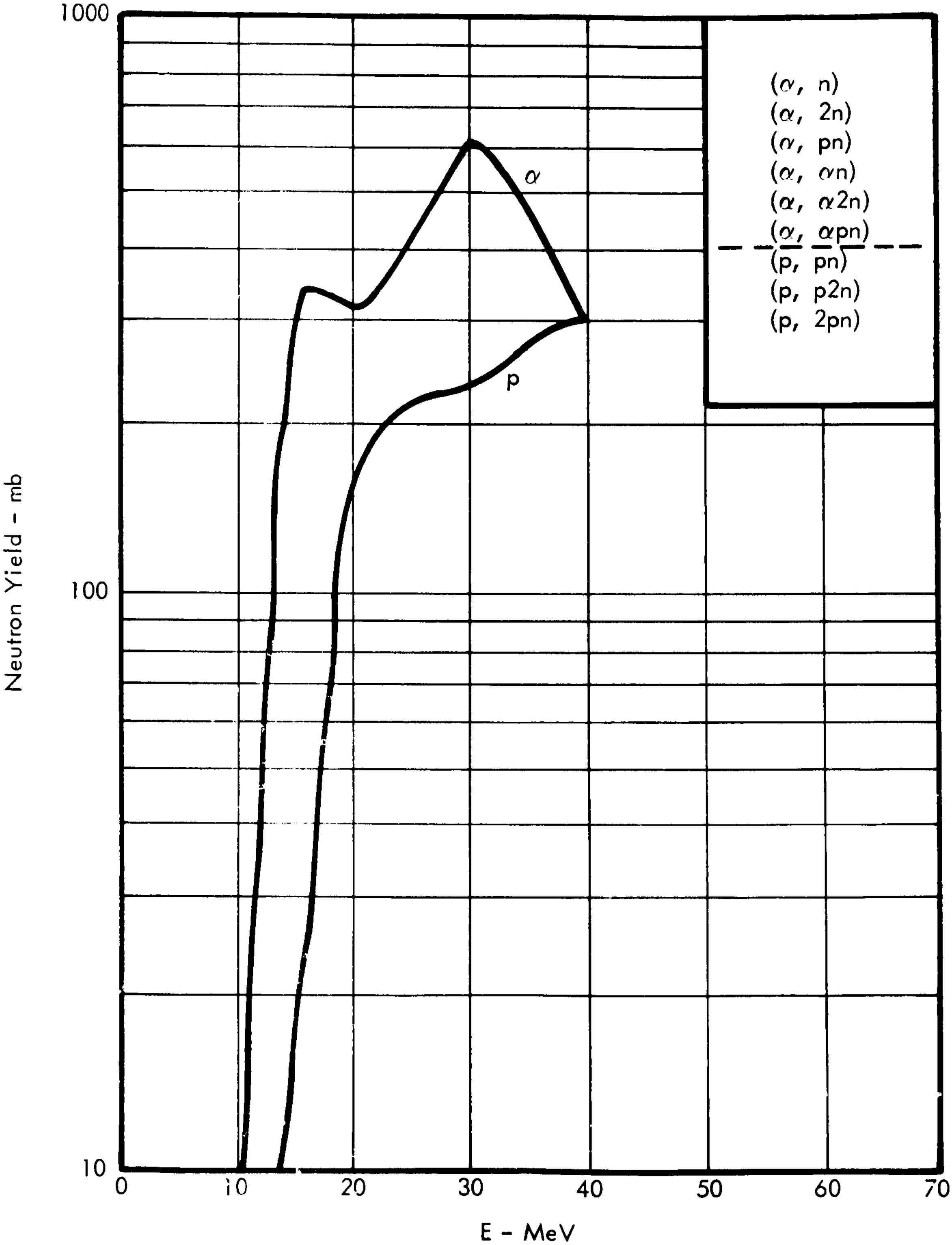

FIGURE F3 NEUTRON YIELD FROM NICKEL - 58[31]

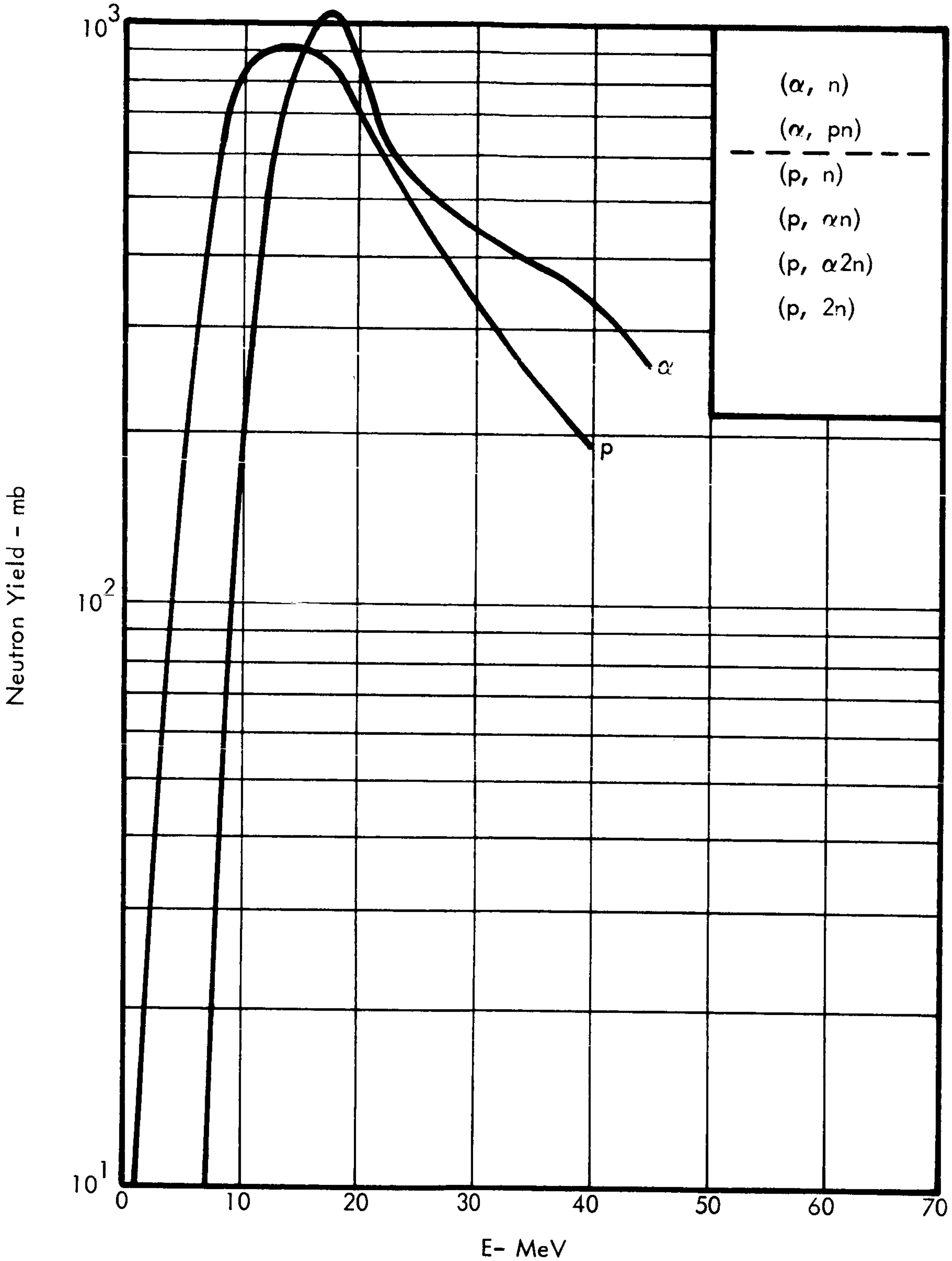

FIGURE F4 NEUTRON YIELD FROM NICKEL - 62[31]

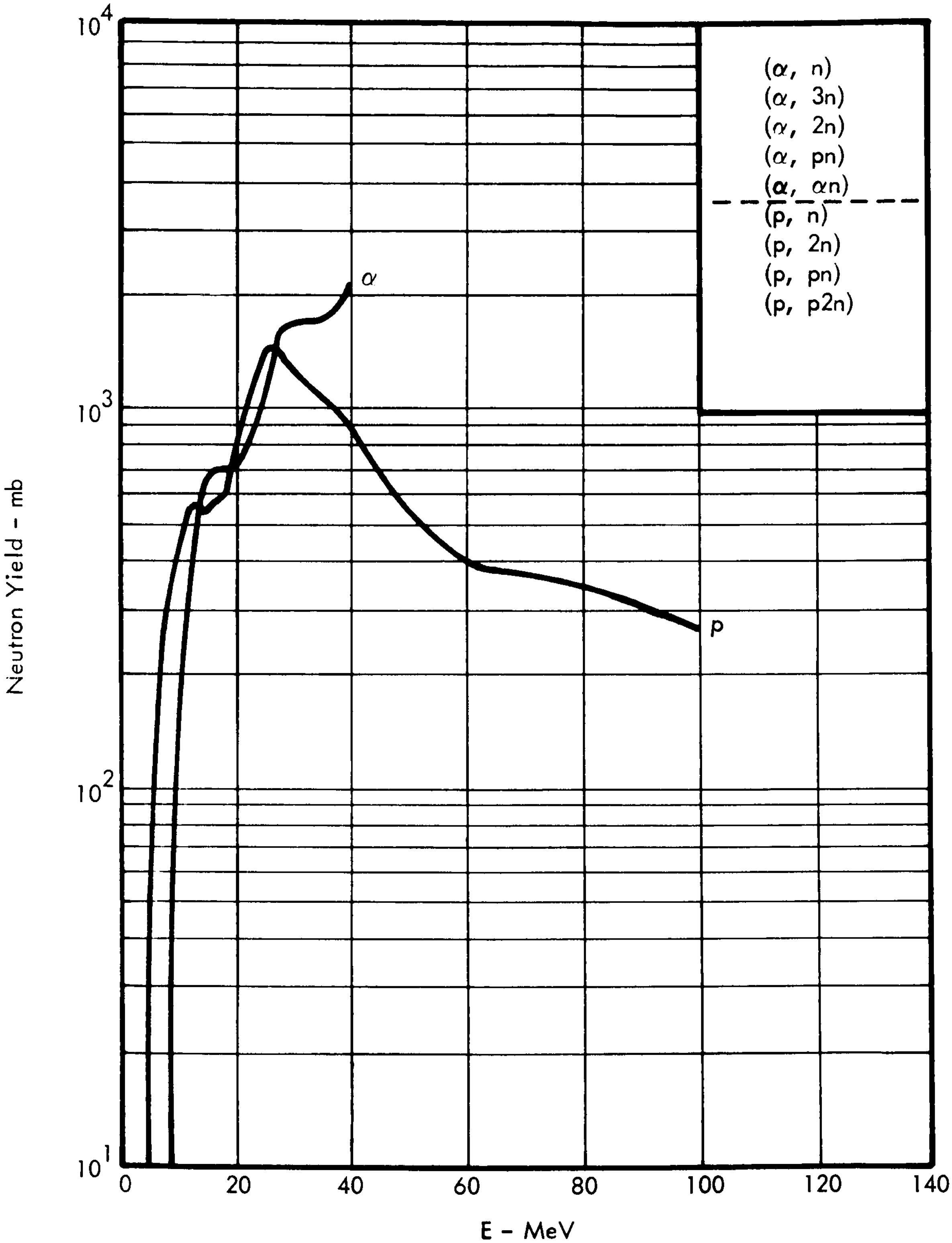

FIGURE F5 NEUTRON YIELD FROM COPPER - 63[31]

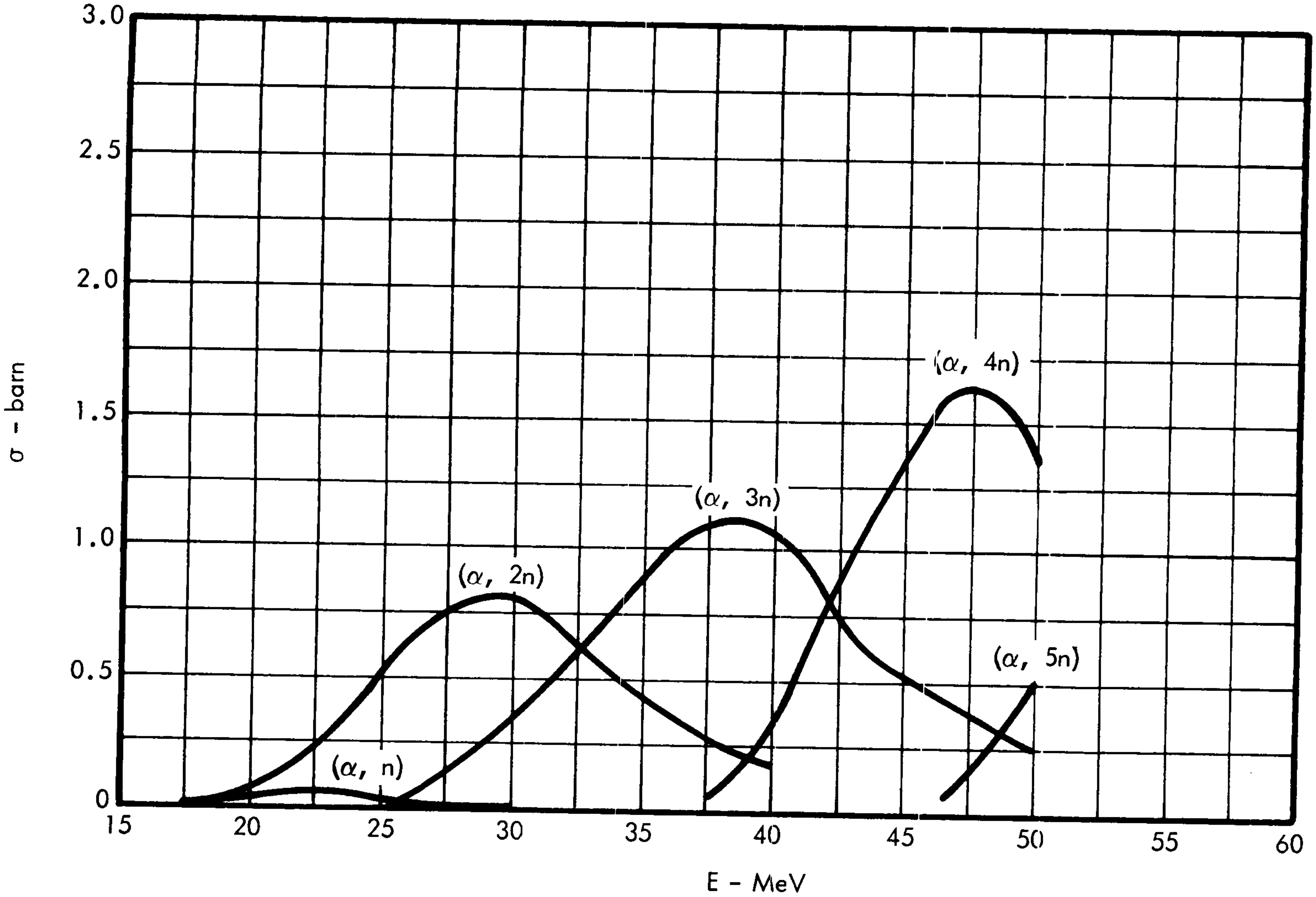

FIGURE F6 NEUTRON YIELD CROSS SECTIONS FOR ALPHA BOMBARDMENT OF GOLD - 197[38]

APPENDIX G

Flare Program Input And Output Listings

The input data in Table G1 is identical for the IBM 7094 and IBM System 360/50 Fortran IV versions of the Flare program except for the preceding $DATA card and the final end-of-file card.

The first output listing, Table G2, results from an IBM 7094 run. The second output listing, Table G3, results from an IBM System 360/50 run. Differences in the output values reflect the difference in computer word lengths.

RECEDING PAGE BLANK NOT FILMED.

TABLE G1 FLARE PROGRAM INPUT DATA

```
$DATA
1784322405
MARS MISSION.  LAUNCH - 9 OCT. 1977   443 DAYS DURATION
1400.      2600.      2050.      15.       11.       3.       .4
.5         1.
       200    2443426    2443868    2443624    2443644
351.62     498.05     192.58     474.34     0.299     0.557
```

ECEDING PAGE BLANK NOT FILMED.

RECEDING PAGE BLANK NOT FILMED.

TABLE G2 FLARE PROGRAM OUTPUT LISTING - IBM 7094

MARS MISSION. LAUNCH - 9 OCT. 1977 443 DAYS DURATION

T1	T2	T3	Y1	Y2	Y3	C	SEC	SIZE
1400.0	2600.0	2050.0	15.00000	11.00000	3.00000	0.40000	0.50000	1.00000

NMIS	JLE	JRE	JAP	JLP
200	2443426	2443868	2443624	2443644

TH1	TH2	TH3	TH4	E1	E2
351.615555	456.849999	192.560000	474.340000	0.299000	0.557000

0.00 PERCENT OF MISSIONS ENCOUNTERED NO FLUX EVENTS

T	R	F	T	R	F	T	R	F	T	R	F
649.0	0.9962	4.551E-03	650.0	0.9957	4.565E-03	651.0	0.9953	4.579E-03	652.0	0.9949	4.593E-03
653.0	0.9946	4.607E-03	654.0	0.9945	4.620E-03	655.0	0.9944	4.633E-03	656.0	0.9944	4.646E-03
657.0	0.9945	4.659E-03	658.0	0.9947	4.672E-03	659.0	0.9950	4.685E-03	660.0	0.9953	4.697E-03
661.0	0.9958	4.709E-03	662.0	0.9963	4.721E-03	663.0	0.9969	4.733E-03	664.0	0.9977	4.745E-03
665.0	0.9965	4.757E-03	666.0	0.9994	4.769E-03	667.0	1.0003	4.781E-03	668.0	1.0014	4.793E-03
669.0	1.0026	4.804E-03	670.0	1.0038	4.816E-03	671.0	1.0051	4.828E-03	672.0	1.0065	4.840E-03
673.0	1.0080	4.851E-03	674.0	1.0096	4.863E-03	675.0	1.0112	4.875E-03	676.0	1.0129	4.887E-03
677.0	1.0147	4.899E-03	678.0	1.0166	4.911E-03	679.0	1.0186	4.923E-03	680.0	1.0206	4.936E-03
681.0	1.0227	4.948E-03	682.0	1.0249	4.961E-03	683.0	1.0272	4.974E-03	684.0	1.0295	4.987E-03
685.0	1.0319	5.001E-03	686.0	1.0344	5.014E-03	687.0	1.0370	5.029E-03	688.0	1.0396	5.043E-03
689.0	1.0422	5.058E-03	690.0	1.0450	5.073E-03	691.0	1.0478	5.088E-03	692.0	1.0507	5.104E-03
693.0	1.0536	5.120E-03	694.0	1.0566	5.137E-03	695.0	1.0596	5.154E-03	696.0	1.0627	5.172E-03
697.0	1.0659	5.190E-03	698.0	1.0691	5.209E-03	699.0	1.0724	5.228E-03	700.0	1.0757	5.248E-03
701.0	1.0791	5.269E-03	702.0	1.0825	5.290E-03	703.0	1.0860	5.312E-03	704.0	1.0895	5.334E-03
705.0	1.0931	5.358E-03	706.0	1.0967	5.382E-03	707.0	1.1004	5.407E-03	708.0	1.1041	5.433E-03
709.0	1.1078	5.459E-03	710.0	1.1116	5.487E-03	711.0	1.1154	5.515E-03	712.0	1.1193	5.545E-03
713.0	1.1231	5.575E-03	714.0	1.1271	5.606E-03	715.0	1.1310	5.639E-03	716.0	1.1350	5.672E-03
717.0	1.1391	5.707E-03	718.0	1.1431	5.742E-03	719.0	1.1472	5.779E-03	720.0	1.1513	5.817E-03
721.0	1.1555	5.856E-03	722.0	1.1596	5.897E-03	723.0	1.1638	5.939E-03	724.0	1.1680	5.982E-03
725.0	1.1723	6.026E-03	726.0	1.1765	6.072E-03	727.0	1.1808	6.119E-03	728.0	1.1851	6.168E-03
729.0	1.1894	6.218E-03	730.0	1.1938	6.270E-03	731.0	1.1981	6.323E-03	732.0	1.2025	6.378E-03
733.0	1.2069	6.434E-03	734.0	1.2113	6.492E-03	735.0	1.2157	6.552E-03	736.0	1.2201	6.613E-03
737.0	1.2246	6.676E-03	738.0	1.2290	6.741E-03	739.0	1.2335	6.807E-03	740.0	1.2380	6.876E-03
741.0	1.2424	6.946E-03	742.0	1.2469	7.018E-03	743.0	1.2514	7.093E-03	744.0	1.2559	7.169E-03
745.0	1.2604	7.247E-03	746.0	1.2649	7.327E-03	747.0	1.2694	7.409E-03	748.0	1.2740	7.493E-03
749.0	1.2785	7.579E-03	750.0	1.2830	7.668E-03	751.0	1.2875	7.759E-03	752.0	1.2920	7.851E-03
753.0	1.2966	7.946E-03	754.0	1.3011	8.044E-03	755.0	1.3056	8.143E-03	756.0	1.3101	8.245E-03
757.0	1.3146	8.349E-03	758.0	1.3192	8.456E-03	759.0	1.3237	8.565E-03	760.0	1.3282	8.676E-03
761.0	1.3327	8.790E-03	762.0	1.3372	8.906E-03	763.0	1.3417	9.025E-03	764.0	1.3461	9.146E-03
765.0	1.3506	9.270E-03	766.0	1.3551	9.396E-03	767.0	1.3595	9.525E-03	768.0	1.3640	9.656E-03
769.0	1.3684	9.791E-03	770.0	1.3729	9.927E-03	771.0	1.3773	1.007E-02	772.0	1.3817	1.021E-02
773.0	1.3861	1.035E-02	774.0	1.3905	1.050E-02	775.0	1.3949	1.065E-02	776.0	1.3993	1.080E-02
777.0	1.4037	1.096E-02	778.0	1.4080	1.112E-02	779.0	1.4124	1.128E-02	780.0	1.4167	1.144E-02
781.0	1.4210	1.161E-02	782.0	1.4253	1.178E-02	783.0	1.4296	1.195E-02	784.0	1.4339	1.213E-02
785.0	1.4381	1.231E-02	786.0	1.4424	1.249E-02	787.0	1.4466	1.267E-02	788.0	1.4508	1.286E-02
789.0	1.4550	1.305E-02	790.0	1.4592	1.324E-02	791.0	1.4634	1.344E-02	792.0	1.4675	1.364E-02
793.0	1.4716	1.384E-02	794.0	1.4758	1.404E-02	795.0	1.4799	1.425E-02	796.0	1.4839	1.446E-02
797.0	1.4880	1.468E-02	798.0	1.4921	1.489E-02	799.0	1.4961	1.511E-02	800.0	1.5001	1.533E-02
801.0	1.5041	1.556E-02	802.0	1.5081	1.578E-02	803.0	1.5120	1.602E-02	804.0	1.5160	1.625E-02
805.0	1.5199	1.649E-02	806.0	1.5238	1.672E-02	807.0	1.5277	1.697E-02	808.0	1.5315	1.721E-02
809.0	1.5354	1.746E-02	810.0	1.5392	1.771E-02	811.0	1.5430	1.796E-02	812.0	1.5468	1.822E-02
813.0	1.5505	1.848E-02	814.0	1.5543	1.874E-02	815.0	1.5580	1.900E-02	816.0	1.5617	1.927E-02
817.0	1.5654	1.954E-02	818.0	1.5690	1.981E-02	819.0	1.5727	2.008E-02	820.0	1.5763	2.036E-02
821.0	1.5799	2.064E-02	822.0	1.5835	2.092E-02	823.0	1.5870	2.121E-02	824.0	1.5905	2.150E-02
825.0	1.5940	2.179E-02	826.0	1.5975	2.208E-02	827.0	1.6010	2.237E-02	828.0	1.6044	2.267E-02
829.0	1.6078	2.297E-02	830.0	1.6112	2.327E-02	831.0	1.6146	2.357E-02	832.0	1.6180	2.388E-02
833.0	1.6213	2.418E-02	834.0	1.6246	2.449E-02	835.0	1.6279	2.480E-02	836.0	1.6311	2.512E-02

TABLE G2 FLARE PROGRAM OUTPUT LISTING - IBM 7094
(Continued)

837.0	1.6344	2.543E-02	838.0	1.6376	2.575E-02	839.0	1.6408	2.607E-02	840.0	1.6439	2.639E-02
841.0	1.6471	2.671E-02	842.0	1.6502	2.704E-02	843.0	1.6533	2.736E-02	844.0	1.6564	2.769E-02
845.0	1.6594	2.802E-02	846.0	1.6624	2.835E-02	847.0	1.6654	2.868E-02	848.0	1.6654	2.902E-02
849.0	1.6654	2.935E-02	850.0	1.6654	2.969E-02	851.0	1.6654	3.002E-02	852.0	1.6654	3.036E-02
853.0	1.6654	3.070E-02	854.0	1.6654	3.104E-02	855.0	1.6654	3.138E-02	856.0	1.6654	3.172E-02
857.0	1.6654	3.207E-02	858.0	1.6654	3.241E-02	859.0	1.6654	3.275E-02	860.0	1.6654	3.310E-02
861.0	1.6654	3.344E-02	862.0	1.6654	3.379E-02	863.0	1.6654	3.413E-02	864.0	1.6654	3.448E-02
865.0	1.6654	3.482E-02	866.0	1.6654	3.517E-02	867.0	1.6654	3.552E-02	868.0	1.6569	3.586E-02
869.0	1.6544	3.621E-02	870.0	1.6519	3.656E-02	871.0	1.6493	3.690E-02	872.0	1.6466	3.725E-02
873.0	1.6439	3.759E-02	874.0	1.6411	3.794E-02	875.0	1.6383	3.828E-02	876.0	1.6354	3.862E-02
877.0	1.6324	3.897E-02	878.0	1.6294	3.931E-02	879.0	1.6264	3.965E-02	880.0	1.6232	3.999E-02
881.0	1.6200	4.033E-02	882.0	1.6168	4.067E-02	883.0	1.6135	4.100E-02	884.0	1.6101	4.134E-02
885.0	1.6067	4.167E-02	886.0	1.6032	4.201E-02	887.0	1.5996	4.234E-02	888.0	1.5960	4.267E-02
889.0	1.5923	4.299E-02	890.0	1.5886	4.332E-02	891.0	1.5848	4.365E-02	892.0	1.5809	4.397E-02
893.0	1.5770	4.429E-02	894.0	1.5730	4.461E-02	895.0	1.5690	4.492E-02	896.0	1.5649	4.524E-02
897.0	1.5607	4.555E-02	898.0	1.5565	4.586E-02	899.0	1.5522	4.616E-02	900.0	1.5478	4.647E-02
901.0	1.5434	4.677E-02	902.0	1.5389	4.707E-02	903.0	1.5343	4.736E-02	904.0	1.5297	4.766E-02
905.0	1.5251	4.795E-02	906.0	1.5203	4.823E-02	907.0	1.5155	4.852E-02	908.0	1.5106	4.880E-02
909.0	1.5057	4.908E-02	910.0	1.5007	4.935E-02	911.0	1.4957	4.962E-02	912.0	1.4905	4.989E-02
913.0	1.4853	5.015E-02	914.0	1.4801	5.041E-02	915.0	1.4748	5.067E-02	916.0	1.4694	5.092E-02
917.0	1.4639	5.117E-02	918.0	1.4584	5.142E-02	919.0	1.4528	5.166E-02	920.0	1.4471	5.189E-02
921.0	1.4414	5.213E-02	922.0	1.4356	5.236E-02	923.0	1.4298	5.258E-02	924.0	1.4238	5.280E-02
925.0	1.4178	5.302E-02	926.0	1.4118	5.323E-02	927.0	1.4056	5.344E-02	928.0	1.3994	5.364E-02
929.0	1.3932	5.384E-02	930.0	1.3868	5.403E-02	931.0	1.3804	5.422E-02	932.0	1.3739	5.441E-02
933.0	1.3674	5.459E-02	934.0	1.3608	5.476E-02	935.0	1.3541	5.493E-02	936.0	1.3473	5.510E-02
937.0	1.3405	5.526E-02	938.0	1.3336	5.541E-02	939.0	1.3266	5.556E-02	940.0	1.3196	5.571E-02
941.0	1.3124	5.585E-02	942.0	1.3052	5.598E-02	943.0	1.2980	5.611E-02	944.0	1.2906	5.624E-02
945.0	1.2832	5.636E-02	946.0	1.2757	5.647E-02	947.0	1.2682	5.658E-02	948.0	1.2605	5.669E-02
949.0	1.2528	5.679E-02	950.0	1.2450	5.688E-02	951.0	1.2372	5.697E-02	952.0	1.2293	5.705E-02
953.0	1.2212	5.713E-02	954.0	1.2132	5.720E-02	955.0	1.2050	5.727E-02	956.0	1.1968	5.733E-02
957.0	1.1885	5.739E-02	958.0	1.1801	5.744E-02	959.0	1.1716	5.749E-02	960.0	1.1631	5.753E-02
961.0	1.1545	5.756E-02	962.0	1.1458	5.759E-02	963.0	1.1370	5.762E-02	964.0	1.1282	5.764E-02
965.0	1.1192	5.765E-02	966.0	1.1103	5.766E-02	967.0	1.1012	5.766E-02	968.0	1.0920	5.766E-02
969.0	1.0828	5.766E-02	970.0	1.0735	5.764E-02	971.0	1.0641	5.763E-02	972.0	1.0547	5.760E-02
973.0	1.0452	5.758E-02	974.0	1.0356	5.755E-02	975.0	1.0259	5.751E-02	976.0	1.0161	5.747E-02
977.0	1.0063	5.742E-02	978.0	0.9964	5.737E-02	979.0	0.9865	5.731E-02	980.0	0.9764	5.725E-02
981.0	0.9663	5.718E-02	982.0	0.9562	5.711E-02	983.0	0.9459	5.704E-02	984.0	0.9356	5.696E-02
985.0	0.9252	5.687E-02	986.0	0.9148	5.678E-02	987.0	0.9043	5.669E-02	988.0	0.8938	5.659E-02
989.0	0.8832	5.649E-02	990.0	0.8725	5.638E-02	991.0	0.8618	5.627E-02	992.0	0.8510	5.616E-02
993.0	0.8402	5.604E-02	994.0	0.8294	5.592E-02	995.0	0.8185	5.579E-02	996.0	0.8076	5.566E-02
997.0	0.7966	5.553E-02	998.0	0.7857	5.539E-02	999.0	0.7747	5.525E-02	1000.0	0.7637	5.511E-02
1001.0	0.7527	5.496E-02	1002.0	0.7417	5.481E-02	1003.0	0.7307	5.466E-02	1004.0	0.7197	5.450E-02
1005.0	0.7088	5.434E-02	1006.0	0.6979	5.418E-02	1007.0	0.6870	5.402E-02	1008.0	0.6763	5.385E-02
1009.0	0.6656	5.368E-02	1010.0	0.6549	5.351E-02	1011.0	0.6444	5.334E-02	1012.0	0.6341	5.316E-02
1013.0	0.6238	5.298E-02	1014.0	0.6138	5.281E-02	1015.0	0.6039	5.262E-02	1016.0	0.5942	5.244E-02
1017.0	0.5847	5.225E-02	1018.0	0.5755	5.207E-02	1019.0	0.5666	5.188E-02	1020.0	0.5580	5.169E-02
1021.0	0.5497	5.150E-02	1022.0	0.5418	5.131E-02	1023.0	0.5343	5.112E-02	1024.0	0.5273	5.093E-02
1025.0	0.5207	5.074E-02	1026.0	0.5146	5.055E-02	1027.0	0.5090	5.035E-02	1028.0	0.5040	5.016E-02
1029.0	0.4995	4.997E-02	1030.0	0.4957	4.978E-02	1031.0	0.4925	4.959E-02	1032.0	0.4899	4.939E-02
1033.0	0.4881	4.920E-02	1034.0	0.4869	4.901E-02	1035.0	0.4864	4.882E-02	1036.0	0.4866	4.864E-02
1037.0	0.4875	4.845E-02	1038.0	0.4891	4.826E-02	1039.0	0.4913	4.808E-02	1040.0	0.4942	4.790E-02
1041.0	0.4978	4.772E-02	1042.0	0.5020	4.754E-02	1043.0	0.5068	4.736E-02	1044.0	0.5121	4.719E-02
1045.0	0.5180	4.702E-02	1046.0	0.5244	4.685E-02	1047.0	0.5313	4.668E-02	1048.0	0.5386	4.651E-02
1049.0	0.5463	4.635E-02	1050.0	0.5544	4.620E-02	1051.0	0.5629	4.604E-02	1052.0	0.5717	4.589E-02
1053.0	0.5808	4.574E-02	1054.0	0.5901	4.560E-02	1055.0	0.5997	4.546E-02	1056.0	0.6095	4.532E-02
1057.0	0.6195	4.519E-02	1058.0	0.6297	4.506E-02	1059.0	0.6400	4.493E-02	1060.0	0.6505	4.481E-02
1061.0	0.6610	4.470E-02	1062.0	0.6717	4.459E-02	1063.0	0.6824	4.449E-02	1064.0	0.6933	4.438E-02
1065.0	0.7041	4.429E-02	1066.0	0.7151	4.420E-02	1067.0	0.7260	4.412E-02	1068.0	0.7370	4.404E-02
1069.0	0.7480	4.397E-02	1070.0	0.7590	4.390E-02	1071.0	0.7700	4.384E-02	1072.0	0.7810	4.378E-02
1073.0	0.7920	4.373E-02	1074.0	0.8029	4.369E-02	1075.0	0.8138	4.366E-02	1076.0	0.8247	4.363E-02
1077.0	0.8356	4.361E-02	1078.0	0.8464	4.359E-02	1079.0	0.8572	4.358E-02	1080.0	0.8679	4.358E-02
1081.0	0.8786	4.359E-02	1082.0	0.8893	4.360E-02	1083.0	0.8998	4.362E-02	1084.0	0.9104	4.365E-02

TABLE G2 FLARE PROGRAM OUTPUT LISTING - IBM 7094
(Continued)

1085.0	0.9208	4.368E-02	1086.0	0.9312	4.373E-02	1087.0	0.9415	4.378E-02	1088.0	0.9518	4.384E-02
1089.0	0.9620	4.390E-02	1090.0	0.9721	4.398E-02	1091.0	0.9822	4.406E-02			

INPUT RN	FIRST RN	LAST RN
1764322405	1764322405	11533795569

TABLE G2 FLARE PROGRAM OUTPUT LISTING - IBM 7094
(Continued)

PROTON FLUX FREQUENCY DISTRIBUTION
(PERCENT OF MISSIONS WHICH ENCOUNTER FLUXES GREATER THAN OR EQUAL TO PHI(E) - P/CM**2-MISSION)

				ENERGY-MEV					
PHI	10.00	30.00	50.00	100.00	200.00	400.00	1000.00	1500.00	PHI
1.0E 02	100.00	100.00	100.00	100.00	100.00	100.00	89.50	61.50	1.0E 02
2.0E 02	100.00	100.00	100.00	100.00	100.00	100.00	87.00	46.00	2.0E 02
4.0E 02	100.00	100.00	100.00	100.00	100.00	100.00	80.00	35.50	4.0E 02
6.0E 02	100.00	100.00	100.00	100.00	100.00	100.00	76.50	29.00	6.0E 02
8.0E 02	100.00	100.00	100.00	100.00	100.00	100.00	73.00	24.50	8.0E 02
1.0E 03	100.00	100.00	100.00	100.00	100.00	100.00	70.00	22.00	1.0E 03
2.0E 03	100.00	100.00	100.00	100.00	100.00	100.00	61.00	15.50	2.0E 03
4.0E 03	100.00	100.00	100.00	100.00	100.00	100.00	45.50	10.00	4.0E 03
6.0E 03	100.00	100.00	100.00	100.00	100.00	99.00	39.00	7.50	6.0E 03
8.0E 03	100.00	100.00	100.00	100.00	100.00	98.50	33.50	7.50	8.0E 03
1.0E 04	100.00	100.00	100.00	100.00	100.00	98.00	30.50	6.00	1.0E 04
2.0E 04	100.00	100.00	100.00	100.00	100.00	91.50	21.00	6.00	2.0E 04
4.0E 04	100.00	100.00	100.00	100.00	100.00	86.00	15.00	4.00	4.0E 04
6.0E 04	100.00	100.00	100.00	100.00	100.00	81.50	11.50	3.00	6.0E 04
8.0E 04	100.00	100.00	100.00	100.00	100.00	76.50	8.50	2.00	8.0E 04
1.0E 05	100.00	100.00	100.00	100.00	99.00	72.00	8.50	1.50	1.0E 05
2.0E 05	100.00	100.00	100.00	100.00	98.00	60.00	6.00	1.00	2.0E 05
4.0E 05	100.00	100.00	100.00	100.00	91.50	45.50	4.50	0.50	4.0E 05
6.0E 05	100.00	100.00	100.00	99.50	86.00	38.50	4.00	0.50	6.0E 05
8.0E 05	100.00	100.00	100.00	99.50	82.50	35.00	3.00	0.50	8.0E 05
1.0E 06	100.00	100.00	100.00	99.00	78.00	30.50	3.00	0.50	1.0E 06
2.0E 06	100.00	100.00	99.50	96.00	59.50	21.50	1.50	0.00	2.0E 06
4.0E 06	100.00	100.00	99.00	88.00	51.00	14.00	0.50	0.00	4.0E 06
6.0E 06	100.00	99.50	97.50	81.50	41.50	12.50	0.50	0.00	6.0E 06
8.0E 06	100.00	99.00	97.50	75.50	38.00	10.00	0.50	0.00	8.0E 06
1.0E 07	100.00	99.00	96.00	70.50	32.00	8.50	0.50	0.00	1.0E 07
2.0E 07	100.00	97.00	88.00	58.00	23.50	7.50	0.00	0.00	2.0E 07
4.0E 07	98.50	90.00	77.50	42.00	14.50	4.50	0.00	0.00	4.0E 07
6.0E 07	97.50	86.00	71.00	33.00	13.50	2.50	0.00	0.00	6.0E 07
8.0E 07	97.00	80.50	69.50	31.00	11.00	1.00	0.00	0.00	8.0E 07
1.0E 08	96.00	78.00	58.50	27.00	9.00	1.00	0.00	0.00	1.0E 08
2.0E 08	89.00	64.50	42.00	17.00	7.50	0.00	0.00	0.00	2.0E 08
4.0E 08	79.50	47.00	29.00	11.50	3.50	0.00	0.00	0.00	4.0E 08
6.0E 08	72.00	38.50	24.00	9.50	2.50	0.00	0.00	0.00	6.0E 08
8.0E 08	64.50	33.50	18.00	8.00	2.00	0.00	0.00	0.00	8.0E 08
1.0E 09	60.00	32.50	14.50	6.50	2.00	0.00	0.00	0.00	1.0E 09
2.0E 09	45.00	17.00	9.50	4.00	0.00	0.00	0.00	0.00	2.0E 09
4.0E 09	31.00	10.50	6.50	2.50	0.00	0.00	0.00	0.00	4.0E 09
6.0E 09	26.50	8.00	4.50	2.00	0.00	0.00	0.00	0.00	6.0E 09
8.0E 09	21.50	6.50	4.50	1.00	0.00	0.00	0.00	0.00	8.0E 09
1.0E 10	16.00	6.00	4.50	1.00	0.00	0.00	0.00	0.00	1.0E 10
2.0E 10	11.50	4.00	3.00	0.00	0.00	0.00	0.00	0.00	2.0E 10
4.0E 10	6.00	4.00	1.50	0.00	0.00	0.00	0.00	0.00	4.0E 10
6.0E 10	4.50	2.00	0.50	0.00	0.00	0.00	0.00	0.00	6.0E 10
8.0E 10	4.50	2.00	0.00	0.00	0.00	0.00	0.00	0.00	8.0E 10
1.0E 11	4.50	1.00	0.00	0.00	0.00	0.00	0.00	0.00	1.0E 11
2.0E 11	2.50	0.00	0.00	0.00	0.00	0.00	0.00	0.00	2.0E 11
4.0E 11	2.00	0.00	0.00	0.00	0.00	0.00	0.00	0.00	4.0E 11
6.0E 11	0.50	0.00	0.00	0.00	0.00	0.00	0.00	0.00	6.0E 11
8.0E 11	0.50	0.00	0.00	0.00	0.00	0.00	0.00	0.00	8.0E 11
1.0E 12	0.50	0.00	0.00	0.00	0.00	0.00	0.00	0.00	1.0E 12
2.0E 12	0.00	0.00	0.00	0.00	0.00	0.00	0.00	0.00	2.0E 12
4.0E 12	0.00	0.00	0.00	0.00	0.00	0.00	0.00	0.00	4.0E 12
6.0E 12	0.00	0.00	0.00	0.00	0.00	0.00	0.00	0.00	6.0E 12
8.0E 12	0.00	0.00	0.00	0.00	0.00	0.00	0.00	0.00	8.0E 12

TABLE G2 FLARE PROGRAM OUTPUT LISTING - IBM 7094
(Continued)

ALPHA FLUX FREQUENCY DISTRIBUTION
(PERCENT OF MISSIONS WHICH ENCOUNTER FLUXES GREATER THAN OR EQUAL TO PHI(E) - A/CM**2-MISSION)

ENERGY-MEV

PHI	10.00	30.00	50.00	100.00	200.00	400.00	1000.00	1500.00	PHI
1.0E 02	100.00	100.00	100.00	100.00	100.00	100.00	38.50	53.50	1.0E 02
2.0E 02	100.00	100.00	100.00	100.00	100.00	100.00	32.50	37.50	2.0E 02
4.0E 02	100.00	100.00	100.00	100.00	100.00	100.00	67.50	28.50	4.0E 02
6.0E 02	100.00	100.00	100.00	100.00	100.00	100.00	61.50	23.50	6.0E 02
8.0E 02	100.00	100.00	100.00	100.00	100.00	100.00	58.00	19.00	8.0E 02
1.0E 03	100.00	100.00	100.00	100.00	100.00	100.00	50.50	17.00	1.0E 03
2.0E 03	100.00	100.00	100.00	100.00	100.00	100.00	40.50	13.00	2.0E 03
4.0E 03	100.00	100.00	100.00	100.00	100.00	98.50	30.50	8.00	4.0E 03
6.0E 03	100.00	100.00	100.00	100.00	100.00	96.00	24.00	6.50	6.0E 03
8.0E 03	100.00	100.00	100.00	100.00	100.00	93.00	20.50	6.50	8.0E 03
1.0E 04	100.00	100.00	100.00	100.00	100.00	90.50	19.00	5.50	1.0E 04
2.0E 04	100.00	100.00	100.00	100.00	100.00	81.00	12.00	3.00	2.0E 04
4.0E 04	100.00	100.00	100.00	100.00	99.50	66.00	8.50	1.50	4.0E 04
6.0E 04	100.00	100.00	100.00	100.00	98.50	59.00	7.00	0.50	6.0E 04
8.0E 04	100.00	100.00	100.00	100.00	97.50	55.00	6.50	0.50	8.0E 04
1.0E 05	100.00	100.00	100.00	100.00	97.00	51.00	6.00	0.50	1.0E 05
2.0E 05	100.00	100.00	100.00	100.00	90.00	39.50	3.50	0.00	2.0E 05
4.0E 05	100.00	100.00	100.00	99.00	77.50	26.50	1.00	0.00	4.0E 05
6.0E 05	100.00	100.00	100.00	98.50	70.00	21.00	0.50	0.00	6.0E 05
8.0E 05	100.00	100.00	100.00	97.00	63.50	19.50	0.00	0.00	8.0E 05
1.0E 06	100.00	100.00	100.00	95.50	57.00	16.50	0.00	0.00	1.0E 06
2.0E 06	100.00	100.00	99.00	87.50	43.00	12.00	0.00	0.00	2.0E 06
4.0E 06	100.00	99.50	97.50	78.00	32.00	7.50	0.00	0.00	4.0E 06
6.0E 06	100.00	99.00	94.50	71.00	26.00	5.50	0.00	0.00	6.0E 06
8.0E 06	100.00	98.00	92.50	64.00	23.50	3.50	0.00	0.00	8.0E 06
1.0E 07	100.00	97.50	89.50	55.50	19.00	3.50	0.00	0.00	1.0E 07
2.0E 07	99.00	93.00	80.50	41.50	11.50	2.50	0.00	0.00	2.0E 07
4.0E 07	98.00	86.50	65.50	29.50	8.00	1.00	0.00	0.00	4.0E 07
6.0E 07	96.50	78.50	56.00	22.50	6.00	0.50	0.00	0.00	6.0E 07
8.0E 07	95.00	71.00	49.50	20.50	5.00	0.00	0.00	0.00	8.0E 07
1.0E 08	92.00	67.50	47.50	18.00	4.50	0.00	0.00	0.00	1.0E 08
2.0E 08	83.00	54.50	33.50	9.50	3.50	0.00	0.00	0.00	2.0E 08
4.0E 08	71.50	41.00	23.00	7.00	2.50	0.00	0.00	0.00	4.0E 08
6.0E 08	63.00	32.00	16.50	5.50	1.00	0.00	0.00	0.00	6.0E 08
8.0E 08	57.50	27.50	11.00	5.00	1.00	0.00	0.00	0.00	8.0E 08
1.0E 09	53.00	24.50	10.00	4.00	1.00	0.00	0.00	0.00	1.0E 09
2.0E 09	39.50	13.00	8.00	3.50	0.00	0.00	0.00	0.00	2.0E 09
4.0E 09	26.50	9.50	5.50	2.00	0.00	0.00	0.00	0.00	4.0E 09
6.0E 09	22.50	6.00	4.00	1.00	0.00	0.00	0.00	0.00	6.0E 09
8.0E 09	19.00	5.50	4.00	0.50	0.00	0.00	0.00	0.00	8.0E 09
1.0E 10	16.00	5.00	3.50	0.50	0.00	0.00	0.00	0.00	1.0E 10
2.0E 10	9.50	3.50	2.50	0.00	0.00	0.00	0.00	0.00	2.0E 10
4.0E 10	6.00	3.50	1.00	0.00	0.00	0.00	0.00	0.00	4.0E 10
6.0E 10	4.00	1.50	0.50	0.00	0.00	0.00	0.00	0.00	6.0E 10
8.0E 10	4.00	1.50	0.00	0.00	0.00	0.00	0.00	0.00	8.0E 10
1.0E 11	4.00	1.00	0.00	0.00	0.00	0.00	0.00	0.00	1.0E 11
2.0E 11	2.00	0.00	0.00	0.00	0.00	0.00	0.00	0.00	2.0E 11
4.0E 11	2.00	0.00	0.00	0.00	0.00	0.00	0.00	0.00	4.0E 11
6.0E 11	0.50	0.00	0.00	0.00	0.00	0.00	0.00	0.00	6.0E 11
8.0E 11	0.50	0.00	0.00	0.00	0.00	0.00	0.00	0.00	8.0E 11
1.0E 12	0.50	0.00	0.00	0.00	0.00	0.00	0.00	0.00	1.0E 12
2.0E 12	0.00	0.00	0.00	0.00	0.00	0.00	0.00	0.00	2.0E 12
4.0E 12	0.00	0.00	0.00	0.00	0.00	0.00	0.00	0.00	4.0E 12
6.0E 12	0.00	0.00	0.00	0.00	0.00	0.00	0.00	0.00	6.0E 12
8.0E 12	0.00	0.00	0.00	0.00	0.00	0.00	0.00	0.00	8.0E 12

MARS MISSION. LAUNCH - 9 OCT. 1977 443 DAYS DURATION

T1	T2	T3	Y1	Y2	Y3	C	SEC	SIZE
1400.0	2600.0	2050.0	15.00000	11.00000	3.00000	0.40000	0.50000	1.00000

NHIS	JLE	JRE	JAP	JLP
200	2443426	2443868	2443624	2443644

TH1	TH2	TH3	TH4	E1	E2
351.619873	498.049805	192.579987	474.339844	0.299000	0.557000

0.0 PERCENT OF MISSIONS ENCOUNTERED NO FLUX EVENTS

T	R	F	T	R	F	T	R	F	T	R	F
649.0	0.9962	4.552E-03	650.0	0.9957	4.567E-03	651.0	0.9952	4.581E-03	652.0	0.9949	4.594E-03
653.0	0.9946	4.608E-03	654.0	0.9945	4.621E-03	655.0	0.9944	4.635E-03	656.0	0.9944	4.648E-03
657.0	0.9945	4.660E-03	658.0	0.9947	4.673E-03	659.0	0.9950	4.686E-03	660.0	0.9953	4.698E-03
661.0	0.9958	4.710E-03	662.0	0.9963	4.723E-03	663.0	0.9969	4.735E-03	664.0	0.9977	4.747E-03
665.0	0.9985	4.759E-03	666.0	0.9994	4.770E-03	667.0	1.0003	4.782E-03	668.0	1.0014	4.794E-03
669.0	1.0025	4.806E-03	670.0	1.0038	4.817E-03	671.0	1.0051	4.829E-03	672.0	1.0065	4.841E-03
673.0	1.0080	4.852E-03	674.0	1.0096	4.864E-03	675.0	1.0112	4.876E-03	676.0	1.0129	4.888E-03
677.0	1.0147	4.900E-03	678.0	1.0166	4.912E-03	679.0	1.0186	4.924E-03	680.0	1.0206	4.937E-03
681.0	1.0227	4.950E-03	682.0	1.0249	4.962E-03	683.0	1.0272	4.975E-03	684.0	1.0295	4.988E-03
685.0	1.0319	5.002E-03	686.0	1.0344	5.016E-03	687.0	1.0370	5.030E-03	688.0	1.0396	5.044E-03
689.0	1.0422	5.059E-03	690.0	1.0450	5.074E-03	691.0	1.0478	5.089E-03	692.0	1.0507	5.105E-03
693.0	1.0536	5.121E-03	694.0	1.0566	5.138E-03	695.0	1.0596	5.155E-03	696.0	1.0627	5.173E-03
697.0	1.0659	5.191E-03	698.0	1.0691	5.210E-03	699.0	1.0724	5.229E-03	700.0	1.0757	5.249E-03
701.0	1.0791	5.270E-03	702.0	1.0825	5.291E-03	703.0	1.0860	5.313E-03	704.0	1.0895	5.336E-03
705.0	1.0931	5.359E-03	706.0	1.0967	5.383E-03	707.0	1.1004	5.408E-03	708.0	1.1041	5.434E-03
709.0	1.1078	5.461E-03	710.0	1.1116	5.488E-03	711.0	1.1154	5.517E-03	712.0	1.1192	5.546E-03
713.0	1.1231	5.576E-03	714.0	1.1271	5.608E-03	715.0	1.1310	5.640E-03	716.0	1.1350	5.674E-03
717.0	1.1391	5.708E-03	718.0	1.1431	5.744E-03	719.0	1.1472	5.781E-03	720.0	1.1513	5.819E-03
721.0	1.1555	5.858E-03	722.0	1.1596	5.898E-03	723.0	1.1638	5.940E-03	724.0	1.1680	5.983E-03
725.0	1.1723	6.028E-03	726.0	1.1765	6.074E-03	727.0	1.1808	6.121E-03	728.0	1.1851	6.169E-03
729.0	1.1894	6.220E-03	730.0	1.1938	6.271E-03	731.0	1.1981	6.324E-03	732.0	1.2025	6.379E-03
733.0	1.2069	6.436E-03	734.0	1.2113	6.493E-03	735.0	1.2157	6.553E-03	736.0	1.2201	6.615E-03
737.0	1.2246	6.678E-03	738.0	1.2290	6.742E-03	739.0	1.2335	6.809E-03	740.0	1.2380	6.878E-03
741.0	1.2424	6.948E-03	742.0	1.2469	7.020E-03	743.0	1.2514	7.094E-03	744.0	1.2559	7.170E-03
745.0	1.2604	7.248E-03	746.0	1.2649	7.329E-03	747.0	1.2694	7.411E-03	748.0	1.2740	7.495E-03
749.0	1.2785	7.581E-03	750.0	1.2830	7.670E-03	751.0	1.2875	7.760E-03	752.0	1.2920	7.853E-03
753.0	1.2966	7.948E-03	754.0	1.3011	8.046E-03	755.0	1.3056	8.145E-03	756.0	1.3101	8.247E-03
757.0	1.3146	8.351E-03	758.0	1.3192	8.458E-03	759.0	1.3237	8.567E-03	760.0	1.3282	8.678E-03
761.0	1.3327	8.792E-03	762.0	1.3372	8.908E-03	763.0	1.3417	9.027E-03	764.0	1.3461	9.148E-03
765.0	1.3506	9.272E-03	766.0	1.3551	9.398E-03	767.0	1.3595	9.527E-03	768.0	1.3640	9.659E-03
769.0	1.3684	9.793E-03	770.0	1.3729	9.930E-03	771.0	1.3773	1.007E-02	772.0	1.3817	1.021E-02
773.0	1.3861	1.036E-02	774.0	1.3905	1.050E-02	775.0	1.3949	1.065E-02	776.0	1.3993	1.081E-02
777.0	1.4037	1.096E-02	778.0	1.4080	1.112E-02	779.0	1.4124	1.128E-02	780.0	1.4167	1.145E-02
781.0	1.4210	1.161E-02	782.0	1.4253	1.178E-02	783.0	1.4296	1.196E-02	784.0	1.4339	1.213E-02
785.0	1.4381	1.231E-02	786.0	1.4424	1.249E-02	787.0	1.4466	1.268E-02	788.0	1.4508	1.286E-02
789.0	1.4550	1.305E-02	790.0	1.4592	1.325E-02	791.0	1.4633	1.344E-02	792.0	1.4675	1.364E-02
793.0	1.4716	1.384E-02	794.0	1.4758	1.405E-02	795.0	1.4799	1.425E-02	796.0	1.4839	1.447E-02
797.0	1.4880	1.468E-02	798.0	1.4921	1.489E-02	799.0	1.4961	1.511E-02	800.0	1.5001	1.534E-02
801.0	1.5041	1.556E-02	802.0	1.5081	1.579E-02	803.0	1.5120	1.602E-02	804.0	1.5160	1.625E-02
805.0	1.5199	1.649E-02	806.0	1.5238	1.673E-02	807.0	1.5277	1.697E-02	808.0	1.5315	1.722E-02
809.0	1.5354	1.746E-02	810.0	1.5392	1.771E-02	811.0	1.5430	1.797E-02	812.0	1.5468	1.822E-02
813.0	1.5505	1.848E-02	814.0	1.5543	1.874E-02	815.0	1.5580	1.901E-02	816.0	1.5617	1.927E-02
817.0	1.5654	1.954E-02	818.0	1.5690	1.982E-02	819.0	1.5727	2.009E-02	820.0	1.5763	2.037E-02
821.0	1.5799	2.065E-02	822.0	1.5835	2.093E-02	823.0	1.5870	2.121E-02	824.0	1.5905	2.150E-02
825.0	1.5940	2.179E-02	826.0	1.5975	2.208E-02	827.0	1.6010	2.238E-02	828.0	1.6044	2.267E-02
829.0	1.6078	2.297E-02	830.0	1.6112	2.327E-02	831.0	1.6146	2.358E-02	832.0	1.6180	2.388E-02

PRECEDING PAGE BLANK NOT FILMED.

TABLE G3 FLARE PROGRAM OUTPUT LISTING - IBM SYSTEM 360/50
(Continued)

833.0	1.6213	2.419E-02	834.0	1.6246	2.450E-02	835.0	1.6279	2.481E-02	836.0	1.6311	2.512E-02
837.0	1.6344	2.544E-02	838.0	1.6376	2.576E-02	839.0	1.6408	2.608E-02	840.0	1.6439	2.640E-02
841.0	1.6471	2.672E-02	842.0	1.6502	2.704E-02	843.0	1.6533	2.737E-02	844.0	1.6564	2.770E-02
845.0	1.6594	2.803E-02	846.0	1.6624	2.836E-02	847.0	1.6654	2.869E-02	848.0	1.6654	2.902E-02
849.0	1.6654	2.936E-02	850.0	1.6654	2.969E-02	851.0	1.6654	3.003E-02	852.0	1.6654	3.037E-02
853.0	1.6654	3.071E-02	854.0	1.6654	3.105E-02	855.0	1.6654	3.139E-02	856.0	1.6654	3.173E-02
857.0	1.6654	3.207E-02	858.0	1.6654	3.242E-02	859.0	1.6654	3.276E-02	860.0	1.6654	3.311E-02
861.0	1.6654	3.345E-02	862.0	1.6654	3.380E-02	863.0	1.6654	3.414E-02	864.0	1.6654	3.449E-02
865.0	1.6654	3.483E-02	866.0	1.6654	3.518E-02	867.0	1.6654	3.553E-02	868.0	1.6569	3.587E-02
869.0	1.6544	3.622E-02	870.0	1.6519	3.656E-02	871.0	1.6493	3.691E-02	872.0	1.6466	3.726E-02
873.0	1.6439	3.760E-02	874.0	1.6411	3.795E-02	875.0	1.6383	3.829E-02	876.0	1.6354	3.863E-02
877.0	1.6324	3.898E-02	878.0	1.6294	3.932E-02	879.0	1.6264	3.966E-02	880.0	1.6232	4.000E-02
881.0	1.6200	4.034E-02	882.0	1.6168	4.068E-02	883.0	1.6135	4.101E-02	884.0	1.6101	4.135E-02
885.0	1.6067	4.168E-02	886.0	1.6032	4.202E-02	887.0	1.5996	4.235E-02	888.0	1.5960	4.268E-02
889.0	1.5923	4.300E-02	890.0	1.5886	4.333E-02	891.0	1.5848	4.366E-02	892.0	1.5809	4.398E-02
893.0	1.5770	4.430E-02	894.0	1.5730	4.462E-02	895.0	1.5690	4.493E-02	896.0	1.5649	4.525E-02
897.0	1.5607	4.556E-02	898.0	1.5565	4.587E-02	899.0	1.5522	4.617E-02	900.0	1.5478	4.648E-02
901.0	1.5434	4.678E-02	902.0	1.5389	4.708E-02	903.0	1.5343	4.738E-02	904.0	1.5297	4.767E-02
905.0	1.5251	4.796E-02	906.0	1.5203	4.825E-02	907.0	1.5155	4.853E-02	908.0	1.5106	4.881E-02
909.0	1.5057	4.909E-02	910.0	1.5007	4.936E-02	911.0	1.4957	4.963E-02	912.0	1.4905	4.990E-02
913.0	1.4853	5.016E-02	914.0	1.4801	5.043E-02	915.0	1.4748	5.068E-02	916.0	1.4694	5.093E-02
917.0	1.4639	5.118E-02	918.0	1.4584	5.143E-02	919.0	1.4528	5.167E-02	920.0	1.4471	5.191E-02
921.0	1.4414	5.214E-02	922.0	1.4356	5.237E-02	923.0	1.4298	5.259E-02	924.0	1.4238	5.282E-02
925.0	1.4178	5.303E-02	926.0	1.4118	5.324E-02	927.0	1.4056	5.345E-02	928.0	1.3994	5.365E-02
929.0	1.3932	5.385E-02	930.0	1.3868	5.405E-02	931.0	1.3804	5.424E-02	932.0	1.3739	5.442E-02
933.0	1.3674	5.460E-02	934.0	1.3608	5.477E-02	935.0	1.3541	5.494E-02	936.0	1.3473	5.511E-02
937.0	1.3405	5.527E-02	938.0	1.3336	5.543E-02	939.0	1.3266	5.558E-02	940.0	1.3196	5.572E-02
941.0	1.3124	5.586E-02	942.0	1.3052	5.600E-02	943.0	1.2980	5.613E-02	944.0	1.2906	5.625E-02
945.0	1.2832	5.637E-02	946.0	1.2757	5.649E-02	947.0	1.2682	5.660E-02	948.0	1.2605	5.670E-02
949.0	1.2528	5.680E-02	950.0	1.2450	5.690E-02	951.0	1.2372	5.698E-02	952.0	1.2293	5.707E-02
953.0	1.2212	5.715E-02	954.0	1.2132	5.722E-02	955.0	1.2050	5.728E-02	956.0	1.1968	5.735E-02
957.0	1.1885	5.740E-02	958.0	1.1801	5.746E-02	959.0	1.1716	5.750E-02	960.0	1.1631	5.754E-02
961.0	1.1545	5.758E-02	962.0	1.1458	5.761E-02	963.0	1.1370	5.763E-02	964.0	1.1282	5.765E-02
965.0	1.1192	5.767E-02	966.0	1.1103	5.767E-02	967.0	1.1012	5.768E-02	968.0	1.0920	5.768E-02
969.0	1.0828	5.767E-02	970.0	1.0735	5.766E-02	971.0	1.0641	5.764E-02	972.0	1.0547	5.762E-02
973.0	1.0452	5.759E-02	974.0	1.0356	5.756E-02	975.0	1.0259	5.752E-02	976.0	1.0161	5.748E-02
977.0	1.0063	5.743E-02	978.0	0.9964	5.738E-02	979.0	0.9865	5.732E-02	980.0	0.9764	5.726E-02
981.0	0.9663	5.720E-02	982.0	0.9562	5.712E-02	983.0	0.9459	5.705E-02	984.0	0.9356	5.697E-02
985.0	0.9252	5.688E-02	986.0	0.9148	5.680E-02	987.0	0.9043	5.670E-02	988.0	0.8938	5.660E-02
989.0	0.8832	5.650E-02	990.0	0.8725	5.640E-02	991.0	0.8618	5.629E-02	992.0	0.8510	5.617E-02
993.0	0.8402	5.605E-02	994.0	0.8294	5.593E-02	995.0	0.8185	5.580E-02	996.0	0.8076	5.567E-02
997.0	0.7966	5.554E-02	998.0	0.7857	5.540E-02	999.0	0.7747	5.526E-02	1000.0	0.7637	5.512E-02
1001.0	0.7527	5.497E-02	1002.0	0.7417	5.482E-02	1003.0	0.7307	5.467E-02	1004.0	0.7197	5.451E-02
1005.0	0.7088	5.436E-02	1006.0	0.6979	5.419E-02	1007.0	0.6870	5.403E-02	1008.0	0.6763	5.386E-02
1009.0	0.6656	5.369E-02	1010.0	0.6550	5.352E-02	1011.0	0.6444	5.335E-02	1012.0	0.6341	5.317E-02
1013.0	0.6238	5.300E-02	1014.0	0.6138	5.282E-02	1015.0	0.6039	5.263E-02	1016.0	0.5942	5.245E-02
1017.0	0.5847	5.227E-02	1018.0	0.5755	5.208E-02	1019.0	0.5666	5.189E-02	1020.0	0.5580	5.171E-02
1021.0	0.5497	5.152E-02	1022.0	0.5418	5.133E-02	1023.0	0.5343	5.114E-02	1024.0	0.5273	5.094E-02
1025.0	0.5207	5.075E-02	1026.0	0.5146	5.056E-02	1027.0	0.5090	5.037E-02	1028.0	0.5040	5.017E-02
1029.0	0.4995	4.998E-02	1030.0	0.4957	4.979E-02	1031.0	0.4925	4.960E-02	1032.0	0.4899	4.941E-02
1033.0	0.4881	4.922E-02	1034.0	0.4869	4.903E-02	1035.0	0.4864	4.884E-02	1036.0	0.4866	4.865E-02
1037.0	0.4875	4.846E-02	1038.0	0.4891	4.828E-02	1039.0	0.4913	4.809E-02	1040.0	0.4942	4.791E-02
1041.0	0.4978	4.773E-02	1042.0	0.5020	4.755E-02	1043.0	0.5068	4.737E-02	1044.0	0.5121	4.720E-02
1045.0	0.5180	4.703E-02	1046.0	0.5244	4.686E-02	1047.0	0.5313	4.669E-02	1048.0	0.5386	4.653E-02
1049.0	0.5463	4.637E-02	1050.0	0.5544	4.621E-02	1051.0	0.5629	4.605E-02	1052.0	0.5717	4.590E-02
1053.0	0.5808	4.575E-02	1054.0	0.5901	4.561E-02	1055.0	0.5997	4.547E-02	1056.0	0.6095	4.533E-02
1057.0	0.6195	4.520E-02	1058.0	0.6297	4.507E-02	1059.0	0.6400	4.495E-02	1060.0	0.6505	4.483E-02
1061.0	0.6610	4.471E-02	1062.0	0.6717	4.460E-02	1063.0	0.6824	4.450E-02	1064.0	0.6933	4.440E-02
1065.0	0.7041	4.430E-02	1066.0	0.7151	4.421E-02	1067.0	0.7260	4.413E-02	1068.0	0.7370	4.405E-02
1069.0	0.7480	4.398E-02	1070.0	0.7590	4.391E-02	1071.0	0.7700	4.385E-02	1072.0	0.7810	4.379E-02
1073.0	0.7920	4.375E-02	1074.0	0.8029	4.370E-02	1075.0	0.8138	4.367E-02	1076.0	0.8247	4.364E-02

TABLE G3 FLARE PROGRAM OUTPUT LISTING - IBM SYSTEM 360/50
(Continued)

1077.0	0.8356	4.362E-02	1078.0	0.8464	4.360E-02	1079.0	0.8572	4.359E-02	1080.0	0.8679	4.359E-02
1081.0	0.8786	4.360E-02	1082.0	0.8893	4.361E-02	1083.0	0.8998	4.363E-02	1084.0	0.9104	4.366E-02
1085.0	0.9208	4.369E-02	1086.0	0.9312	4.374E-02	1087.0	0.9415	4.379E-02	1088.0	0.9518	4.385E-02
1089.0	0.9620	4.391E-02	1090.0	0.9721	4.399E-02	1091.0	0.9822	4.407E-02			

INPUT RN	FIRST RN	LAST RN
1784322405	1784322405	1980663811

TABLE G3 FLARE PROGRAM OUTPUT LISTING - IBM SYSTEM 360/50
(Continued)

PROTON FLUX FREQUENCY DISTRIBUTION
(PERCENT OF MISSIONS WHICH ENCOUNTER FLUXES GREATER THAN OR EQUAL TO PHI(E) - P/CM**2-MISSION)

				ENERGY-MEV					
PHI	10.00	30.00	50.00	100.00	200.00	400.00	1000.00	1500.00	PHI
1.0E 02	100.00	100.00	100.00	100.00	100.00	100.00	91.00	54.00	1.0E 02
2.0E 02	100.00	100.00	100.00	100.00	100.00	100.00	85.00	45.50	2.0E 02
4.0E 02	100.00	100.00	100.00	100.00	100.00	100.00	76.00	33.50	4.0E 02
6.0E 02	100.00	100.00	100.00	100.00	100.00	100.00	74.00	30.00	6.0E 02
8.0E 02	100.00	100.00	100.00	100.00	100.00	100.00	68.50	27.00	8.0E 02
1.0E 03	100.00	100.00	100.00	100.00	100.00	100.00	67.50	25.00	1.0E 03
2.0E 03	100.00	100.00	100.00	100.00	100.00	100.00	57.00	19.50	2.0E 03
4.0E 03	100.00	100.00	100.00	100.00	100.00	99.50	43.00	13.50	4.0E 03
6.0E 03	100.00	100.00	100.00	100.00	100.00	98.50	36.50	10.50	6.0E 03
8.0E 03	100.00	100.00	100.00	100.00	100.00	98.00	32.00	8.50	8.0E 03
1.0E 04	100.00	100.00	100.00	100.00	100.00	97.00	30.00	7.50	1.0E 04
2.0E 04	100.00	100.00	100.00	100.00	100.00	92.50	23.00	5.00	2.0E 04
4.0E 04	100.00	100.00	100.00	100.00	100.00	84.50	16.00	3.00	4.0E 04
6.0E 04	100.00	100.00	100.00	100.00	99.50	79.50	13.00	2.50	6.0E 04
8.0E 04	100.00	100.00	100.00	100.00	99.00	75.00	11.50	1.50	8.0E 04
1.0E 05	100.00	100.00	100.00	100.00	98.50	71.50	11.00	1.00	1.0E 05
2.0E 05	100.00	100.00	100.00	100.00	96.50	63.50	7.00	1.00	2.0E 05
4.0E 05	100.00	100.00	100.00	99.50	92.50	47.50	6.00	1.00	4.0E 05
6.0E 05	100.00	100.00	100.00	99.00	88.00	40.00	2.50	0.50	6.0E 05
8.0E 05	100.00	100.00	100.00	98.50	78.50	35.50	2.00	0.50	8.0E 05
1.0E 06	100.00	100.00	100.00	98.00	77.00	32.50	1.00	0.50	1.0E 06
2.0E 06	100.00	100.00	99.50	95.00	66.50	20.50	1.00	0.50	2.0E 06
4.0E 06	100.00	99.50	98.50	90.00	52.50	14.50	1.00	0.0	4.0E 06
6.0E 06	100.00	99.50	97.50	80.50	45.00	12.50	0.50	0.0	6.0E 06
8.0E 06	100.00	99.50	97.50	75.50	38.50	11.00	0.50	0.0	8.0E 06
1.0E 07	100.00	98.50	96.00	71.50	37.00	9.50	0.50	0.0	1.0E 07
2.0E 07	99.50	97.50	89.50	60.00	26.00	5.00	0.50	0.0	2.0E 07
4.0E 07	99.50	93.00	76.00	48.50	15.50	4.00	0.0	0.0	4.0E 07
6.0E 07	98.50	86.00	68.50	42.00	12.00	2.50	0.0	0.0	6.0E 07
8.0E 07	96.50	80.00	63.50	36.50	10.50	2.00	0.0	0.0	8.0E 07
1.0E 08	96.00	75.50	60.00	33.00	8.50	1.00	0.0	0.0	1.0E 08
2.0E 08	91.00	63.00	51.50	20.50	5.50	1.00	0.0	0.0	2.0E 08
4.0E 08	76.50	56.50	36.00	11.50	2.50	0.50	0.0	0.0	4.0E 08
6.0E 08	68.50	45.00	29.50	9.50	2.50	0.50	0.0	0.0	6.0E 08
8.0E 08	62.50	40.50	24.00	8.00	2.00	0.0	0.0	0.0	8.0E 08
1.0E 09	61.50	36.00	20.50	5.50	1.00	0.0	0.0	0.0	1.0E 09
2.0E 09	48.50	23.00	13.50	3.00	1.00	0.0	0.0	0.0	2.0E 09
4.0E 09	37.50	16.50	6.00	2.00	0.0	0.0	0.0	0.0	4.0E 09
6.0E 09	31.50	13.00	5.00	1.00	0.0	0.0	0.0	0.0	6.0E 09
8.0E 09	27.00	9.00	3.50	0.50	0.0	0.0	0.0	0.0	8.0E 09
1.0E 10	21.00	7.00	3.50	0.50	0.0	0.0	0.0	0.0	1.0E 10
2.0E 10	15.00	4.50	2.00	0.0	0.0	0.0	0.0	0.0	2.0E 10
4.0E 10	9.50	2.00	0.50	0.0	0.0	0.0	0.0	0.0	4.0E 10
6.0E 10	7.50	1.50	0.0	0.0	0.0	0.0	0.0	0.0	6.0E 10
8.0E 10	5.00	1.50	0.0	0.0	0.0	0.0	0.0	0.0	8.0E 10
1.0E 11	4.00	0.50	0.0	0.0	0.0	0.0	0.0	0.0	1.0E 11
2.0E 11	1.50	0.0	0.0	0.0	0.0	0.0	0.0	0.0	2.0E 11
4.0E 11	1.00	0.0	0.0	0.0	0.0	0.0	0.0	0.0	4.0E 11
6.0E 11	0.50	0.0	0.0	0.0	0.0	0.0	0.0	0.0	6.0E 11
8.0E 11	0.50	0.0	0.0	0.0	0.0	0.0	0.0	0.0	8.0E 11
1.0E 12	0.50	0.0	0.0	0.0	0.0	0.0	0.0	0.0	1.0E 12
2.0E 12	0.0	0.0	0.0	0.0	0.0	0.0	0.0	0.0	2.0E 12
4.0E 12	0.0	0.0	0.0	0.0	0.0	0.0	0.0	0.0	4.0E 12
6.0E 12	0.0	0.0	0.0	0.0	0.0	0.0	0.0	0.0	6.0E 12
8.0E 12	0.0	0.0	0.0	0.0	0.0	0.0	0.0	0.0	8.0E 12

TABLE G3 FLARE PROGRAM OUTPUT LISTING - IBM SYSTEM 360/50
(Continued)

ALPHA FLUX FREQUENCY DISTRIBUTION
(PERCENT OF MISSIONS WHICH ENCOUNTER FLUXES GREATER THAN OR EQUAL TO PHI(E) - A/CM**2-MISSION)

PHI	10.00	30.00	50.00	ENERGY-MEV 100.00	200.00	400.00	1000.00	1500.00	PHI
1.0E 02	100.00	100.00	100.00	100.00	100.00	100.00	88.00	52.00	1.0E 02
2.0E 02	100.00	100.00	100.00	100.00	100.00	100.00	79.50	35.00	2.0E 02
4.0E 02	100.00	100.00	100.00	100.00	100.00	100.00	70.50	25.50	4.0E 02
6.0E 02	100.00	100.00	100.00	100.00	100.00	100.00	64.00	22.00	6.0E 02
8.0E 02	100.00	100.00	100.00	100.00	100.00	100.00	61.50	19.50	8.0E 02
1.0E 03	100.00	100.00	100.00	100.00	100.00	100.00	57.50	17.00	1.0E 03
2.0E 03	100.00	100.00	100.00	100.00	100.00	99.00	40.00	13.50	2.0E 03
4.0E 03	100.00	100.00	100.00	100.00	100.00	97.50	31.00	9.50	4.0E 03
6.0E 03	100.00	100.00	100.00	100.00	100.00	95.50	21.50	6.50	6.0E 03
8.0E 03	100.00	100.00	100.00	100.00	100.00	93.50	20.00	5.00	8.0E 03
1.0E 04	100.00	100.00	100.00	100.00	100.00	91.50	17.50	4.50	1.0E 04
2.0E 04	100.00	100.00	100.00	100.00	100.00	84.00	13.50	2.00	2.0E 04
4.0E 04	100.00	100.00	100.00	100.00	99.00	65.50	9.00	2.00	4.0E 04
6.0E 04	100.00	100.00	100.00	100.00	98.00	60.00	6.50	0.50	6.0E 04
8.0E 04	100.00	100.00	100.00	100.00	97.50	57.50	5.00	0.50	8.0E 04
1.0E 05	100.00	100.00	100.00	100.00	95.50	52.50	4.50	0.50	1.0E 05
2.0E 05	100.00	100.00	100.00	100.00	89.50	42.00	3.00	0.50	2.0E 05
4.0E 05	100.00	100.00	100.00	99.00	77.50	31.50	1.50	0.50	4.0E 05
6.0E 05	100.00	100.00	100.00	98.00	69.50	24.50	1.00	0.0	6.0E 05
8.0E 05	100.00	100.00	100.00	97.50	65.50	21.50	1.00	0.0	8.0E 05
1.0E 06	100.00	100.00	100.00	96.50	60.00	18.50	0.50	0.0	1.0E 06
2.0E 06	100.00	100.00	99.00	89.50	52.00	11.50	0.50	0.0	2.0E 06
4.0E 06	100.00	99.50	97.50	76.50	41.50	7.00	0.0	0.0	4.0E 06
6.0E 06	100.00	99.50	95.50	67.00	30.50	4.50	0.0	0.0	6.0E 06
8.0E 06	100.00	98.50	94.50	62.00	26.00	3.50	0.0	0.0	8.0E 06
1.0E 07	100.00	97.50	91.50	59.00	23.00	2.50	0.0	0.0	1.0E 07
2.0E 07	99.50	93.50	80.00	52.00	14.00	2.00	0.0	0.0	2.0E 07
4.0E 07	99.50	86.50	64.00	35.00	8.50	0.50	0.0	0.0	4.0E 07
6.0E 07	96.00	78.00	60.50	27.50	6.50	0.50	0.0	0.0	6.0E 07
8.0E 07	93.50	70.00	57.50	25.00	3.50	0.50	0.0	0.0	8.0E 07
1.0E 08	92.50	68.00	53.50	22.00	3.50	0.50	0.0	0.0	1.0E 08
2.0E 08	86.00	56.50	36.50	16.00	2.00	0.0	0.0	0.0	2.0E 08
4.0E 08	69.50	43.50	27.50	7.00	1.00	0.0	0.0	0.0	4.0E 08
6.0E 08	62.00	35.50	23.50	5.00	0.50	0.0	0.0	0.0	6.0E 08
8.0E 08	56.00	32.50	20.50	4.00	0.50	0.0	0.0	0.0	8.0E 08
1.0E 09	53.00	31.00	16.50	3.50	0.0	0.0	0.0	0.0	1.0E 09
2.0E 09	40.50	18.50	9.50	2.00	0.0	0.0	0.0	0.0	2.0E 09
4.0E 09	35.00	13.00	5.00	0.50	0.0	0.0	0.0	0.0	4.0E 09
6.0E 09	28.00	10.50	3.50	0.0	0.0	0.0	0.0	0.0	6.0E 09
8.0E 09	23.00	8.50	2.50	0.0	0.0	0.0	0.0	0.0	8.0E 09
1.0E 10	17.50	6.50	2.50	0.0	0.0	0.0	0.0	0.0	1.0E 10
2.0E 10	14.00	3.50	1.00	0.0	0.0	0.0	0.0	0.0	2.0E 10
4.0E 10	9.00	1.00	0.0	0.0	0.0	0.0	0.0	0.0	4.0E 10
6.0E 10	6.00	1.00	0.0	0.0	0.0	0.0	0.0	0.0	6.0E 10
8.0E 10	3.50	1.00	0.0	0.0	0.0	0.0	0.0	0.0	8.0E 10
1.0E 11	2.50	0.50	0.0	0.0	0.0	0.0	0.0	0.0	1.0E 11
2.0E 11	1.00	0.0	0.0	0.0	0.0	0.0	0.0	0.0	2.0E 11
4.0E 11	1.00	0.0	0.0	0.0	0.0	0.0	0.0	0.0	4.0E 11
6.0E 11	0.50	0.0	0.0	0.0	0.0	0.0	0.0	0.0	6.0E 11
8.0E 11	0.50	0.0	0.0	0.0	0.0	0.0	0.0	0.0	8.0E 11
1.0E 12	0.50	0.0	0.0	0.0	0.0	0.0	0.0	0.0	1.0E 12
2.0E 12	0.0	0.0	0.0	0.0	0.0	0.0	0.0	0.0	2.0E 12
4.0E 12	0.0	0.0	0.0	0.0	0.0	0.0	0.0	0.0	4.0E 12
6.0E 12	0.0	0.0	0.0	0.0	0.0	0.0	0.0	0.0	6.0E 12
8.0E 12	0.0	0.0	0.0	0.0	0.0	0.0	0.0	0.0	8.0E 12

APPENDIX H

Dose Program Input And Output Listings

Dose program test case input is shown in Table H1. The output listing is shown in Table H2.

This program requires an input tape prepared by the Geometry program sample problem (Volume II).

TABLE H1 DOSE PROGRAM INPUT DATA

```
*     DATA
N31 PHI E MAT SA SB R1 HEAD NPHI NM N2 ND BIN FDC UNITS FF AT EE NE FI C
 A CB  Z AW CC NDM AA AB AR1 EA PHA NPHA
5HEAD 20 OUTPUT TEST.   * * * * * * * * * * * * * * * * * * * * * * *
 * * * * * * * * ** * * * * * * * * * * * * * * * * * * * * *
5UNITS 3  RAD/MISSION
5BIN 1 C0184
4NM 7 MAT 1 2 3 4 5 201 221 N2 26 ND 4 $9
3Z 13/5 7/2 AW 27/5 18/2 AT 0/4 FDC 1.27324-9 $9
3AT 27/5 18/2 $9
3CA .061729277 CB 1.6119395 CC .2460117 $9
4NPHI 8 NPHA 8 NDM 1 $9
3E 10 30 50 100 200 400 1+3 1500 EA 10 30 50 100 200 400 1+3 1500
3PHI 1.098+9 8.446+7 2.052+7 2.97+6 3.551+5 1.884+4 7.869+1 4.386
3PHA 5.666+8 5.843+7 1.404+7 1.496+6 1.125+5 4.468+3 37.55 2.452
3FI 4.57+12 9.99+11 8.2+10 7.46+8 7.76+6 9.01+4 1.7+3 $9  10000 - 30
4NE 7 $3EE .5 1 2 4 6 8 10 $9    ELECTRON FLUX ENERGIES
3SA 2.7938117-3/5 2.15442-3 1.932865-3 SB 2.34551-6/5 2.0318594-6 2.1622
 7-6 R1 1.775/6 1.8 $9  PROTON
3AA 2.8722918-4/5 2.1542266-4 1.8668739-4 AB 2.8692487-7/5 6.5164801-9 4
 .9534441-8 AR1 1.75/6 1.775 $9  ALPHA
=FF .2/5 1/2 $9
N4 NAR POLA AZIM NSKIP
4NSKIP 1 NAR 3 $=POLA 0 180 0 90 20 160 AZIM 0 180 0 90 315 45 $9
=
=
=
N31 PHI E MAT SA SB R1 HEAD NPHI NM N2 ND BIN FDC UNITS FF AT EE NE FI C
 A CB  Z AW CC NDM AA AB AR1 EA PHA NPHA
'ND 0 $9
8
```

RECEDING PAGE BLANK NOT FILMED.

TABLE H2 DOSE PROGRAM OUTPUT LISTING

MATERIALS LIST FOR THIS CASE

SHIELD ***	PROTON		***	***	ALPHA		*** ***	PARAMETERS			***
MATERIAL	SA	SB	R1	AA	AB	AR1	FF	AT	Z	AW	
1	2.7938-03	2.3455-06	1.7750+00	2.8723-04	2.8692-07	1.7500+00	2.0000-01	2.7000+01	1.3000+01	2.7000+01	
2	2.7938-03	2.3455-06	1.7750+00	2.8723-04	2.8692-07	1.7500+00	2.0000-01	2.7000+01	1.3000+01	2.7000+01	
3	2.7938-03	2.3455-06	1.7750+00	2.8723-04	2.8692-07	1.7500+00	2.0000-01	2.7000+01	1.3000+01	2.7000+01	
4	2.7938-03	2.3455-06	1.7750+00	2.8723-04	2.8692-07	1.7500+00	2.0000-01	2.7000+01	1.3000+01	2.7000+01	
5	2.7938-03	2.3455-06	1.7750+00	2.8723-04	2.8692-07	1.7500+00	2.0000-01	2.7000+01	1.3000+01	2.7000+01	
201	2.1544-03	2.0319-06	1.7750+00	2.1542-04	6.5165-09	1.7500+00	1.0000+00	1.8000+01	7.0000+00	1.8000+01	

DETECTOR ***	PROTON		***	***	ALPHA		*** ***	ELECTRON		***
MATERIAL	SA	SB	R1	AA	AB	AR1	CA	CB	CC	
221	1.9329-03	2.1623-06	1.8000+00	1.8669-04	4.9534-08	1.7750+00	6.1729-02	1.6119+00	2.4601-01	

BIN = 00184 FCC = 1.2732-05

ALPHA SPECTRUM

EA(I)	PHA(I)	HA(I)	QA(I)
1.00000+01	5.66600+08	6.62491+10	2.06790+00
3.00000+01	5.84300+07	7.76021+11	2.79140+00
5.00000+01	1.40400+07	4.32169+12	3.23036+00
1.00000+02	1.49600+06	4.37681+13	3.73311+00
2.00000+02	1.12500+05	5.76097+15	4.65415+00
4.00000+02	4.46800+03	1.66519+17	5.21562+00
1.00000+03	3.75500+01	5.81472+21	6.72997+00
1.50000+03	2.45200+00	0.	0.

PROTON SPECTRUM

E(I)	PHI(I)	H(I)	Q(I)
1.00000+01	1.09800+09	2.37321+11	2.33473+00
3.00000+01	8.44600+07	1.04223+12	2.76979+00
5.00000+01	2.05200+07	1.12137+12	2.78850+00
1.00000+02	2.97000+06	3.99105+12	3.06417+00
2.00000+02	3.55100+05	1.98760+15	4.23635+00
4.00000+02	1.88400+04	6.79203+19	5.97869+00
1.00000+03	7.86900+01	1.80843+23	7.12046+00
1.50000+03	4.38600+00	0.	0.

ELECTRON SPECTRUM

EE(I)	FI(I)
5.00000-01	4.57000+12
1.00000+00	9.59000+11
2.00000+00	8.20000+10
4.00000+00	7.46000+08
6.00000+00	7.76000+06
8.00000+00	9.01000+04
1.00000+01	1.76000+03

TABLE H2 DOSE PROGRAM OUTPUT LISTING
(Continued)

```
OUTPUT TEST.  * * * * * * * * * * * * * * * * * * * * * * *   * * * * * * * * ** * * * * * * * * * * * * * * * * * * * *

DETECTOR IN RIGHT EYE - LEFT MODULE.
XD =     4.666     YD =    34.750      ZD =     26.000
DETECTOR MATERIAL NUMBER IS 221

        ***  DETECTOR   1  DOSE UNITS ARE  RAD/MISSION        ***

TOTAL PROTON DOSE     TOTAL ALPHA DOSE     TOTAL ELECTRON DOSE     TOTAL BREMSSTRAHLUNG DOSE
    1.76E+02              1.835+01              4.800+00                  0.
```

POLA	AZIM	PROTON PARTIAL DOSE	WEIGHT FRACTION	ALPHA PARTIAL DOSE	WEIGHT FRACTION	ELECTRON PARTIAL DOSE	WEIGHT FRACTION	BREMSSTRAHLUNG PARTIAL DOSE	WEIGHT FRACTION	SOLID ANGLE
0. / 180.00	0. / 180.00	5.856+01	0.69	5.953+00	0.65	1.483+00	0.62	0.	0.	6.278+00
0. / 90.00	0. / 90.00	3.555+01	1.42	3.852+00	1.43	1.061+00	1.59	0.	0.	1.849+00
20.00 / 160.00	315.00 / 45.00	8.362+01	2.16	9.620+00	2.33	2.615+00	2.42	0.	0.	2.828+00
REMAINDER		6.546E+01	1.04	7.400+00	1.03	1.956+00	1.04	0.	0.	4.932+00

TABLE H2 DOSE PROGRAM OUTPUT LISTING
(Continued)

OUTPUT TEST. *

DETECTOR IN ABDOMEN - LEFT MODULE.
XD = 0. YD = 36.000 ZD = -1.000
DETECTOR MATERIAL NUMBER IS 221

*** DETECTOR 2 DOSE UNITS ARE RAD/MISSION ***

TOTAL PROTON DOSE	TOTAL ALPHA DOSE	TOTAL ELECTRON DOSE	TOTAL BREMSSTRAHLUNG DOSE
5.210+00	6.594-02	0.	0.

POLA	AZIM	PROTON PARTIAL DOSE	WEIGHT FRACTION	ALPHA PARTIAL DOSE	WEIGHT FRACTION	ELECTRON PARTIAL DOSE	WEIGHT FRACTION	BREMSSTRAHLUNG PARTIAL DOSE	WEIGHT FRACTION	SOLID ANGLE
0. 180.00	0. 180.00	2.811+00	1.04	3.548-02	1.03	0.	0.	0.	0.	6.551+00
0. 90.00	0. 90.00	6.449-01	0.98	8.168-03	0.99	0.	0.	0.	0.	1.579+00
20.00 160.00	315.00 45.00	1.369+00	1.18	1.683-02	1.20	0.	0.	0.	0.	2.679+00
REMAINDER		1.762+00	0.90	2.228-02	0.90	0.	0.	0.	0.	4.714+00

TABLE H2 DOSE PROGRAM OUTPUT LISTING
(Continued)

```
OUTPUT TEST.  * * * * * * * * * * * * * * * * * * * * * * * *   * * * * * * * ** * * * * * * * * * * * * * * * * *

DETECTOR IN RIGHT EYE - RIGHT MODULE.
XC =    -4.006      YD =   -37.250      ZD =    -26.000
DETECTOR MATERIAL NUMBER IS 221

        ***  DETECTOR   3  DOSE UNITS ARE  RAD/MISSION        ***


TOTAL PROTON DOSE      TOTAL ALPHA DOSE      TOTAL ELECTRON DOSE      TOTAL BREMSSTRAHLUNG DOSE
     1.550+02              2.164+01               5.903+00                    0.


  POLA    AZIM      PROTON       WEIGHT       ALPHA        WEIGHT      ELECTRON      WEIGHT  BREMSSTRAHLUNG  WEIGHT
   0.      0.    PARTIAL DOSE  FRACTION  PARTIAL DOSE   FRACTION  PARTIAL DOSE  FRACTION  PARTIAL DOSE  FRACTION  SOLID ANGLE
 180.00  180.00    5.461+01      0.56      5.604+00       0.52      1.452+00      0.49       0.            0.        6.249+00

  POLA    AZIM      PROTON       WEIGHT       ALPHA        WEIGHT      ELECTRON      WEIGHT  BREMSSTRAHLUNG  WEIGHT
   0.      0.    PARTIAL DOSE  FRACTION  PARTIAL DOSE   FRACTION  PARTIAL DOSE  FRACTION  PARTIAL DOSE  FRACTION  SOLID ANGLE
  90.00   90.00    5.773-01      0.03      8.697-03       0.00      0.            0.         0.            0.        1.351+00

  POLA    AZIM      PROTON       WEIGHT       ALPHA        WEIGHT      ELECTRON      WEIGHT  BREMSSTRAHLUNG  WEIGHT
  20.00  315.00  PARTIAL DOSE  FRACTION  PARTIAL DOSE   FRACTION  PARTIAL DOSE  FRACTION  PARTIAL DOSE  FRACTION  SOLID ANGLE
 160.00   45.00    4.510+00      0.12      1.918-01       0.05      1.745-03      0.00       0.            0.        2.429+00

REMAINDER          1.366+02      1.73      1.586+01       1.81      4.449+00      1.86       0.            0.        5.087+00
```

TABLE H2 DOSE PROGRAM OUTPUT LISTING
(Continued)

OUTPUT TEST. *

DETECTOR IN ABDOMEN - RIGHT MODULE.
XD = 0. YD = -36.000 ZD = 1.600
DETECTOR MATERIAL NUMBER IS 221

*** DETECTOR 4 DOSE UNITS ARE RAD/MISSION ***

TOTAL PROTON DOSE	TOTAL ALPHA DOSE	TOTAL ELECTRON DOSE	TOTAL BREMSSTRAHLUNG DOSE
5.213+00	6.596-02	0.	0.

POLA	AZIM	PROTON PARTIAL DOSE	WEIGHT FRACTION	ALPHA PARTIAL DOSE	WEIGHT FRACTION	ELECTRON PARTIAL DOSE	WEIGHT FRACTION	BREMSSTRAHLUNG PARTIAL DOSE	WEIGHT FRACTION	SOLID ANGLE
0. 180.00	0. 180.00	2.389+00	0.96	3.037-02	0.96	0.	0.	0.	0.	6.015+00
0. 90.00	0. 90.00	5.616-01	0.85	6.950-03	0.83	0.	0.	0.	0.	1.592+00
20.00 160.00	315.00 45.00	1.231+00	1.11	1.549-02	1.10	0.	0.	0.	0.	2.677+00
REMAINDER		2.180+00	1.02	2.750-02	1.02	0.	0.	0.	0.	5.133+00

REFERENCES

1. Abetti, G.: Solar Research, The MacMillan Co.; New York, N. Y.; 1963.

2. Adamson, D.; Davidson, R. E.: Statistics of Solar Cosmic Rays as Inferred from Correlation with Intense Geomagnetic Storms, NASA TN D-1010; Washington, D. C.; February, 1962.

3. Allen, C. W. (ed.): Tenth Report on Solar - Terrestrial Relations, Planetary and Space Science, Vol. 12; May, 1964.

4. Allen, C. W.: The Influence of the Sunspot Cycle on Phenomena at the Bottom of the Atmosphere, Planetary and Space Science, Vol. 12, p. 327; May, 1964.

5. Allen, R. I.; Bly, F. T.; Dressler, A. J.; Douglass, C. C.; Perkins, J. F.; Price, H. C.; Schofield, W. M.; Smith, E. C.: Shielding Problems in Manned Space Vehicles, NR 140; Lockheed-Georgia Co., Marietta, Ga.; September, 1961.

6. Anderson, K. A.: Preliminary Study of Prediction Aspects of Solar Cosmic Ray Events, NASA TN D-700; Washington, D. C.; April, 1961.

7. Antalova, A.; Gnevyshev, M. N.: Principal Characteristics of the 11-Year Solar Activity Cycle, Soviet Astronomy - AJ, Vol. 9, no. 2, p. 198; September - October, 1965.

8. Bailey, D. K.: Polar - Cap Absorption, Tenth Report on Solar - Terrestrial Relations, Planetary and Space Science, Vol. 12, p. 495; May, 1964.

9. Bailey, L. E.: Angle and Energy Distributions of Charged Particles from the High - Energy Nuclear Bombardment of Various Elements, UCRL 3334; Berkeley, California; 1956.

10. Baktai, M.; Feyesh, I.; Horvat, A.: Reflection of Solar Activity in the Behavior of the Annual Rings of "Pinus Tarnocienzica" of the Miocene Period, Soviet Astronomy - AJ Vol. 8, no. 2, p. 322; September - October, 1964.

11. Berger, M. J.; Seltzer, S. M.: Energy Spectra and Angular Distributions of Electrons Transmitted Through Sapphire (Al_2O_3) Foils, NASA SP-3008; Washington, D. C.; 1964.

12. Berger, M. J.; Seltzer, S. M.: Transmission of 1 - MeV Electrons Through Aluminum, NBS Report 8900; U. S. Department of Commerce; National Bureau of Standards, Washington, D. C.; June 1965.

13. Berger, M. J.; Seltzer, S. M.: Tables of Energy Losses and Ranges of Electrons and Positrons, NASA SP-3012; Washington, D. C.; 1964.

14. Billingham, J.: Apollo Dose Limits, Second Symposium on Protection Against Radiations in Space, Gatlinburg, Tenn., October 12 through 14, 1964; NASA SP-71, p. 139; 1965.

15. Brooks, C. E. P.: Seventh Report on Solar - Terrestrial Relations, Planetary and Space Science, p. 183; 1951.

16. Burrell, M. O.: The Calculation of Proton Penetration and Dose Rates, Second Symposium on Protection Against Radiations in Space, Gatlinberg, Tenn., October 12 through 14, 1964; NASA SP-71, p. 493; 1965.

17. Burrell, M. O.: Private Communication.

18. Crespo, V. P.; Alexander, J. M.; Hyde, E. K.: Ejection of Large Fragments in High-Energy Nuclear Reactions, Phys. Rev., Vol. 131, no. 4, p. 1765; August, 1963.

19. Goldstein, H.: Fundamental Aspects of Reactor Shielding, Addison-Wesley Publishing Co., Inc., Reading, Mass.; 1959.

20. Gnevyshev, M. N.: New Data on Solar Activity and its Influence on the Earth, Akademiya Navk SSSR, Vestnik, no. 5, p. 67; 1965.

21. Gregory, J. B.: Particle Influx at High Latitudes, 2. Solar Protons, J. Geophys. Res., Vol. 68, no. 10, p. 3097; May, 1963.

22. Hess, W. N. (ed.): AAS - NASA Symposium on the Physics of Solar Flares, Greenbelt, Maryland, October 28 through 30, 1963, NASA SP-50; 1964.

23. Hill, C. W.; Douglass, C. C.; Ritchie, W. B.; Simpson, K. M., Jr.: Computer Programs for Shielding Problems in Manned Space Vehicles, ER 6643, Lockheed-Georgia Co., Marietta, Ga.; January, 1964.

24. Hill, C. W.; Ritchie, W. B.; Simpson, K. M., Jr.: Data Compilation and Evaluation of Space Shielding Problems - Range and Stopping Power Data, Volume I, ER 7777, Lockheed-Georgia Co., Marietta, Ga.; July 1965.

25. Hill, C. W., Ritchie, W. B.; Simpson, K. M., Jr.: Data Compilation and Evaluation of Space Shielding Problems - Dose Calculations In Space Vehicles, Volume II, ER 7777, Lockheed-Georgia Co., Marietta, Ga.; August, 1965.

26. Hodgman, C. D. (ed.): Mathematical Tables from Handbook of Chemistry and Physics, Chemical Rubber Publishing Co., Cleveland, Ohio; 1954.

27. Korteling, R. G.; Hyde, E. K.: Interaction of High-Energy Protons and Helium Ions with Niobium, Phys, Rev., Vol. 136, no. 2B, p. B425; October, 1964.

28. Malitson, H. H.; Webber, W. R.: A Summary of Solar Cosmic Ray Events, Solar Proton Manual, NASA TR R-169, p. 1, Washington, D. C.; 1963.

29. Mar, B. W.: Electron Shielding Codes for Evaluation of Space Radiation Hazards, D2-90414, The Boeing Co., Seattle, Wash.; 1963.

30. McGowan, F. K.; Milner, W. T.; Kim, H. J.: Nuclear Cross Sections for Charged-Particle Induced Reactions - Mn, Fe, Co, ORNL - CPX 1; 1964.

31. McGowan, F. K.; Milner, W. T.; Kim, H. J.: Nuclear Cross Sections for Charged-Particle Induced Reactions - Ni, Cu, ORNL - CPX 2; September, 1964.

32. Modisette, J. L.: Apollo Radiation Environment Analysis, Second Symposium on Protection Against Radiations in Space, Gatlinburg, Tenn., October 12 through 14, 1964, NASA SP-71, p. 147; 1965.

33. Parker, E. N.: Interplanetary Dynamical Processes, Interscience Publishers, John Wiley and Sons, New York, N. Y.; 1963.

34. Scott, M.: Mechanics, p. 304, McGraw-Hill Book Co., Inc., New York, N. Y., 1949.

35. Smith, H. J.; Smith, E. v. P.: Solar Flares, The MacMillan Co., New York, N. Y.; 1963.

36. Vette, J. I.: Models of the Trapped Radiation Environment, Volume I, Inner Zone Protons and Electrons, NASA SP-3024, Washington, D. C.; 1966.

37. Vette, J. I.: Private Communication.

38. van de Vijver, R.: Excitation Function for Alpha-Induced Reactions on Gold, Physica, Vol. 29, p. 1214; 1963.

39. Warwick, C. S.: Propagation of Solar Particles in the Interplanetary Magnetic Field, J. Geophys. Res., Vol. 67, p. 1333; 1962.

40. Webber, W. R.: A Review of Solar Cosmic Ray Events, AAS - NASA Symposium on the Physics of Solar Flares, Greenbelt, Maryland, October 28 through 30, 1963., NASA SP-50, p. 215; 1964.